

Dissecting the Development of plasmacytoid Dendritic Cells

Inauguraldissertation

zur

Erlangung der Würde eines Doktors der Philosophie

vorgelegt der

Philosophisch-Naturwissenschaftlichen Fakultät

der Universität Basel

von

Patrick Fernandes Rodrigues

Aus Montalegre, Portugal

2020

Originaldokument gespeichert auf dem Dokumentenserver der Universität Basel

edoc.unibas.ch

Genehmigt von der Philosophisch-Naturwissenschaftlichen Fakultät auf Antrag von

(Mitglieder des Dissertationskomitees: Prof. Dr. R. Zeller, Prof. Dr. R. Tussiwand, Prof. Dr. C. King)

Basel, den 19.02.2019

Prof. Dr. Martin Spiess

Dekan

Table of Contents

Summary:	1
Introduction:	2
<i>History of pDCs:</i>	2
<i>The development of pDCs:</i>	4
Hematopoiesis:	4
Required cytokines and known progenitors in pDC development:	6
Lineage restricted reporters:	7
Cellular Barcoding:	10
Transcription factors required during pDC development:	11
<i>The function of pDCs:</i>	16
Trafficking of pDCs:	16
The role of TLR7 and TLR9 in viral sensing:.....	17
The role of other innate immune sensors:.....	19
<i>pDCs in health and disease:</i>	20
The regulation of type I IFN production:	20
The role of pDCs in antigen presentation:	21
pDCs in acute vs chronic viral infections:	22
pDCs in autoimmunity:	24
pDCs in cancer:.....	25
Heterogeneity of pDCs:.....	26
Aim of the project:	27
Results:	28
<i>Distinct progenitor lineages contribute to the heterogeneity of plasmacytoid dendritic cells</i>	28
Abstract	29
Results.....	30
Discussion	39
Methods.....	41
<i>Supplementary Information</i>	43
Supplementary Figures.....	44
Supplementary Methods.....	52
Supplementary Tables	52
Discussion:	56

Abbreviations:	61
Acknowledgment:	65
References:	66
Appendix:	86

Summary:

Plasmacytoid dendritic cells (pDCs) are an immune subset specialized in the production of Type I Interferons (IFNs). Conventional dendritic cells (cDCs) originate mostly from a common dendritic cell progenitor (CDP), whereas pDCs have been shown to develop from both CDPs as well as common lymphoid progenitors (CLPs). In contrast to the current literature, we here show that pDCs mostly differentiate from an IL-7R expressing lymphoid progenitor. IL-7R⁺ progenitors can be subdivided into three distinct subsets based on the expression of SiglecH and Ly6D: double negative (DN), Ly6D⁺ single positive (SP) and double positive (DP) progenitors. Each of these subsets identifies a specific developmental stage along the pDC lineage, where commitment by IL-7R⁺ progenitors is achieved upon expression of Ly6D and SiglecH (DP pre-pDCs). Further, RNA sequencing analysis of IL-7R⁺ lymphoid progenitor subsets revealed the transcriptional landscape of pDC development along the lymphoid branch, where high expression of the transcription factor IRF8 marks pDC commitment and anticipates the increase of TCF4 levels. The transcriptional signature of DP pre-pDCs correlates with the lineage potential assessed in vitro, in which DP pre-pDCs are fully committed to the pDC lineage. Moreover, single cell RNA sequencing on bone marrow and splenic pDCs revealed pDC heterogeneity in both tissues and further supported the dual origin of pDC from myeloid and lymphoid precursors. While all pDCs have the potential to secrete Type I IFNs and have high expression levels of pDC-specific transcript, only myeloid-derived pDCs share with cDCs the capacity to process and present antigen, suggesting that functional specification is directly linked to developmental origin.

Introduction:

pDCs are an immune subset specialized in the production of Type I IFNs. They have been long considered as part of the dendritic cell (DC) subset, even though their morphological appearance, migratory behavior, transcriptional signature and activation pattern seem to be distinct from those of conventional DCs (cDCs). The identification of a myeloid progenitor capable of generating all subtypes of DCs, including pDCs, led to the idea that the majority of pDCs are generated by a myeloid precursor rather than by any other lineage. However, conflicting evidence was present in the literature supporting a lymphoid origin of pDCs, which prompted us to dissect more in detail the developmental pathway of pDCs. The following chapter gives a short summary on the history of pDCs and recapitulates our current knowledge and understanding on pDC hematopoiesis as well as its role in the immune system.

pDCs: an historical perspective

The first description of pDCs dates back to 1958, where clusters of lymphoid cells were identified in human lymph nodes¹. Those cell clusters were morphologically characterized by electron microscopy studies and revealed a well-structured rough endoplasmatic reticulum, thus being interpreted as a special type of plasma cell lacking the expression of lineage markers and the potential to produce immunoglobulins^{2,3}. Their close localization within T cell regions, their presence within thymic lobes and their expression of some T cell-associated antigens such as CD4, led in 1983 to the designation of “plasmacytoid T-cells”⁴. Facchetti et al performed in 1988 a more detailed immunophenotypical characterization. The absence of B, T and granulocyte-associated antigens and the presence of myelomonocytic markers such as CD36, HLA and the invariant chain CD74 challenged the idea of the lymphoid origin of plasmacytoid T-cells, suggesting a myeloid developmental pathway. This hypothesis led to a new definition of the subset: “plasmacytoid monocytes”⁵. Around the same year, several independent studies identified a small subset of leukocytes in human peripheral blood, which similarly as plasmacytoid monocytes, lacked the expression of lineage markers and produced high levels of IFNs in response to enveloped viruses, bacteria and tumor cells, which led to the term “natural IFN-producing cells” (IPCs)^{6,7,8,9,10,11,12}. Since their discovery it has been difficult to assign these cells to a specific lineage as they resembled plasma blasts and expressed both lymphoid as well as myeloid antigens^{8,9,12,13}. The observation that stimulation of these cells

with IL-3 and CD40L induced their maturation into T helper type 2 (Th2) priming mature dendritic cells (DCs), led Grouard et al in 1997 to assign them to the dendritic cell lineage¹⁴. It took two additional years until Cella et al¹⁵ and Siegal et al¹⁶ demonstrated that IPCs, plasmacytoid monocytes and plasmacytoid T cells were de facto the same cell, which produced high amounts of IFNs during antiviral immune reactions. In 2000, their ability to induce also TH1 priming, similar to conventional DCs (cDCs), led to the new and definitive nomenclature of plasmacytoid DCs (pDCs)¹⁷.

In 2001 three independent groups identified pDCs in mouse tissues. Similar to their human counterpart, murine pDCs showed the same morphology as well as capacity to produce IFN but were characterized by high B220 and Ly6C expression levels, whereas CD123 (IL-3R α), MHC-II and co-stimulatory molecules were low under steady state conditions and only increased upon Flt3L or CpG ODN stimulation, respectively^{18, 19, 20}. Collectively, their expression of MHC-II, of co-stimulatory molecules, and of the integrin receptor Itgax (CD11c), consistent with their capacity to prime T cell responses, further supported their assignment to the DC lineage^{18, 19, 20} (Figure 1).

The identification of pDC specific cell surface markers facilitated future work that aimed at a better characterization and definition of their functional properties. In humans, two novel antigens were identified: BDCA-2 (CD303) and BDCA-4 (CD304)²¹ (Figure 1). BDCA-2 is a type II C-type lectin transmembrane glycoprotein, which if crosslinked with monoclonal antibodies, suppresses the production of IFN- α/β by pDCs²². BDCA-4 is a neuronal receptor of the class 3 semaphorin subfamily, which also functions as a coreceptor of endothelia or tumor cell produced vascular and endothelial growth factor A (VEGF-A). Stimulation of BDCA-4 by monoclonal antibodies does not alter the function of pDCs, making it a perfect choice for pDC purification assays²³ (Figure 1). In mice, two independent groups generated antibodies targeting Bone marrow Stromal antigen (BST2, clone 927 and 120G8) and Sialic acid binding immunoglobulin-like lectin H (SiglecH, clone 440c or 551)^{24, 25, 26} (Figure 1). BST2 was shown to be specifically expressed by pDCs under steady state conditions and mice treated *in vivo* with α BST2 monoclonal antibodies are effectively depleted of pDCs. However, since BST2 is upregulated on other cell subsets such as B lymphocytes or endothelial cells following exposure to Type I or II IFNs, caution is necessary in using this antibody to identify pDCs, or interpreting results of mice treated with this antibody. Additionally, *in vitro* activation of α BST2 purified pDCs shows a reduction of IFN- α secretion, implicating an important role for BST2 in the regulation of pDC function. SiglecH is highly expressed on pDCs but not

exclusively. A specialized macrophage subset present in the spleen, lymph node and brain as well as progenitor cells in the BM show expression of SiglecH^{26,27}. Similar to BST2, α SiglecH monoclonal antibodies profoundly impair IFN- α secretion in response to CpG stimulation, whereas the production of other cytokines such as IL6, IL-10 or TNF- α is not affected. Remarkably, no depletion of pDCs was observed *in vivo* upon α SiglecH treatment^{25, 26, 27} (Figure 1).

Markers	Antibodies	Advantages	Caveats
Siglec-H ⁺	agonistic mAb (clone 440c)	rapid functional impairment	transient, may affect other cells
Bst2 ⁺	depleting mAb (clone 120G8, 927)	rapid depletion	transient, may affect other cells
Ly6C ⁺	mAb (HK1.4)	no functional impairment	unspecific, recognizes granulocytes
CD11c ⁺	mAb (clone 418)	no functional impairment	unspecific, recognizes DCs
B220 ⁺	mAb (clone RA3-6B2)	no functional impairment	unspecific, recognizes B cells
CD45RA ⁺	depleting mAb (clone 14.8)	no functional impairment	unspecific, recognizes B and T cells
CD123 (IL-3R α) ⁺	mAb (clone CSL362)	efficient depletion	unspecific, blocks IL-3 signalling
MHC-II ⁺	mAb (clone M5/114.15.2)	no functional impairment	unspecific, recognizes all APCs
CD74 ⁺	mAb (clone In1/CD74)	no functional impairment	unspecific, recognizes all APCs
BDCA2 (CD303) ⁺	agonistic mAb (clone 24F4A)	rapid functional impairment	not demonstrated in humans
BDCA4 (CD304) ⁺	mAb (clone 12c2)	no functional impairment	unspecific, recognizes other cells

Figure 1: Shown are surface markers expressed on murine (blue) and human (pink) pDCs. Markers shared between mouse and human pDCs are indicated by the overlap (purple). Additionally, antibody clones are depicted which are used for functional detection, modulation or depletion of pDCs.

The development of pDCs:

Hematopoiesis:

Hematopoiesis is a hierarchical process in which self-renewing multipotent hematopoietic stem cells (HSCs) generate all downstream progenitors as well as all mature blood cells (Figure 2)^{28,29}. It was shown that a fraction of active HSCs can generate different subsets of multipotent progenitors (MPPs)³⁰ that further differentiate into two separate branches, becoming either common lymphoid progenitors (CLPs)³¹ or common myeloid progenitors (CMPs)³². CLPs generate all lymphoid cells, namely ILCs, NK-, B- and T cells but lack the potential to generate myeloid and erythroid cells. CMPs can differentiate into megakaryocyte and erythrocyte progenitors (MEP) as well as granulocyte and macrophage precursors (GMP)³². Within the GMP precursors, a monocyte and dendritic cell progenitor (MDP) with the potential to generate monocytes as well as DCs but not neutrophils was recently identified and characterized^{33,34}. MDPs can be further segregate into common monocyte progenitors (cMoPs) and common dendritic cell precursors (CDPs). Adoptively transferred cMoPs give rise to Ly6C^{hi} and

Ly6C^{low} monocytes³⁵, whereas CDPs have the potential to generate pDCs as well as cDC1 and cDC2³⁶. Immediate precursors with exclusive differentiation potential have been identified for both cDC subsets³⁷. Although the molecular mechanism defining cDC1 lineage specification has been characterized, cDC2 specification is still unclear³⁷. Multiple pathways appear to converge into a phenotypically homogenous but transcriptionally heterogeneous cDC2 lineage^{38, 39, 40}. In addition, the developmental trajectory leading to pDC commitment seems to be uncertain, since both the myeloid derived CDPs as well as lymphoid derived CLPs were shown to have the potential to generate pDCs, as shown in Figure 2^{36, 41, 42, 43}.

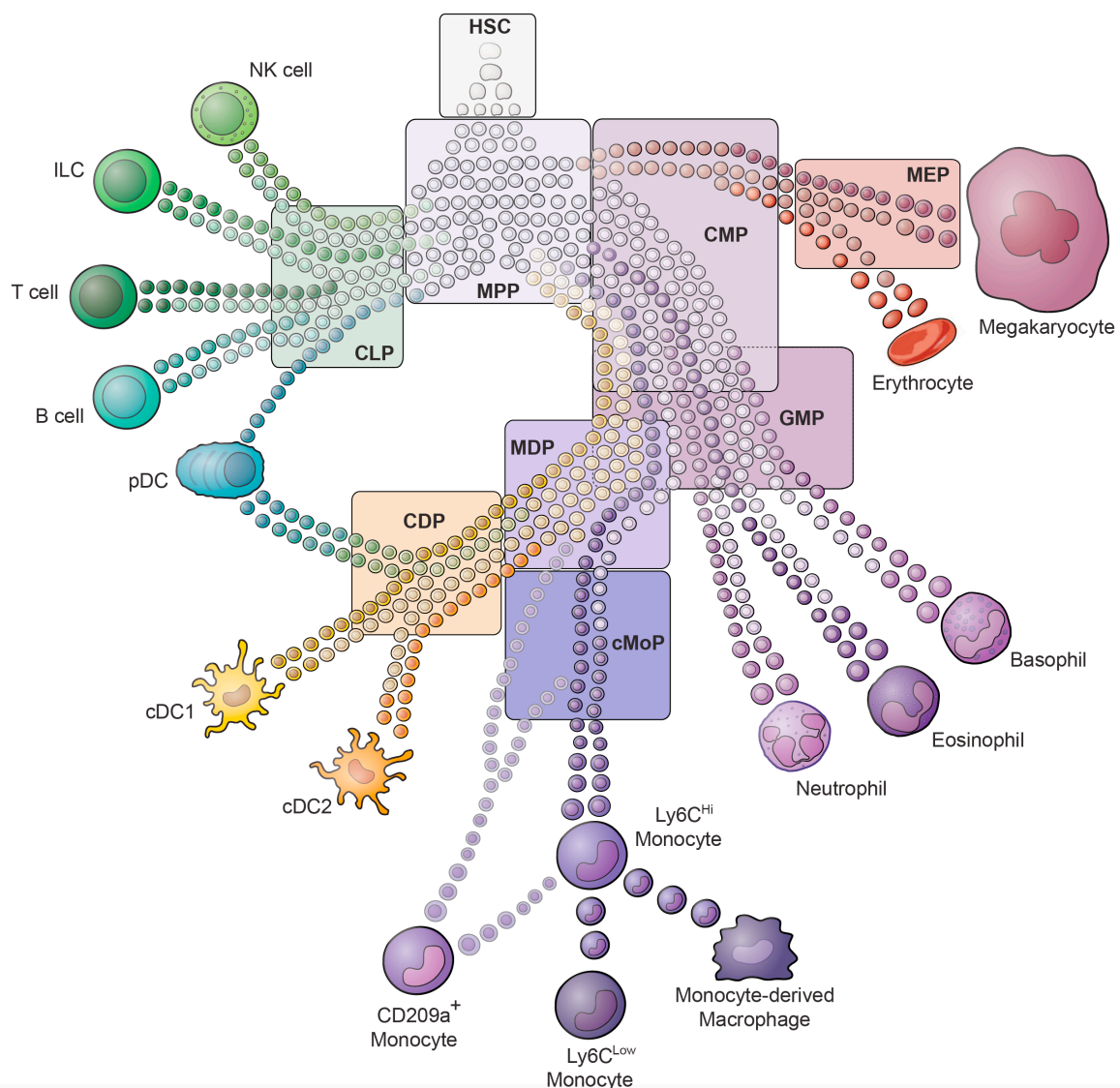


Figure 2: Hematopoietic development in the Bone Marrow. Shown are the progressive developmental stages which occur during hematopoiesis and that lead to the formation of distinct immune cells. Abbreviations: Hematopoietic Stem Cell (HSC); Multipotent precursor (MPP); Common Lymphoid Progenitor (CLP); Natural Killer Cell (NK cell); Innate Lymphoid Cell (ILC); Common Myeloid Precursor (CMP); Myeloid and Erythroid Precursor (MEP); Granulocyte Macrophage Precursor (GMP); Macrophage and Dendritic Cell Precursor (MDP); common Monocyte Precursor (cMoP); Common Dendritic cell Precursor (CDP); conventional Dendritic cell (cDC) and plasmacytoid Dendritic cell (pDC).

Required cytokines and known progenitors in pDC development:

The developmental path and lineage affiliation of pDCs have since their discovery been controversial, partly because these cells show features associated to the myeloid as well as the lymphoid branch. The expression of surface markers as well as their ability to prime T cells led to their assignment to the DC lineage, which separates pDCs from cDCs. In support of a common origin is also the expression of the Fms-like tyrosine kinase 3 receptor (Flt3) as well as the dependency of its corresponding ligand Flt3L by both subsets cDCs and pDCs.^{44, 45}. However, since myeloid as well as lymphoid subsets show massive perturbations in Flt3 or Flt3L deficient mice, the argument for a common developmental lineage trajectory remains questionable^{46, 47}. BM progenitors, cultured in the presence of Flt3L develop into cDCs and pDCs, suggesting an instructive role for this cytokine. Generation of pDCs and cDCs results from the phosphorylation of signal transducer and activator of transcription 3 (STAT3) and phosphoinositide 3-kinase (PI3K) mediated activation of mammalian target of rapamycin (mTOR)^{48, 49}. Interestingly, it was shown that the synergistic interaction of Flt3L and Type I IFN induce the generation of pDCs from CLPs, hinting towards a lymphoid developmental pathway during inflammatory conditions⁵⁰.

Collectively, the question whether pDCs derive from lymphoid or myeloid progenitors has not been solved since their identification and characterization in 1958. Several groups showed that both, CLPs as well as CMPs have the potential to generate pDCs^{41, 42}. Corcoran et al proposed a developmental progression through a lymphoid pathway, since around 30% of splenic and thymic pDCs undergo D_H-J_H rearrangements, a process occurring early and exclusively during lymphoid development⁵¹. Additionally, Bendriss-Vermare et al and Res et al showed that pre-T cell receptor α (pT α) transcripts are present in human thymic pDCs^{52, 53}. The manifestation of classical B as well as T cell lymphoid lineage markers, therefore suggests a possible contribution of the lymphoid developmental pathway. Nevertheless, earlier studies showed that the induction of lymphoid transcriptional programs are not only restricted on CLP derived pDCs, but that also a small fraction of CMP derived pDCs exhibited rearrangements of the immunoglobulin heavy chain^{41, 42}. However, caution is needed as recent single cell technologies supported the evidence that, the so far identified progenitors, including CMPs, are a rather heterogeneous population⁵⁴. Olweus et al placed pDCs within the myeloid branch due to the pDC generation potential of CD34⁺ progenitors which express the granulomonocytic marker M-CSFR⁵⁵. Indeed, pDCs can be derived from M-CSFR⁺ CDPs, a myeloid progenitor that has the potential to differentiate to all DC subsets⁵⁶. Additionally, in the absence of its

ligand M-CSF, mice have impaired DC development, showing a 50-70% reduction of all DC subsets⁵⁷. However, a decrease was not only observed within the myeloid compartment, also lymphoid derived cells such as splenic B and T cells were reduced in M-CSF deficient mice. This might be explained by the fact that these mice are severely osteopetrotic and therefore have significantly reduced BM cavities which lead to disrupted BM niches⁵⁸. Nevertheless, the addition of M-CSF seems to support the development of pDCs *in vitro* and *in vivo* in the absence of FLT3L⁵⁹. Interestingly, progenitors with the highest potential to generate pDCs upon M-CSF stimulation were CLPs and not the myeloid progenitors CMPs nor GMPs, despite the absence of detectable surface M-CSFR expression⁵⁹. A recent study identified a pDC progenitor with clonogenic pDC developmental potential within a precursor population that lacks expression of myeloid M-CSFR and lymphoid markers IL-7R, defined as M-CSFR⁻CDPs⁶⁰. This progenitor population arises directly from Lymphoid-primed Multi Potent Progenitors (LMPPs)⁶⁰. A similar study identified the immediate BST2⁺CCR9⁻ pDC precursors within the mature compartment⁶¹, which led to the hypothesis that CCR9⁻ pDC precursors circulate and seed tissues before undergoing final maturation in pDCs⁶².

Lineage restricted reporters:

To better understand DC development, experiments were performed by several groups in which the relationship of a precursor cell and its progeny can be defined *in vivo*. The most common method uses the lineage restricted expression of the Cre recombinase which mediates the site-specific excision of loxP-flanked chromosomal DNA sequences⁶³. Mice expressing Cre under lineage specific promoter genes were crossed with mice, which have an inserted loxP-flanked STOP sequence followed by the Enhanced Yellow Fluorescent Protein gene (EYFP) in the ubiquitously expressed ROSA 26 locus (Rosa26^{LSL-EYFP})⁶⁴.

In order to study DC development several lineage specific Cre lines were generated and used: the myeloid specific M-CSFR Cre (Csf1r^{Cre})⁶⁵, the lymphoid specific IL-7R Cre (IL-7R^{Cre})⁶⁶ and hCD2 Cre (hCD2^{Cre})⁶⁷ or the DC specific CD11c Cre (Itgax^{Cre})⁶⁸, Zbtb46 Cre (Zbtb46^{Cre})⁶⁵ and Clec9a Cre (Clec9a^{Cre})⁶⁹ (Figure 3A). Labeling of precursor cells and its progeny by crossing these cre lines with Rosa26^{LSL-EYFP} allowed for more detailed characterizations of developmental trajectories.

Most known myeloid progenitors such as MDPs, cMoPs and CDPs are characterized by the expression of M-CSFR. Therefore, it is not surprising that Csf1r^{Cre} x Rosa26^{LSL-EYFP} mice show over 95% labelling of all myeloid cells such as the pre DCs, cDCs, red pulp

macrophages and monocytes⁶⁵. In addition, about 70% of pDCs are labelled, indicating and further supporting the original idea of a myeloid origin of the majority of pDCs. However, whether cre mediated deletion occurred in cell types other than myeloid cells, especially in the lymphoid lineage such as the CLPs or the mature compartment of B, T and NK cells, was not evaluated. Interestingly, two recent studies showed that not only myeloid cells express high levels of *Csf1r* transcripts, but also 50% to 70% of lymphoid derived T and B cells expressed during their development *Csf1r*, justifying a broader labeling capacity in the *Csf1r*-Cre lineage tracer mice and therefore not allowing for a clear answer about developmental origins of DC subsets^{70, 71}.

Interleukin-7 receptor (IL-7R) is the most crucial cytokine receptor driving lymphopoiesis *in vivo* and a key cell surface marker for discriminating lymphoid progenitors in the BM. An *Il-7R^{Cre}* mouse was generated in 2010 by Schlenner et al and used to characterize and trace lymphocyte development⁶⁶. The cre mediated deletion was evident in about 10% LMPPs and over 85% of CLPs, whereas myeloid CMP and GMP as well as erythroid MEP progenitors had infrequent labeling below 5%. As expected, the majority of splenic lymphocytes were irreversibly labeled in *Il-7R^{Cre}* x *Rosa26^{LSL-EYFP}* mice, with B-, T and NK cells being more than 95% EYFP positive. Myeloid cells, on the other hand, showed cre induced labelling of approximately 3% within Macrophages or neutrophils. Interestingly, the labeling efficiency within the DC compartment varied: while more than 85% of pDCs were EYFP positive, only 10% of cDCs were EYFP positive. Nevertheless, as correctly stated by the authors, no conclusion on lymphoid or nonlymphoid origins of pDCs can be drawn, since these high labeling frequencies likely result on IL-7R expression in mature pDCs⁶⁶. Another cre transgenic mouse which is acting specifically within the lymphoid lineage was characterized in 2003. De Boer et al generated a transgenic line that expressed iCre under the control of the *hCD2* promoter⁶⁷. The authors showed that Cre mediated recombination occurred only in T and B cells⁶⁷. Additional analysis of the *hCD2^{Cre}* x *Rosa26^{LSL-EYFP}* mice by Siegemund et al showed that all lymphoid cells, such as B, T and NK cells, and only a small fraction below 5% of myeloid cells such as Granulocytes and macrophages were labeled. Interestingly, all pDCs as well as 20% of the cDCs showed the recombination of the *LoxP* sites, indicating a lymphoid origin of the majority of pDCs and a small fraction of cDCs⁷².

Later studies aimed at specifically labelling all or some of the DC subsets to understand the relation among them and their lineage of origin. Transgenic mice in which the *CD11c* promoter drives the expression of EYFP were extensively studied and showed that more than 95% of splenic cDCs and around 86% of pDCs were labelled^{68, 73}. However, cre mediated

deletion was additionally observed in 100% alveolar macrophages, 70% splenic red pulp macrophages, 35% of marginal zone macrophages, 30% of blood monocytes and 20% peritoneal macrophages⁷³. The awareness that *Itgax*^{Cre} mice did not show the desired DC specificity, moved the scientific community to develop more specific Cre lines. The group of Nussenzweig generated a Cre line, in which an IRES Cre cassette was inserted into the 3' UTR of the endogenous cDC specific gene *Zbtb46*⁷⁴. *Zbtb46* is a transcription factor which appears to be exclusively expressed by cDCs, as shown by the group of Ken Murphy⁷⁵. Indeed, *Zbtb46*^{Cre} x *Rosa26*^{LSL-EYFP} mice show a more cDC specific deletion, in which about 65% of cDCs and less than 10% of pDCs, monocytes, red pulp macrophages, small intestine macrophages as well as B and T cell lymphocytes are labeled⁶⁵. Another cDC specific Cre line was generated in 2013 by Schraml et al⁶⁹. *Clec9a* expression is first detected on CDPs and maintained in mature cDC1 and pDCs but not in cDC2^{69, 76, 77}. The *Clec9a*^{Cre} line was generated by substituting the first two exons with a Cre cassette. *Clec9a*^{Cre} x *Rosa26*^{LSL-EYFP} mice show about 10% of labelling in CDPs, whereas mature DCs have distinct labelling resulting in 100% for cDC1, 50% for cDC2 and only 20% for pDCs⁶⁹. Other cells such as monocytes or macrophages remain unlabeled, indicating high DC specificity, even though cre mediated deletion was not observed evenly within the different DC subsets⁶⁹.

In 2016, Sawai et al described a genetic system in which cre mediated permanent labelling is induced in HSCs, thus allowing the assessment of precursors-progeny relationship in unperturbed animals. The authors created a transgenic mouse, which expresses a tamoxifen inducible Cre recombinase estrogen receptor fusion protein (CreER) under the control of the 5' truncated *Pdzk1ip1* BAC clone (*Pdzk1ip1*^{CreER})⁷⁸. *Pdzk1ip1*^{CreER} mice were crossed to *Rosa26*^{LSL-tdTomato} mice (*Pdzk1ip1*^{CreER} x *Rosa26*^{LSL-tdTomato}), and HSCs were permanently labelled upon tamoxifen injections. The labelled HSCs rapidly contributed to committed progenitors of all lineages, where about 25% and 20% of CDPs and CLPs, respectively were labelled after 11 weeks. Splenic cDCs and pDCs were replaced with a fast kinetic by a marked progeny reaching 20% of labelling after 11 weeks. Lymphoid derived showed a different degree of labelling depending of the subset. 10% of immature and about 5% mature B cells in the BM was labelled, while NK cells showed a labelling efficiency of about 18%, reaching comparable percentages as cDCs as well as pDCs⁷⁸. The different degree of labelling was therefore not conclusive in regard to the developmental history of pDCs, since both myeloid as well as lymphoid cells exhibited similar developmental kinetics.

Cellular Barcoding:

The biggest disadvantage in Cre mediated fate mapping experiments is the inability to trace the developmental relationship and plasticity of individual progenitors. Nowadays, this limitation can be circumvented by using “cellular barcoding”, a method in which different progenitors get tagged with semi-random, non-coding DNA sequences. Progenitors and their progeny can be marked either *in vitro* by transducing unique DNA barcodes into target progenitor cells or *in vivo* by Cre mediated excision of artificial DNA cassettes, thus allowing random and large combinatorial diversity⁷⁹. Shalin H. Naik et al developed in 2013 a barcoding assay, in which Lymphoid primed multi potent progenitors (LMPPs) were permanently marked with a library of heritable DNA barcodes and subsequently transferred into sub lethally irradiated hosts.⁸⁰ 14 days later the progeny was analyzed. Interestingly, around 50% of the LMPPs were classified as DC biased, whereas 10% of the progenitors contributed to either B or myeloid cells and only a small fraction of 3% showed multi lineage potential. The authors conclude that the broad developmental potential of LMPPs rather seems to rely on single cell heterogeneity which has imprinted lineage biases rather than single cell multipotentiality⁸⁰. Nevertheless, these barcoding experiments were only performed with LMPPs but not with other downstream progenitors such as the lymphoid or myeloid progenitors CLPs or CDPs, respectively. Therefore, no conclusion on lymphoid or nonlymphoid origins of pDCs can be drawn. Nevertheless, a recent study published by Dawn S. Lin et al combined cellular barcoding with high throughput methods to assess DC development in FLT3L cultures⁸¹. The authors cultured barcode labelled hematopoietic stem and progenitor cells (HSPCs) under FLT3L conditions and serially measured barcode signatures from different DC subsets. They visualized these multidimensional data using developmental interpolated t-distributed stochastic neighborhood embedding (DiSNE) time laps movies and were able to show that cDC and pDC development bifurcation already occurs early during hematopoiesis and does not go over a common progenitor such as CDP⁸¹. Helft et al and Lee et al additionally showed that early lineage and even DC subset imprinting on clonal basis takes place within individual human HSPCs^{82, 83} supporting the early developmental bifurcation of cDCs and pDCs which was suggested by Lin et al⁸¹.

In 2017 Pei et al performed cellular barcoding experiments by taking advantage of the Polylox mouse system. The polylox mice contains multiple barcoding elements composed out of ten LoxP sites in alternating orientations and spaced apart with unique 178 bp in the Rosa26 locus, thus allowing specific and unique tagging of single cells and their progeny upon Cre

mediated recombination⁷⁹. Most HSC clones gave rise to multilineage or oligolineage fates, arguing against early lineage priming of HSCs. Further, they confirmed the classical model of hematopoietic lineage specification by revealing a basic split between common lymphocyte development and common erythroid and myeloid development. Unfortunately, no information was provided by the authors on the developmental trajectories from HSCs to the DC lineages.

Transcription factors required during pDC development:

CDPs are thought to be the progenitor stage, at which the developmental bifurcation of cDC1, cDC2 and pDCs occurs. Molecularly, the divergence of pDCs from cDCs as well as the final maturation steps involve a number of different transcription factors, including Pu.1, Irf8, Ikaros, Bcl11a, Tcf4, Id2, Zeb2, SpiB and Runx2 (Figure 3B).

The transcription factor PU.1 plays an essential role in lymphoid as well as myeloid development by directly regulating the expression of Flt3⁸⁴. PU.1 deficiency results in dramatic perturbations of several immune cell subsets: granulocytes are expanded, while lymphoid as well as myeloid development is greatly impaired as a consequence of the loss of their corresponding progenitors^{85,86}. PU.1 was shown to bind to closed chromatin and prime enhancers by recruiting IRF8. This interaction results in histone H3-Lysin-27 acetylation (H3K27ac), resulting in an open conformation at enhancer elements and determining the induction of the myeloid transcriptional program that ultimately leads to the generation of monocytes and DCs^{87,88}. This hypothesis is further supported by a recent study, which showed skewing within the DC lineages, where pDC numbers are increased at the expense of cDCs, upon conditional ablation of PU.1 in CD11c expressing cells⁸⁹.

While PU.1 is supposed to act as a pioneer factor for multiple lineages, IRF8 can function as a transcriptional activator or repressor depending on the context and on its binding partners^{91,92,93,94}. Within the lymphoid branch, IRF8 was shown to play an intrinsic role in cell fate decision of pre-pro B cells. Binding of Irf8 and PU.1 at EICE (Ets-IRF composite elements) is key for the induction of the B cell specific transcription factor *Ebfl*⁹⁵. Within the myeloid branch, Irf8 deficiency results in disordered enhancer landscapes, which leads to impaired monocyte and cDC1 development while development and production of neutrophils is greatly enhanced in humans and mice^{96,97,98,99,100}. Interestingly, pDCs were shown to be absent in humans which have point mutations affecting the DNA binding domain of IRF8, an observation which was also described in Irf8 deficient mice in 2002 by Schiavoni et al^{101,102}, but revised in 2016 by Sichien et al¹⁰⁰. In the latter study, the group of Guilliams showed that

complete or late deletion of IRF8 had no impact on pDC development. Nevertheless, *Irf8* deficient pDCs were altered in their transcriptional signature, leading to a pDC with atypical surface marker expression and functional properties¹⁰⁰. Interestingly, IRF8 and IRF4 double deficient mice were completely devoid of pDCs, highlighting a possible compensatory role of IRF4 in IRF8 deficient mice^{100, 103}.

Another transcription factor important in early hematopoiesis is Ikaros (also known as *Ikzf1*). Ikaros is a zinc finger transcription factor which is essential for the development of several hematopoietic cell lineages^{104, 105, 106, 107, 108}. It acts mainly as a repressor by binding DNA as homodimer or heterodimer with other members of the Ikaros family, such as Helios, a transcription factor expressed in early hematopoietic progenitor, or Aiolos, a zinc finger protein being expressed in B and T cells^{109, 110, 111, 112}. Not much is known about the role of Ikaros during DC development. The expression of a dominant negative form results in complete abrogation of cDC development, while a null mutation in Ikaros specifically inhibits the development of cDC2 but not cDC1¹¹³. Allman et al showed in 2006 that splenic pDCs but not cDCs are greatly reduced in mice which have the hypomorphic mutation in the Ikaros locus (*Ikaros*^{L/L})¹¹⁴. Interestingly, *Ikaros*^{L/L} mice still generate an early pDC progenitor population in the BM that appears to be developmentally blocked. This population expresses genes, that are normally not present in WT pDCs but expressed on lymphocytes such as *Vpreb1*, *Lck*, *Tcrb-V13*, *Ptcr* and *Hes1*¹¹⁴. The same group also showed that Ikaros cooperates with Notch signaling, promoting pDC differentiation and cell fate decision by correctly regulating the expression of DC specific target genes and antagonizing TGF β signaling¹¹⁵. Additionally, a recent independent study on humans shows that a heterozygous mutation in *IKZF1* decreases pDC numbers and expands cDC1¹¹⁶. Further, it was shown that treatment with lenalidomide, a drug which induces proteasomal degradation of IKZF1, effectively reduces pDC numbers *in vivo*¹¹⁶.

Bcl11a encodes a Krüppel-like zinc finger transcription factor which is known to regulate early hematopoiesis. *Bcl11a* is essential for the development of B cells and thymocyte maturation¹¹⁷ and was also shown to silence the fetal hemoglobin locus in cooperation with the transcription factor SOX6 along the erythroid lineage^{118, 119}. The first publication assessing the role of *Bcl11a* in pDC development was published in 2013 by Wu et al. The authors showed, that *Bcl11a* in fetal progenitors is necessary for the expression of FLT3 and IL-7R and that fetal liver reconstituted wild type mice have severely reduced numbers of pDCs¹²⁰. Further, adult *Bcl11a* floxed mice crossed with the *Vav-icre* line (*Bcl11a*^{fl/fl} x *Vav*^{iCre}) had

severely decreased BM and splenic pDCs, confirming the requirement of Bcl11a for pDC development. Additionally, genome wide analysis of DNA binding revealed that Bcl11a regulates the expression of transcription factors important during DC specification such as the E protein transcription factor Tcf4, the inhibitor of DNA binding (Id) protein Id2 and the ETO family protein Mtg16 ¹²¹.

E proteins form homodimers or heterodimers with class II basic helix loop helix (bHLH) proteins, which function as transcriptional activators or repressors through the recruitment of distinct co-activator or repressor complexes. Four E protein transcription factors were identified in mice: TCFE2A and TCF3 (also known as E12 and E47), two isoforms generated by the *Tcf3* gene (also known as *E2a*), TCF12 (also known as HEB) and TCF4 (also known as E2-2) ¹²². Cisse et al and Nagasawa et al showed that pDC lineage specification and transcriptional regulation in mice and humans is mediated by Tcf4 ^{123, 124}, suggesting this transcription factor as the master regulator for pDCs development. Furthermore, they could show that continuous expression of TCF4 is essential for pDC maintenance, regulating a large proportion of pDC-specific genes ^{123, 124}. Constitutive deletion of *Tcf4* leads to an exclusive block of pDC development but not of other lineages, whereas deletion in mature pDCs has a severe impact on the identity of pDCs, inducing the loss of pDC associated markers, spontaneous dendrite formation, upregulation of MHC-II molecules and ultimately to an increased antigen presentation capacity ^{123, 125}. Despite the major advances in understanding the differentiation of the pDC, the transcriptional regulatory network that promotes the commitment and lineage determination is still not fully understood. E proteins were shown to heterodimerize with Id proteins, which express an HLH domain without the basic region, therefore preventing E proteins from binding to DNA ¹²⁶. Development into cDC1 depends on the expression of ID2, which was shown to specifically inhibit TCF4 and therefore pDC lineage commitment ^{125, 127}. Indeed, while Id2 deficient mice show a severe defect in cDC1 development, pDC numbers seem to be increased ¹²⁷. These studies support the hypothesis that the balance of ID2 and TCF4 at the CDP stage determines lineage specification towards these two lineages. In particular, it was shown by Grajakowska et al that the pDC specific long isoform of TCF4 (TCF4_L) in complex with the MTG16 induces transcription of pDC-related genes while repressing *Id2* and therefore cDC1 commitment ¹²⁸. However, the mechanism which controls the level of Tcf4, Id2 and Mtg16 at CDP stage and during pDC specification is still unclear and an active topic of investigation.

Zeb2 is a potential modulator which was recently described to be important in lymphoid as well as myeloid development. It belongs to the family of zinc-finger E-box-binding

transcription factors and plays an important role in cell fate decisions of melanocytes¹²⁹ and neuronal oligodendrocytes^{130, 131, 132}. Furthermore, during embryonic development it acts as a modulator of epithelial-to-mesenchymal-transition (EMT)^{133, 134}. Although its role in hematopoiesis is largely unknown, it was recently shown that Vav-iCre mediated deletion of Zeb2 led to neonatal lethality which was induced by intracerebral hemorrhages¹³⁵. Zeb2 deficient HSCs have altered adhesion and homing properties, display migratory defects and therefore impaired re-location of hematopoiesis from the fetal liver to BM cavities¹³⁵. Zeb2 was also shown to cooperate with T-bet and thus to promote terminal NK and CD8⁺ T cell maturation^{136, 137}, suggesting also for this TF, multiple actions depending on the cellular context. Deficiency within the hematopoietic compartment results in the expansion of neutrophils and loss of monocytes and of B cells^{138, 139}, suggesting to counteract the effects of IRF8. Recently, two studies showed the importance of Zeb2 also for DC development^{139, 140}. Deficiency in CD11c expressing cells results in decreased pDCs and cDC2 numbers, with an expansion of the cDC1 compartment. Overexpression of Zeb2 leads into slightly decreased cDC1 but unaltered cDC2 and pDCs numbers¹⁴⁰. Interestingly, Zeb2 deficiency is linked to increased Id2 levels in pDCs and cDC2. This led the authors to the interpretation that Zeb2 plays a key role in cDC1, pDC and cDC2 specification and commitment, in which it potentially represses the expression of Id2¹⁴⁰. Nevertheless, the function of Zeb2 in DC development is still a matter of investigation, as the unaltered pDC pool in Zeb2 transgenic mice cannot be explained by the suggested transcription factor network and is probably more complex than the hypothesized pDC–cDC1 dichotomy.

The two transcription factors Spi-B as well as Runx2 were shown to play an essential role during the late phase of pDC development Spi-B also belongs to the ETS family of transcription factors and shares with other members of the group a conserved ETS domain which mediates DNA binding¹⁴¹. In 2004, Schotte et al were able to prove the requirement of Spi-B during human pDC development. Knockdown of Spi-B strongly inhibited the potential of CD34⁺ progenitors to generate pDCs *in vitro* as well as *in vivo*, while enhanced the development of pro-B cells¹⁴². Furthermore, overexpression of Spi-B in hematopoietic CD34⁺ fetal liver stem cells enhanced pDC development, while inhibiting NK-, T- and B cell development¹⁴³. Nagasawa et al suggested in 2008 that cells overexpressing Spi-B had reduced levels of Id2, implying an inhibitory mechanism¹²⁴. However, all experiments performed were based on over-expression or knock-down assays, which might not reflect the physiologic conditions *in vivo*. Indeed, a less severe phenotype was observed in Spi-B knockout mice: only BM pDCs seem to be reduced, whereas splenic, LN and blood pDCs were increased,

suggesting a migratory rather than a developmental defect¹⁴⁴. Nevertheless, the absence of Spi-B, results in a functional impairment of pDCs, which display altered expression of pDC-specific markers, such as reduced expression of the anti-apoptotic BCL2-A as well as defects in TLR7 and TLR9 mediated Type I IFN production^{144, 145}.

Other transcription factors which were shown to play a central role within the hematopoietic system are the Runx genes. The Runx family consists of the three transcription factors Runx1, Runx2 and Runx3. These proteins are orthologues of the RUNT protein in *Drosophila melanogaster* and regulate the expression of target genes by forming heterodimers with the common subunit CBF β . While the repressor function of Runx1 and Runx3 was extensively studied in CD4-CD8 T cell lineage choices, only little is known about the role of Runx2 within the hematopoietic system¹⁴⁶. Runx2 was described as master regulator of bone development, where it acts primarily as activator, facilitating the generation of osteoblasts and therefore being indispensable for bone formation¹⁴⁷. Sawai et al reported in 2013 that Runx2 is specifically expressed in pDCs in a Tcf4 dependent manner, where it regulates the expression of Ccr5 allowing for pDC migration to the periphery¹⁴⁸. An additional study from 2016 further highlighted the essential role of Runx2 in the localization and function of pDCs¹⁴⁹. In this study Runx2 appears to be required for the downregulation of CXCR4, the BM homing chemokine receptor, and also essential to mount a robust anti-viral immune response¹⁴⁹.

Despite major advances in our understanding of gene network regulation, we still do not understand how hematopoietic lineage commitment and specification is achieved. Indeed, it becomes apparent that regulation at enhancer as well as at promoters defines the transcriptional landscape. However, more efforts are needed to fully grasp the key steps of such a dynamic process, where epigenetic regulatory cis- and transelements cooperate in defining the identity of a cell through its developmental origin.

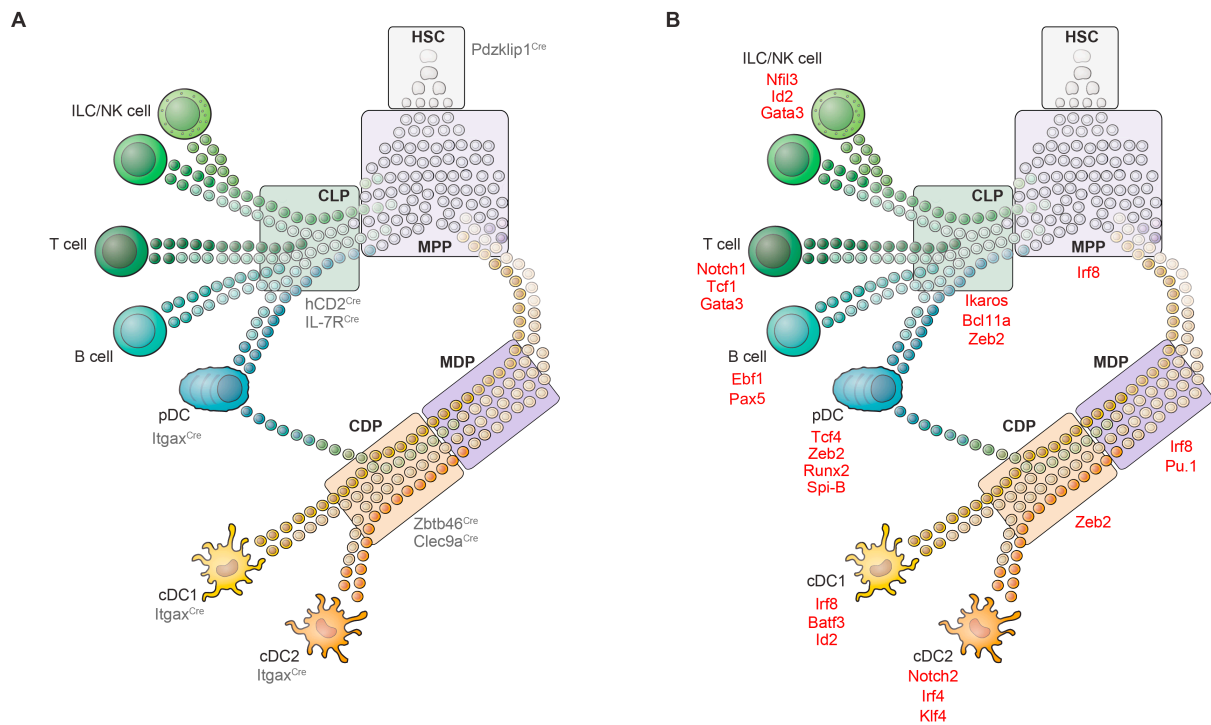


Figure 3: Essential Developmental stages and Transcription factors in lymphocyte and DC hematopoiesis. (A) Shown in dark gray are the different cre transgenic mouse lines and the specific developmental stages, in which the cre is active. (B) Indicated in red are the transcription factors required for the depicted cell populations. Abbreviations: Hematopoietic Stem Cell (HSC); Multipotent precursor (MPP); Common Lymphoid Progenitor (CLP); Natural Killer Cell (NK cell); Innate Lymphoid Cell (ILC); Common Myeloid Precursor (CMP); Myeloid and Erythroid Precursor (MEP); Granulocyte Macrophage Precursor (GMP); Macrophage and Dendritic Cell Precursor (MDP); common Monocyte Precursor (cMoP); Common Dendritic cell Precursor (CDP); conventional Dendritic cell (cDC) and plasmacytoid Dendritic Cell (pDC).

The function of pDCs:

Trafficking of pDCs:

DCs are key players of the immune system that operate at the boundary of innate and adaptive immunity. The migratory capacity of DCs was associated with tissue tolerance and the pathogenesis of a range of diseases. Initial studies demonstrate that the migratory pattern of pDCs differs from that of cDCs: final matured BM pDCs exit the BM via the bloodstream and migrate to secondary lymphoid organs such as the LNs by entering through the high endothelial venules (HEV) and not the afferent lymphatics, as it is the case for mature cDCs. The egression of pDCs from the BM is achieved by a tightly controlled process, in which the expressions of distinct chemokine receptor is regulated. While CXCR4 is involved in the retention of immature pDCs within the correct BM stromal niche¹⁴⁸, CCR2 and CCR5 are progressively being expressed during maturation, allowing the egression from the BM into the blood^{149, 150}. CCR2 was additionally shown to drive the recruitment of pDCs to skin regions

which were topically treated with imiquimod, a process which leads to apoptosis in keratinocytes and therefore to CCL2 production in mast cells¹⁵⁰. The migration of pDCs into the splenic white pulp is mediated by the co-expression of CXCR4 and CCR7¹⁵¹, whereas high CXCL12 gradients in tumor areas result in infiltrations of pDCs which express CXCR4¹⁵². Additional chemokine receptors were shown to drive pDC migration into different tissues: CXCR3 and CCR5 mediate the migration towards inflamed tissues^{153,154}, whereas CCR6 and CCR10, chemokine receptors expressed on human pDCs, induce the translocation towards inflamed tissues in response to CCL20 and CCL27¹⁵⁵. The recruitment of pDCs into the small intestine and the thymus are dependent on the expression of CCR9^{156,157}, whereas pDC migration into the colon seems to be CCR9 independent¹⁵⁸. Interestingly, the migration into the mucosal intraepithelial compartment is mediated by Mucosal addressin cell adhesion molecule 1 (MadCAM-1) and β 7 integrins¹⁵⁹. pDCs also express the receptors C3aR and C5aR, which allows them to sense the anaphylatoxins C3a and C5a and therefore to migrate into lesions of inflammatory skin diseases such as cutaneous lupus erythematosus and allergic contact dermatitis¹⁶⁰. The expression of Cx3cr1 was also described, however its role in pDC migration and homeostasis is unknown and still matter of investigation.

The role of TLR7 and TLR9 in viral sensing:

The recognition of viruses or self-nucleic acids in pDCs is mediated by Toll like receptor 7 (TLR-7) and TLR-9. Both are located in the endosomal compartment and induce the secretion of either Type I IFNs or pro-inflammatory cytokines, a process which is mediated by the myeloid differentiation primary response protein 88 (MyD88)-IRF7 or the MyD88-nuclear factor-kB (NF-kB) pathway, respectively^{161,162,163}. TLR7 was shown to recognize RNA viruses, endogenous RNA and synthetically produced oligoribonucleotides, whereas TLR9 senses DNA viruses containing unmethylated CpG-rich DNA regions, endogenous DNA as well as synthetic CpG oligodeoxyribonucleotides (ODN). Whether engagement of TLR7 and TLR9 results in the production of Type I IFNs or proinflammatory cytokines is dependent on the localization in which the interaction between the receptors and their corresponding ligands occurs. It was shown that multimeric CpG-A oligonucleotides preferentially aggregate in early endosomes, where they induce the secretion of Type I IFNs via the MyD88-IRF7 pathway¹⁶⁴. Monomeric CpG-B stimulation on the other hand leads to the activation of TLR9 in the endolysosomal compartment, a process which activates the MyD88-NF-kB pathway and therefore the upregulation of co-stimulatory molecules as well as the secretion of the pro-

inflammatory cytokines TNF α , IL-6 and IL12p40¹⁶⁴. The reason why CpG-A and CpG-B localize to different endosomal compartments is still matter of investigation. Studies suggest that the structural conformation of different CpGs determines their distinct localization. This theory was proposed after the observation that CpG-B complexed with the cationic lipid DOTAP (dioleoyloxytrimethylammoniumpropane) results in the localization of CpG-B within the early endosomal compartment in pDCs. This re-localization mediates the expression of Type I IFN production and not to the production of pro-inflammatory cytokines^{164, 165}. Nevertheless, further studies are required to fully understand the mechanisms that lead to the distribution of different ligands to distinct cellular endosomal compartments and therefore to the expression of Typ I IFNs or proinflammatory cytokines.

There are different theories on how pDCs are able to sense ongoing viral infections. An important mechanism of viral pathogen sensing is the direct recognition of viral particles. In this process pDCs get activated by directly internalizing replication deficient viruses, leading to endosomal TLR signaling^{20, 166, 167, 168}. Another mechanism is the antibody-Fc mediated stimulation of pDCs. Fc receptor Fc γ RIIA promotes the uptake of antibody coated viral or endogeneous nucleic acids which then induces TLR mediated secretion of IFNs in pDCs^{169, 170}. Nevertheless, the IRF7 mediated secretion of IFNs in pDCs makes them largely resistant to viral infections, suggesting that recognition of viruses occurs via mechanisms that are distinct from direct pDC infections^{167, 171}. This new paradox of viral sensing was introduced by several studies in which they used Vesicular stomatitis Virus (VSV) or the hepatocyte specific hepatitis C virus (HCV) as an infection model. Both studies showed that cells which are infected with these RNA viruses trigger a robust IFN response in pDCs, a process which requires an active viral replication and which is cell-cell contact as well as TLR-7 signaling dependent^{172, 173}. Additionally, it was shown that the release of exosomes containing HCV derived RNA by infected hepatocytes mediated the activation of pDCs¹⁷⁴, a mechanism which is also observed with other RNA viruses such as retroviruses^{175, 176}, lymphocytic choriomeningitis virus (LCMV)¹⁷⁷, Dengue and West Nile viruses¹⁷⁸, hepatitis-A virus¹⁷⁹ as well as Epstein Barr Virus (EBV)¹⁸⁰. Interestingly, TLR-9 mediated recognition of infected cells has only be described partially. In 2007 Megjugorac et al suggested that cells infected with the DNA Herpes simplex virus (HSV) secrete viral as well as cellular compartments, which mediate pDCs to produce IFNs¹⁸¹. Further, a more recent publication showed that type I IFN producing pDCs are localized in close proximity to MCMV infected cells. There, the recognition of primary infected cells was achieved by the formation of interferogenic synapses

between pDCs and infected cells. This interaction is established by LFA-1 mediated adhesion and is abrogated in experiments, where LFA-1 was blocked *in vitro*¹⁸² or genetically depleted *in vivo*¹⁸³.

The role of other innate immune sensors:

TLR7 and TLR9 are important viral innate immune sensors in pDCs, but also other pattern recognition receptors (PRR) were shown to play a role in pDC mediated immunity. Dasgupta et al showed in 2014 that pDCs exposed to Polysaccharide A (PSA), an immunomodulatory molecule expressed by the ubiquitous gut microorganism *Bacteroides fragilis*, increase costimulatory molecules and specifically mediate the secretion of IL-10 by CD4⁺ T cells. This process is triggered by TLR2 and was shown to protect against colitis¹⁸⁴. The role of TLR12 was described in 2013 by Koblanksky et al. It was shown that pDCs which recognize toxoplasma gondii profilin by TLR12 induce the secretion of IL-12 and Type I IFN which subsequently results in the activation of NK cells¹⁸⁵. Furthermore, TLR12 deficient mice were shown to be highly susceptible to T.gondii infections, which suggests an important role for pDCs in the induction of innate immune responses and host resistance¹⁸⁵.

Even though TLRs have been established as the main innate receptors involved in pDC activation, other cytosolic sensors were described to be important during immune responses. One group of cytosolic sensors was identified by mass spectrometry analysis, in which purified CpG binding proteins were purified and characterized¹⁸⁶. The authors were able to show that DExD/H-box helicase 36 (DHX36) and DHX9 in pDCs were acting as specific cytosolic sensors for CpG-A and CpG-B, respectively. While binding of CpG-A by DHX36 results in the nuclear translocation of IRF7 and Type I IFN secretion, interaction between CpG-B and DHX9 mediates the activation of the NF- κ B pathway and therefore the secretion of pro-inflammatory cytokines¹⁸⁶. Other major cytosolic sensors, such as cGMP-AMP synthetase (cGAS) and stimulator of IFN genes protein (STING) were also suggested to play a role during the responses to extrinsic or intrinsic derived DNA. Indeed, recent publications suggest that cytosolic DNA activates the cGAS-STING pathway in pDCs, thereby mediating the production of type I IFN independently of TLR9. Further, knockdown of STING resulted in reduced IFN expression, suggesting an important regulatory role of the cGAS-STING pathway in the recognition of cytosolic DNA^{187, 188, 189}. Nevertheless, further studies may provide a better understanding in the crosstalk between different cytosolic proteins and elucidate the molecular mechanisms that is induced during cytosolic mediated immune responses.

pDCs in health and disease:The regulation of type I IFN production:

The potential to produce high levels of type I IFNs is a key hallmark of pDCs. It was shown that IFN secretion by pDCs in response to viral infections seems to have beneficial effects for the host. Nevertheless, a variety of autoimmune diseases are characterized by a high type I IFN signature, which implicates that tightly regulated processes are required which prevent detrimental side effects caused by aberrant IFN production. Indeed, several mechanisms were characterized, which control the amplitude of type I IFN production. Mouse as well as human pDCs express surface receptors, which regulate the secretion of TLR7 or TLR9 mediated IFNs^{190,191}. The murine receptors SiglecH^{25,192}, BST2¹⁹³, Ly49Q¹⁹⁴, PDC-Trem¹⁹⁵, PIR-B¹⁹⁶ and EBI2¹⁹⁷, were shown to modulate the secretion of type I IFN, whereas human pDCs express the regulatory receptors BDCA2, ILT7, NKp44, CD300A and CD300C, DCIR, CD32, BST2 and LAIR1. Many of these receptors either contain intracellular tyrosine based inhibitory motifs (ITIM) or associate with adaptor proteins such as DAP12 or FcεRγ which then deliver signals via an intracellular tyrosine based activation motif (ITAM). Murine SiglecH as well as human BDCA2 and ILT7 inhibit the secretion of IFNs upon engagement with agonistic antibodies and signal through DAP12 or FcεRγ and the tyrosine kinase SYK.

Other mechanisms which were described to modulate the secretion of IFNs are the inhibitory posttranscriptional regulatory mechanisms, mediated by microRNAs as well as hormones. TLR7 and TLR9 induced downstream signaling results in the expression of miR-146a, a microRNA that suppresses NF-κB activation and TLR mediated signaling in pDCs¹⁹⁸. Further, it was shown that TLR7 stimulation induces the expression of miR-155 and its star form partner miR-155*. Both have opposing effects in Type I IFN production, in which miR-155* is induced shortly after TLR7 stimulation and enhances IFN expression by inhibiting IRAK3, whereas miR-155 induction occurs later where it inhibits IFN secretion by inhibiting TAB2 translation¹⁹⁹. Another microRNA which was shown to regulate the function and the survival of pDCs is mir-126: deficient mice for mir-126 show an impairment in pDC homeostasis and their capacity to respond to TLR ligands. This process is mediated by targeting the mTOR pathway and therefore regulating the expression of Tlr7, Tlr9 and Nfkb1²⁰⁰. Recently it was additionally shown that estrogen positively regulates the TLR-7 mediated response of pDCs *in vivo*. This might provide a possible explanation for the observation that pDCs from women produce more type I IFNs in response to HIV than pDCs from men²⁰¹.

The role of pDCs in antigen presentation:

The ability of pDCs to express MHC-class II and the co-stimulatory molecules CD80, CD86 and CD40 opens up the question about the antigen presentation potential of pDCs. Recent studies have proposed that pDCs can present antigens to CD4⁺ T cells, although not as efficient as cDCs^{202, 203}. In murine models, pDCs have mostly been studied for their potential on presenting antigens to CD4⁺ T cells, whereas human studies mostly focused on pDC antigen presentation to CD8⁺ T cells^{204, 205}. Recent studies showed that pDCs can prime the immune system into an activating or tolerogenic state, depending on the stimulation. Activation of pDCs through TLRs or other pattern recognition receptors induce an immunogenic immune response. On the other hand, unstimulated or alternatively activated conditions which induce the expression of indoleamine 2,3-dioxygenase (IDO)^{206, 207, 208, 209}, ICOSL²¹⁰, OX40L²¹¹, programmed cell death protein ligand 1 (PDL1)²¹² or granzyme B²¹³, rather promote a tolerogenic immune response to tumor cells, alloantigens and harmless antigens. Indeed, a CCR9⁺ pDC subset with immunosuppressive characteristics was described in 2008 by Hadeiba et al. The authors showed that these pDCs mediate the generation of regulatory T cells (T_{reg}) and are therefore able to inhibit an acute graft versus host driven immune response in allogeneic CD4⁺ donor T cell experiments²¹⁴. Further, CD8a⁺ pDCs were shown to suppress the development of airway hyper reactivity in a mouse model of lung inflammation by mediating the generation of T_{regs}²¹⁵. Nevertheless, to examine the antigen presentation potential of pDCs *in vivo*, several research groups generated pDC specific antibodies which were conjugating with antigens. A recent study used transgenic mice, in which human BDCA2 is specifically expressed on pDCs. They showed that targeting antigens to BDCA2 resulted in significant suppression of Ag-specific CD4⁺ T cells upon secondary exposure to Ag, a process that involved both the maintenance of T_{regs} and the decrease in effector CD4⁺ T cells²¹⁶. Further, treating mice with antibodies specific for SiglecH which were conjugated with myelin oligodendrocyte glycoprotein (MOG) results in a reduced expansion of Th1 and Th17 cells, subsequently leading to a delayed onset and decreased severity level of MOG-induced experimental autoimmune encephalomyelitis (EAE) disease²¹⁷. Additionally, OVA delivery through BST2 antibodies resulted in robust cellular and humoral immune responses and protected mice against OVA-encoding viruses as well as B16-OVA melanoma cells²¹⁸. Thus, antigen targeting to pDCs can either result in an activating or tolerogenic immune response which is antigen, stimulation as well as delivery dependent.

pDCs in acute vs chronic viral infections:

The *in vivo* role of pDCs during acute or chronic viral infections has since their discovery been surprisingly difficult to demonstrate. The powerful potential of pDCs to produce IFNs in response to nearly all enveloped viruses would suggest their indispensable role during antiviral immune responses. Nevertheless, the potent type I IFN secretion by pDCs in response to acute viral infections is usually limited in time and amplitude. The production of IFNs by pDCs in responses to viruses such as murine cytomegalovirus (MCMV), herpes simplex virus 1 (HSV1), VSV and LCMV is most evident during the early phase in systemic infections and leads to the suppression of viral replication. However, pDC derived IFNs become less important in the late onset of viral infections as other cells become more dominant producers of type I IFNs. Thus, pDCs are not strictly required for the *in vivo* control of such murine model viruses, since the multilayered nature of a viral immune response might compensate for the loss of one immune subset. For instance, cDCs were able to compensate for the absence of pDCs in infections with ectromelia virus or MCMV. Further, alveolar macrophages were shown to be the primary source of type I IFNs during pulmonary infections with Newcastle disease virus (NDV), but when depleted, pDCs take over and become the major source of Type I IFNs²¹⁹. A strict requirement of pDC-derived type I IFNs was only observed in mouse hepatitis virus (MHV) and HSV2 infections. MHV infection is normally controlled in a TLR7 and IFNAR dependent manner and induces a fast and massive production of Type I IFNs in pDCs which is required to sustain the survival of cDCs and Macrophages^{220, 221}. In systemic HSV infections, NK cell activation and survival are mediated by pDC produced Type I IFNs which results in reduced morbidity as well as mortality²²². Further, mouse models in which pDCs were inducibly (BDCA2-DTR mice) or constitutively (Tcf4^{fl/fl} mice) depleted revealed the importance of pDCs in viral infections such as MCMV or LCMV^{223, 224}. pDC depleted mice which were infected with VSV revealed an increased viral burden and impaired survival and accumulation of virus specific cytotoxic T cells²²³. Further, recent publication in human showed that IRF7 deficiency causes a severe defect in pDC function and this resulted in higher susceptibility to influenza virus²²⁵. Additionally, mouse models in which IRF7 signaling is restricted to pDCs showed that IRF7 signaling in pDCs controls both Dengue as well as Chikungunya acute viral infection by amplifying downstream antiviral responses²²⁶. Overall, the impact of pDCs in acute viral infections might depend on several factors such as the infecting virus, the route of infection as well as the genetic background.

Even though the complexity of chronic viral immune responses is still elusive and matter of investigation, an enormous effort was made in the last decade to elucidate and clarify the functional role of pDCs in chronic HIV infections. Recent papers suggest that HIV infections in pDCs mediate the dysregulation of several pDC functions such as cytokine as well as Type I IFN production, migration patterns as well as T cell stimulation potential. HIV induces pDC activation by stimulating TLR7 signaling but can also directly infect pDCs by targeting the cell surface receptors CD4, CXCR4 and CCR5. Patients infected with HIV revealed reduced numbers of pDCs in the blood, which is promoted by the migration to peripheral LNs²²⁷. Further, migratory patterns towards the gut mucosa are observed in simian immunodeficiency virus (SIV) and HIV infections, which correlate with the upregulation of the gut homing molecules $\alpha 4\beta 7$ and CD103 on pDCs^{227, 228} but not with the viral load²²⁹. Whether pDCs contribute to the chronicity of HIV is still not clear. It is known that HIV stimulated pDCs persistently produce Type I IFNs and express low levels of maturation molecules, therefore mediating a low T cell response²³⁰. Furthermore, later stages of chronic viral infections result in pDC exhaustion, which is mediated by impaired development, enhanced self-renewal in the periphery and persistent signaling through TLR7²³¹. Additionally, HIV infected pDCs were shown to promote the expression of IDO, an enzyme which induces the generation of T_{reg} cells²³². Whether pDCs contribute to a beneficial or detrimental outcome in chronic viral infections, might also depend on the time point of their actions. While early administration of IFN $\alpha 2$ in mice infected with SIV increases the expression of Interferon stimulated genes (ISG) and therefore prevents systemic infection, sustained administration of IFN $\alpha 2$ results in type I IFN desensitization, decreased antiviral gene expression, increased viral load and accelerated CD4⁺ T cell loss²³³. Additionally, mice infected with chronic LCMV which are devoid of pDCs or lack the ability to signal through TLR7 and TLR9 have a defect in T cell priming as well as viral clearance^{224, 234}. This dysfunctional T cell priming may be mediated at least partially through the interaction of pDCs with cDCs²³⁵, in particularly the recruitment of cDC1 that induce the activation of cytotoxic CD8⁺ T cells²³⁶. Further, early administration of Type I IFN prevented chronic LCMV infections, whereas late treatment had no beneficial effects²³⁷. Moreover, inhibition of Type I IFN signaling in chronic LCMV infections resulted in improved T cell functions as well as reduced viral loads^{238, 239}.

pDCs in autoimmunity:

The potentially important role of pDCs in autoimmunity was proposed in numerous publications, since a variety of autoimmune diseases are characterized by an elevated type I IFN signature. Several studies proposed that pDCs might be involved in autoreactive immune responses which lead to diseases such as systemic lupus erythematosus (SLE), psoriasis as well as type 1 diabetes (T1D). SLE is characterized by the production of antinuclear antibodies which are able to complex with endogenous nucleic acids. These immune complexes are internalized into the endosome by pDCs via the Fc receptor CD32, where they induce the secretion of Type I IFN by activating TLR7 and TLR9^{169, 170, 240}. This process might further be enhanced by the release of neutrophil extracellular traps (NETs), a process in which neutrophils secrete TLR9 inducing molecules such as chromatin DNA, the antimicrobial peptide LL-37 (also known as CAMP) and HMGB1^{241, 242}. Nevertheless, SLE prone Mrl.Fas^{lpr} mice showed markedly exacerbated lupus when crossed with mice which are not able to secrete NETs (NOX2 deficient mice), suggesting that endogenous nucleic acids might derive from other sources, such as necroptotic or pyroptotic cells or NADPH-independent released mitochondrial DNA²⁴³. Studies confirmed that sustained activation and secretion of Type I IFNs in pDCs contribute to the pathogenesis of SLE. The BXSB lupus prone strain which develops spontaneous autoimmunity, reduces disease severity and extends survival upon early Type I IFN signaling blockade²⁴⁴. Similar results were obtained in Mrl.Fas^{lpr} mice: disruption of Type I IFN results in therapeutic benefits, however does not affect mortality. Further, it was shown that autoimmune skin inflammation which is induced by tape stripping is reduced in lupus prone NZB x NZW F1 mice after antibody mediated pDC depletion or TLR7 and TLR9 blockade²⁴⁵. The *in vivo* role of pDCs in SLE was further specifically addressed in several genetically modified mice. Deletion of IRF8 in NZB mice and a mutation on Slc15a4 in C57BL/6.Fas^{lpr} mice resulted in reduced autoantibody production and overall weaker disease manifestation²⁴⁶. Additionally, characterization of Mrl.Fas^{lpr} mice which lack MyD88 showed that pDCs contribute to SLE pathogenesis, in particular to B lymphopenia but not glomerulonephritis²⁴⁷. The use of mouse models in which pDCs were transiently or constitutively depleted, further confirmed the pathogenic role of pDCs in SLE. Global or CD11c Cre induced Tcf4 deletion in lupus prone mice abolished autoantibody generation as well as glomerulonephritis²⁴⁷. On the other hand, transient depletion of pDCs in BXSB mice resulted in a reduced Type I IFN signature in tissues and abolished activation and expansion of B and T cells, which lead to a reduced production of anti-nuclear antibodies²⁴⁸.

The chronic activation of pDCs and the subsequent production of IFNs and inflammatory cytokines seem to be contributing factors for other autoimmune diseases such as psoriasis as well as T1D. Patients suffering from psoriasis have high pDC infiltrates in early skin lesions, where self-nucleic acids aggregate with anti-microbial peptides and activate pDCs through TLR7 and TLR9^{249, 250, 251}. It was shown that by blocking the secretion of Type I IFN or inducing antibody mediated depletion of pDCs in xenograft psoriasis models resulted in reduced skin lesion formations²⁵². Interestingly, treatment of human and mouse pDCs with the vitamin D analogue calcipotriol resulted in an impaired capacity of pDCs to mediate the activation and differentiation of effector T cells²⁵³. Nevertheless, genetic depletion of pDCs revealed only a negligible role of pDCs in a genetic model of psoriasis²⁵⁴ and no importance at all in chemically induced psoriasis²⁵⁵. The role of pDCs in T1D was suggested, as increased numbers of pDCs in pancreatic islets were observed during the onset of human disease as well in non-obese diabetes (NOD) mouse models^{256, 257}. In NOD mice, secretion of DNA reactive antibodies by B1a cells mediates the release of LL-37 from neutrophils, which subsequently binds to self DNA²⁵⁷. This promotes the generation of DNA/antibody complexes which in turn activate pDCs through TLR9. Indeed, genetic depletion of pDCs in NOD models results in ameliorated insulinitis and decreased incidence of diabetes confirming the pathogenic role of pDCs in NOD induced diabetes²⁵⁸.

pDCs in cancer:

pDCs are regularly found in a wide variety of tumors including tissue carcinomas, melanomas and other hematopoietic malignancies and thought to mediate the interaction between the innate and the adaptive immunity. Tumor infiltrating pDCs in breast and ovarian cancers are associated with a poor prognosis: they were characterized to be poor Type I IFN producers and rather mediate a tolerogenic immune response by inducing T_{reg} differentiation^{259, 260, 261}. The mechanism which lead to the impaired Type I IFN production and the immunosuppressive immune response is dependent on the secretion of transforming growth factor- β (TGF β) and tumor necrosis factor- α (TNF α)²⁶¹. Indeed, genetic pDC depletion models confirm the role of TGF β and the tumor-promoting properties of pDCs²⁶². Nevertheless, pDCs were also shown to contribute to antitumor immunogenic responses. Administration of activated pDCs into melanoma patients lead to desired CD4⁺ and CD8⁺ T cell responses²⁶³. Further, intertumoral injections of TLR7 ligands in murine mammary tumor models resulted in the activation of tumor associated pDCs and therefore to an antitumor

immune response²⁶⁴. Additionally, TLR activated pDCs were shown to induce tumor killing by expressing TRAIL and granzyme B and activate NK cells in the B16 melanoma mouse model^{150, 265}. Overall, pDCs were shown to contribute to both, tumor progression as well as antitumor immune responses. However, the molecular mechanism which determines the pDC fate in tumor environment remains to be fully elucidated and represents an important challenge for the future.

Heterogeneity of pDCs:

The variety of functions ascribed to pDCs suggests two possible scenarios: either different environmental cues mediate responses within the same cell or a heterogeneous pool of mature pDC subsets performs specifically the described functions during an immune response. Bar-On et al characterized a DC subset, which exhibits a unique pDC gene signature but expresses surface markers reminiscent of the cDC lineage²⁶⁶. This CX3CR1⁺ CD8a⁺ DC subset is functionally not able to produce Type I IFNs but is highly dependent on the expression of the key pDC transcription factor TCF4²⁶⁶. A more recent publication further described a CD2^{hi}CD5⁺CD81⁺ pDC subset, which expresses classical pDC markers but does not have the potential to produce Type I IFN upon CpG stimulation²⁶⁷. Furthermore, the authors showed that this subset is a potent stimulator in B cell activation and antibody production and a strong inducer of T cell proliferation and T_{reg} formation²⁶⁷. Additionally, recent single cell RNA seq analysis on human peripheral blood mononuclear cells (PBMCs) revealed a new DC subset that shares common markers with pDCs such as IL3R, BDCA2 and BDCA4^{268, 269, 270}. However, there were some phenotypical as well as functional differences described. In contrary to conventional pDCs, non-canonical pDCs express the cell surface markers AXL, SIGLEC6, CD33 and CX3CR1, do not produce Type I IFNs upon CpG stimulation and potently activate T cells^{268, 269, 270}. The fact that non-canonical pDCs express markers which were used in earlier studies to assess the function of conventional pDCs urges us to reconsider some obtained results and therefore different aspects of pDC biology. Some functional observations might be attributed to the contamination of undetected non-canonical pDCs within the conventional pDC gate, and therefore possibly explaining the controversial results obtained from different studies.

Aim of the project:

Most characterized hematopoietic progenitors are composed of heterogeneous subsets, which contribute to the development of specific blood cells. The origin of pDCs, for instance, has long been controversial and exclusively committed progenitors to this lineage have never been described. The aim of this project is to characterize the developmental stages in which pDC commitment occurs and to further identify a committed progenitor with exclusive pDC potential. Besides, we aim to understand the transcriptional program which regulates pDC lineage specification and that subsequently induces pDC lineage commitment.

Results:

Distinct progenitor lineages contribute to the heterogeneity of plasmacytoid dendritic cells

Patrick Rodrigues Fernandes¹, Lucia Alberti-Servera^{1,2}, Anna Eremin¹, Gary E. Grajales-Reyes³, Robert Ivanek^{1,4}, Roxane Tussiwand^{1*}

¹Department of Biomedicine, University of Basel, 4058 Basel, Switzerland, ²Department of Human Genetics and VIB Center for the Biology of Disease, Leuven, Belgium, ³Department of Pathology and Immunology, Washington University School of Medicine, St. Louis, MO 63110, USA, ⁴Swiss Institute of Bioinformatics, 4058 Basel, Switzerland

July 2018 – Nature Immunology

Distinct progenitor lineages contribute to the heterogeneity of plasmacytoid dendritic cells

Patrick Fernandes Rodrigues¹, Lluïcia Alberti-Servera^{1,2}, Anna Eremin¹, Gary E. Grajales-Reyes³, Robert Ivanek^{1,4} and Roxane Tussiwand^{1*}

Plasmacytoid dendritic cells (pDCs) are an immune subset devoted to the production of high amounts of type 1 interferons in response to viral infections. Whereas conventional dendritic cells (cDCs) originate mostly from a common dendritic cell progenitor (CDP), pDCs have been shown to develop from both CDPs and common lymphoid progenitors. Here, we found that pDCs developed predominantly from IL-7R⁺ lymphoid progenitor cells. Expression of SiglecH and Ly6D defined pDC lineage commitment along the lymphoid branch. Transcriptional characterization of SiglecH⁺Ly6D⁺ precursors indicated that pDC development requires high expression of the transcription factor IRF8, whereas pDC identity relies on TCF4. RNA sequencing of IL-7R⁺ lymphoid and CDP-derived pDCs mirrored the heterogeneity of mature pDCs observed in single-cell analysis. Both mature pDC subsets are able to secrete type 1 interferons, but only myeloid-derived pDCs share with cDCs their ability to process and present antigen.

Dendritic cells (DCs) are a specialized immune subset dedicated to sensing pathogens and inducing the appropriate immune response¹. Under steady-state conditions, DCs can be subdivided into cDCs and pDCs^{2–5}. cDCs are specialized in antigen uptake and presentation to naïve T cells and can be further subdivided into cDC1 and cDC2, expressing the transcription factors IRF8 and IRF4, respectively^{6–8}. pDCs are a distinct lineage dedicated to the production of high amounts of type 1 interferons in response to viral infections^{9–11}. Development of DCs occurs in the bone marrow (BM) and requires a complex transcriptional network, in which progressive lineage specification gradually and hierarchically limits and excludes alternative fates^{4,8}. A CDP able to give rise to both cDCs and pDCs has been described in the BM^{12,13}. Furthermore, cDCs and pDCs share not only their dependency on the cytokine FLT3L but also the expression of several transcription factors, thus suggesting common regulatory networks^{14–16}.

Immediate precursors with exclusive differentiation potential have been identified for both cDC subsets¹⁷. Although the molecular mechanism defining cDC1 lineage specification has been dissected¹⁷, cDC2 commitment is still unclear⁴. Multiple pathways appear to converge into a phenotypically homogenous but transcriptionally heterogeneous cDC2 lineage^{4,5,18,19}. In addition, pDC development seems to be ‘promiscuous’, because both CDPs and common lymphoid progenitors can give rise to pDCs^{13,16,20,21}. Two distinct pDC progenitors have been characterized^{22,23}. Within the BM, CCR9⁺MHC-II^b pDCs have been characterized as the immediate precursors of CCR9⁺ mature pDCs^{22,23}, although these pDC precursors already express mature markers and appear functional. pDCs have also been reported to arise mostly from CD135⁺CD115[−]CD127[−] precursor cells. Despite their greater pDC potential than CDPs, these progenitors maintain the ability to generate cDCs, thus suggesting that they are either heterogeneous or still uncommitted in nature^{22–24}.

Molecularly, pDC development and identity depend on the expression of the transcription factor TCF4 (also referred to as

E2-2)^{25,26}. TCF4 deficiency is prenatally lethal, and haploinsufficiency in humans results in Pitt–Hopkins syndrome, which is characterized by impaired pDC development, thus indicating a conserved requirement of TCF4 across species²⁵. Whereas commitment to pDCs is regulated by the expression of TCF4, development into cDC1 depends on the expression of the transcriptional repressor ID2, which specifically inhibits TCF4 and therefore pDC lineage commitment²⁶. The branching of these two DC subsets at the CDP stage is determined by the balance of ID2 and TCF4. In particular, the long isoform of TCF4 (TCF4_l) in complex with the transcription factor CBFA2T3 (also referred to as MTG16) induces pDC-target genes while repressing *Id2* and therefore cDC1 commitment^{27,28}. The zinc-finger transcription factor ZEB2 has also been shown to be involved in the regulation of early DC development^{29,30}. Zeb2 deficiency results in decreases in pDCs and cDC2, and in an increase of cDC1, whereas its overexpression leads to slightly decreased cDC1 and unaltered numbers of cDC2 and pDCs²⁹. According to these observations, and the elevated expression of *Id2* observed in *Zeb2*^{−/−} mice²⁹, ZEB2 has been suggested to potentially repress *Id2*, which is required for cDC1 commitment. However, the unaltered pDC pool in *Itgax-cre* × *R26-Zeb2*^{fl/fl} mouse progeny indicates that an active lineage commitment involving a more complex, TCF4-dependent transcriptional network that goes beyond the previously supposed cDC1–pDC dichotomy is required during pDC development. Furthermore, these results may also suggest a dual origin of pDCs, in which the requirement for TCF4 and ZEB2 is lineage and stage specific. The complete absence of pDCs in the progeny of *Zeb2*^{fl/fl} crossed to *Mx1-cre*³⁰ mice, and their partial decrease in *Itgax-cre*²⁹, supports either a CDP-independent origin of pDCs or an incomplete deletion of *Zeb2* in CDPs.

A prerequisite for determining the molecular mechanisms involved in lineage specification is to define the developmental stage at which pDC commitment occurs and to identify the pDC-committed precursor (pre-pDC) with exclusive lineage potential. Given the complexity of the transcriptional interactions occurring

¹Department of Biomedicine, University of Basel, Basel, Switzerland. ²Department of Human Genetics and VIB Center for the Biology of Disease, Leuven, Belgium. ³Department of Pathology and Immunology, Washington University School of Medicine, St. Louis, MO, USA. ⁴Swiss Institute of Bioinformatics, Basel, Switzerland. *e-mail: r.tussiwand@unibas.ch

at different stages during pDC and cDC commitment and the possible developmental convergence from lymphoid and myeloid lineages into a single phenotypically consistent population, we decided to perform an in-depth exploration of the paths leading to pDC differentiation. Here, we found that pDCs developed mostly from IL-7R⁺ lymphoid precursor cells (IL-7R⁺ LPs) and identified a bona fide committed pre-pDC with exclusive lineage potential within the IL-7R-expressing pool. In addition, we characterized the transcriptional landscape of pDC development from IL-7R⁺ LPs to mature pDCs. Transcriptionally, the pre-pDC precursors identified here showed high expression of IRF8 before the acquisition of pDC identity and functionality, which was gained only after the expression of TCF4. Finally, we showed, through single-cell analysis, that despite developmental convergence to a phenotypically similar population, lymphoid- and myeloid-derived mature pDCs are transcriptionally and functionally heterogeneous.

Results

pDCs develop primarily from IL-7R⁺ LPs. Both CDPs and common lymphoid progenitors are able to generate pDCs in vitro, but the independent contributions of these two subsets to the mature pDC pool in vivo are unclear^{12,13,16,21}. All DCs, including cDCs and pDCs, originate from Lin⁺B220⁺Ly6C⁺CD117^{int/lo}CD135⁺ hematopoietic progenitor cells. Within this subset, the expression of CD115 (CSF1R) and CD127 (IL-7R) allowed for the identification of three populations: CD115⁺CD127⁻ cells (CDPs hereafter), CD115⁺CD127⁺ cells (IL-7R⁺ LPs hereafter) and CD115⁻CD127⁺ cells (CSF1R-IL-7R⁻ NPs hereafter) (Fig. 1a). The frequency and abundance of CDPs and IL-7R⁺ LPs were similar in the BM of wild-type mice under steady-state conditions (Fig. 1b). To understand the cDC and pDC potential of each BM progenitor subset, we cultured them in the presence of FLT3L and assessed the development of CD45RA⁺CD317⁺ pDCs, CD11c⁺MHC-II^{hi} cDCs, CD11c⁺MHC-II^{hi}CD11b⁺ cDC2 and CD11c⁺MHC-II^{hi} CD24⁺cDC1, unless otherwise specified. IL-7R⁺ LPs generated approximately fivefold more pDCs than did CDPs, which predominantly gave rise to cDCs, and more than threefold more pDCs than did CSF1R-IL-7R⁻ NPs (Fig. 1c,d and Supplementary Fig. 1b). Because IL-7R⁺ LPs represent approximately 0.12% of total BM cells and include approximately 0.04% Sca1⁺ common lymphoid progenitors³¹, which are progenitors of B cells, we assessed the ability of CDPs, IL-7R⁺ LPs and CSF1R-IL-7R⁻ NPs to develop into CD19⁺ B cells by culturing them under B cell-polarizing conditions in the presence of FLT3L and OP9 stromal cells (Methods). Only IL-7R⁺ LPs developed into CD19⁺ B cells and remained the most efficient population at generating pDCs under these B cell-permissive conditions (Supplementary Fig. 1a,c).

To examine the pDC, cDC and B cell potential of these progenitor subsets under competitive conditions, we isolated IL-7R⁺ LPs from the BM of CD45.2 mice and cocultured them with CDPs or CSF1R-IL-7R⁻ NPs from CD45.1 congenic mice (Supplementary Fig. 1i). Regardless of the presence or absence of stromal cells, IL-7R⁺ LPs had significantly greater pDC potential than did CDPs or CSF1R-IL-7R⁻ NPs at all analyzed time points (Fig. 1e,f and Supplementary Fig. 1g) and were the only progenitors able to differentiate into CD19⁺ B cells (Supplementary Fig. 1f,h). To exclude differential proliferative capacity and the possibility that these progenitor subsets might be distinct developmental stages of one another, we performed a time-course analysis (Fig. 1g). The total cell output from CDPs and IL-7R⁺ LPs was comparable and peaked at day 4. However, IL-7R⁺ LP-derived pDCs outnumbered those derived from CDPs at every time point (Supplementary Fig. 1d). In contrast, cDCs were mostly CDP derived (Fig. 1g and Supplementary Fig. 1e). After day 4 of culture, the total cellular output from CDPs was higher than that of IL-7R⁺ LPs (Fig. 1g), thus suggesting that the ability of IL-7R⁺ LPs to generate progeny decreased, that the

IL-7R⁺ LP-derived cells had diminished survival ability in vitro, or a combination of both. To discriminate among these possibilities, we performed the same experiment, using the proliferation tracer CellTrace Violet. We detected no major differences in the proliferation rates of CDP- or IL-7R⁺ LP-derived cells (data not shown), thus suggesting that in vitro-generated pDCs have lower survival ability than in vitro-generated cDCs, independently of their origin, in line with previous reports³².

To assess the pDC, cDC and B cell in vivo potential of these progenitors, we co-transferred IL-7R⁺ LPs isolated from BM in a 1:1 ratio with congenic CSF1R-IL-7R⁻ NPs (Fig. 1h,i) or CDPs (Fig. 1j,k and Supplementary Fig. 1l) into sublethally irradiated mice and analyzed the BM and spleen of the recipient mice by flow cytometry 4 d after transfer (Fig. 1h-k). IL-7R⁺ LPs generated a 5- to 15-fold-higher output of SiglecH⁺CD317⁺ pDCs than CSF1R-IL-7R⁻ NPs or CDPs in both tissues (Fig. 1h-k). Donor-derived CD19⁺ B cells were detected only in the BM and were exclusively IL-7R⁺ LP derived (Fig. 1k and Supplementary Fig. 1l), whereas cDCs, which were recovered only in the spleen, were 80% CDP derived (Fig. 1k and Supplementary Fig. 1l). Early uncommitted Lin⁻c-kit^{hi} BM progenitors, when co-injected, had equal potential to generate SiglecH⁺CD317⁺ BM and splenic pDCs, thus suggesting that both congenic strains had equal pDC reconstitution potential (Supplementary Fig. 1j-k). Collectively, mature BM and splenic pDCs differentiate in vitro and in vivo predominantly from IL-7R-expressing BM progenitors and not from CDPs or CSF1R-IL-7R⁻ NPs.

SiglecH⁺Ly6D⁺ IL-7R⁺ LPs have exclusive pDC potential. We then further investigated the pDC and B cell potential within the IL-7R⁺ LPs. Staining for SiglecH and Ly6D allowed us to subdivide IL-7R⁺ LPs into three fractions with relatively equal distribution: SiglecH⁻Ly6D⁻ (double negative, DN), SiglecH⁻Ly6D⁺ (single positive, SP) and SiglecH⁺Ly6D⁺ (double positive, DP) (Fig. 2a and Supplementary Fig. 2a). All three subsets showed a high differentiation potential into CD317⁺CD45RA⁺ pDCs that increased from DN to SP to DP (Fig. 2b). Furthermore, DP cells had almost exclusive pDC lineage potential, showing a pDC commitment of more than 90% (Fig. 2b). To understand the developmental relationship among DN, SP and DP progenitors, we sorted and performed a time-course analysis examining the pDC output over 7 d of culture. All three subsets had a similar total output of mature pDCs (Fig. 2c). However, DP progenitors developed into mature pDCs faster, peaking at day 3 (Fig. 2c), thus suggesting that DP progenitors may be a more mature subset. In vitro, the pDC developmental ability of DP progenitors was also largely superior to those of CDPs and the previously reported pDC precursors CSF1R-IL-7R⁻ NPs²³ and CD11c⁺CD317⁺CCR9⁻ cells (CCR9⁻ progenitors hereafter)^{22,24} (Supplementary Fig. 2b-d). The percentage of CD317⁺CD45RA⁻ non-pDCs that developed in FLT3L-treated cultures in vitro was approximately 40% for DN cells and 30% for SP cells, and was limited to approximately 5% for DP progenitors (Fig. 2b and Supplementary Fig. 2e). Most of these CD317⁺CD45RA⁻ cells expressed cDC markers such as CD172, CD11b, CD24 and MHC-II. In comparison, CDPs generated approximately 50% cDC1 and 35% cDC2, and showed a pDC output of approximately 15% (Fig. 2d and Supplementary Fig. 2c-e). When we exposed DN, SP and DP cells, CSF1R-IL-7R⁻ NPs, CCR9⁻ progenitors and CDPs to B cell-polarizing conditions (FLT3L and OP9 stromal cells; Supplementary Fig. 2f-j), CSF1R-IL-7R⁻ NPs, CCR9⁻ progenitors and CDPs had no CD19⁺ B cell potential, IL-7R⁺ LPs and SP had CD19⁺ B cell potential, and DP progenitors were unable to develop into CD19⁺ B cells and maintained a high pDC output (Fig. 2d-e and Supplementary Fig. 2f,g,i). SiglecH⁺Ly6D⁺IL-7R⁺ LPs are committed to the pDC lineage: they showed almost exclusive pDC potential in the presence of FLT3L and had no ability to differentiate into B cells when

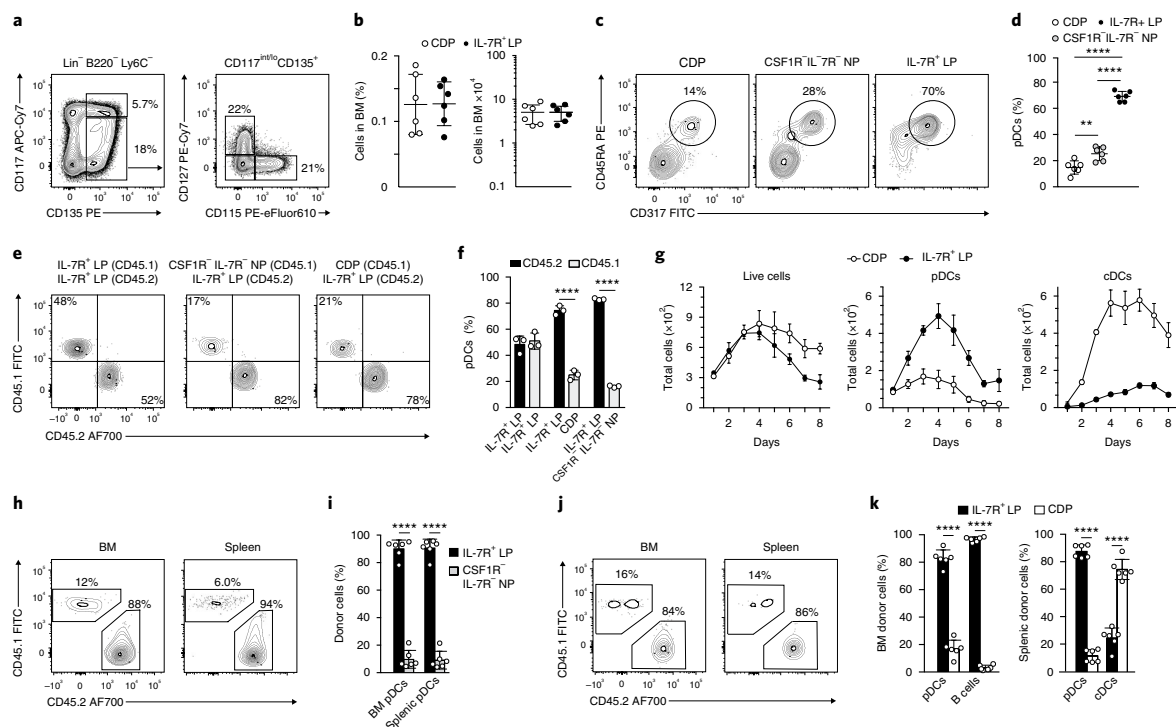


Fig. 1 | pDCs develop primarily from IL-7R⁺ lymphoid progenitors. **a, b**, All subsets are pregated on Lin⁺B220⁺Ly6C⁻CD117^{int/lo}CD135⁺. Shown are the gating strategy (**a**) of CDPs (CD115⁺CD127⁻), IL-7R⁻M-CSFR⁻ NPs (CD115⁺CD127⁻) and IL-7R⁺ LPs (CD115⁺CD127⁺), and the frequency (**b**) of the indicated progenitors in the BM of C57BL/6 mice ($n=6$; each dot represents a mouse, and thin lines represent the mean \pm s.d.). **c, d**, Sort-purified CDPs, IL-7R⁻M-CSFR⁻ NPs and IL-7R⁺ LPs were cultured for 4 d in the presence of FLT3L. pDC output was determined according to the expression of CD317 (Bst2) and CD45RA (**c**) and is shown as percentage output (**d**) ($n=6$; each dot represents a mouse, and thin lines represent the mean \pm s.d.). **e–k**, Sort-purified progenitors isolated from CD45.1 and CD45.2 mice were cocultured (**e, f**) for 4 d in the presence of FLT3L. Shown are two-color histograms for the expression of CD45.1 and CD45.2 pregated on CD45RA⁺CD317⁺ pDCs (**e**) and percentage output (**f**) ($n=3$; each dot represents a mouse, and thin lines represent the mean \pm s.d.). **g**, IL-7R⁺ LPs and CDPs were cultured in competitive settings in a 1:1 ratio. Shown is the total, pDC and cDC output over 8 d of culture ($n=3$ mice; thin lines represent the mean \pm s.e.m.). **h–k**, BM and splenic pDC output was determined 4 d after intravenous co-transfer of CD45.2-positive IL-7R⁺ LPs in competition with CD45.1-positive IL-7R⁻M-CSFR⁻ NPs (**h, i**) or CDPs (**j, k**). Shown are two-color histograms for the expression of CD45.1 and CD45.2 pregated on CD45RA⁺CD317⁺ pDCs (**h, j**) ($n=6$ mice). Shown are percentage donor-derived BM pDCs and B cells and splenic pDCs and cDCs, as indicated (**i, k**) ($n=6$; each dot represents a mouse, and thin lines represent the mean \pm s.d.). Statistical analysis was done with one-way ANOVA with Tukey post-test (**d, f**) or two-tailed Student's *t* test (**i, k**). * $P < 0.05$, ** $P < 0.01$, *** $P < 0.001$, **** $P < 0.0001$.

cultured under B cell-polarizing conditions in the presence of OP9 stromal cells.

SiglecH⁺Ly6D⁺ DP cells are bona fide pDC progenitors. Because SiglecH and Ly6D³³ are expressed on mature pDCs, we phenotypically and functionally compared DP progenitors directly with freshly isolated BM and splenic mature pDCs. We detected higher expression of CD127, CD135, CCR9, CD45RA, Ly6C, B220, CD11c, MHC-II, Sca1 and CD317 on mature SiglecH⁺B220⁺Ly6D⁺Ly6C⁺ pDCs than on DP progenitors (Fig. 3a and Supplementary Fig. 3a). Further, DP progenitors did not express CCR9 (Fig. 3a), thus indicating that pDC progenitors reside within the CCR9⁻ compartment²². In *Zbtb46*^{gfp/+} mice, *Zbtb46*-GFP or CD115, which are cDC-specific markers, were not detected on either DP cells or mature pDCs (Fig. 3a and Supplementary Fig. 3a). Stimulation with CpG-A induced the production of the cytokine IFN- α by mature BM and splenic pDCs, but not by DP progenitors, which acquired this ability after 4 d in culture (Fig. 3b). Similarly, SP and DN progenitors produced type 1 IFN only after 4 d, upon maturation (Supplementary Fig. 3b). Morphologic maturation, as assessed by Giemsa staining,

was achieved by DN, SP and DP progenitors after 4 d in culture (Fig. 3c and Supplementary Fig. 3c).

We next tested whether the DN, SP and DP maturation stages could be recapitulated in vitro. A time-course analysis of cell-sorted DN progenitors showed progressive accumulation of SP and DP cells, which were detectable in culture at day 2 (Fig. 3d). Mature CD45RA⁺SiglecH⁺ pDCs developed from DP progenitors after 2 d of culture, whereas SP progenitors initially upregulated SiglecH at day 1 and transitioned into mature cells from day 3 (Supplementary Fig. 3d,e). Similarly, analysis of proliferation showed that DP cells required fewer divisions than SP and DN cells to develop into mature pDCs (Fig. 3e), thereby indicating progressive maturation from DN via SP to DP status. Thus, DP progenitors acquire the expression of lineage-specific markers, the morphology and the ability to produce IFN- α characteristic of mature splenic pDCs after two cell divisions.

Stage-specific transcriptional signatures define pDC commitment. We next sought to define the transcriptional signature that recapitulates the commitment to pDCs. We performed RNA sequencing on DN, SP and DP progenitors isolated from wild-type

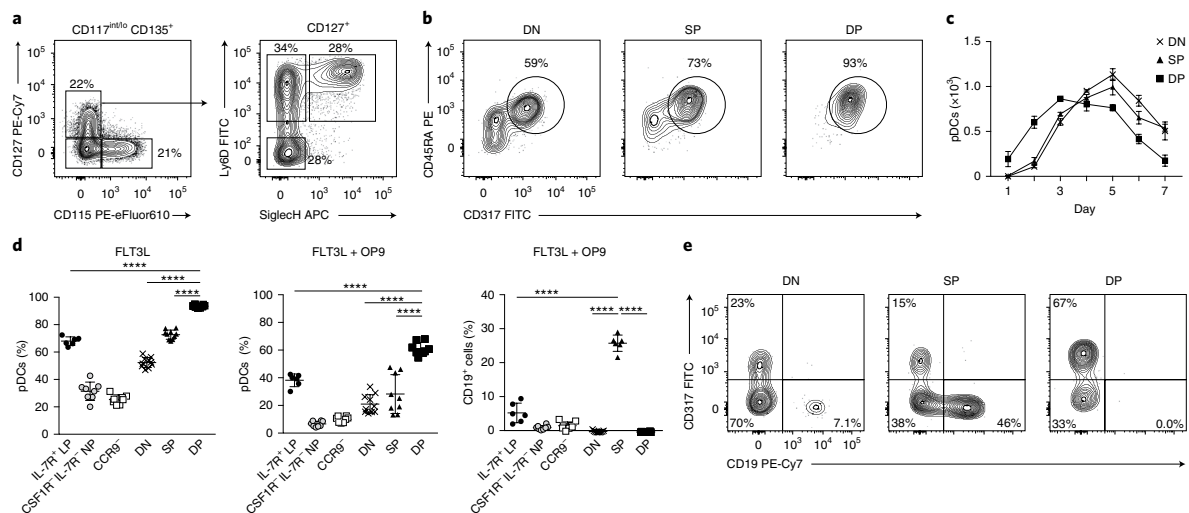


Fig. 2 | SiglecH⁺Ly6D⁺IL-7R⁺ LPs have exclusive pDC potential. **a**, IL-7R⁺ LPs, as defined in Fig. 1a, were further subdivided on the basis of expression of SiglecH and Ly6D. Shown is the gating strategy for DN, Ly6D SP, and SiglecH and Ly6D DP progenitors ($n=6$ mice). **b–e**, Sort-purified IL-7R⁺M-CSFR⁺NPs, IL-7R⁺ LPs, CCR9⁺ (CD317⁺B220⁺CD11c⁺CCR9⁺), DN, SP and DP precursors were cultured in the presence of FLT3L. Two-color histograms for the expression of CD45RA and CD317 (**b**) and the percentage of mature pDCs (**d**) are shown for day 4 of culture ($n=6$ mice, with 1 or 2 technical replicates). Each dot represents a sample, and thin lines represent the mean \pm s.d.). **c**, Total pDCs generated over 7 d of culture from sort-purified DN, SP and DP precursors ($n=3$ mice; thin lines represent the mean \pm s.e.m.). **d,e**, The same progenitors cultured for 4 d in the presence of FLT3L and OP9 stromal cells. Shown are percentages of mature pDCs and B cells (**d**) and two-color histograms for the expression of CD317⁺ pDCs and CD19⁺ B cells (**e**) ($n=6$ mice with 1 or 2 technical replicates; each dot represents a sample, and thin lines represent the mean \pm s.d.). Statistical analysis was done with one-way ANOVA with Tukey post-test. * $P < 0.05$, ** $P < 0.01$, *** $P < 0.001$, **** $P < 0.0001$.

BM and compared their transcriptional landscapes with that of B220⁺SiglecH⁺Ly6C⁺Ly6D⁺ mature BM pDCs. Principal component analysis (PCA) showed individual segregation of mature pDCs and DP progenitors: whereas DN cells and SP cells clustered together and partially shared their transcriptomes, DP cells were a distinct subset also different from mature pDCs (Fig. 4a). Hierarchical clustering of the subsets on the basis of Pearson's correlation coefficient confirmed the results obtained by PCA (Fig. 4b), in which DP cells were transcriptionally closely related to mature pDCs.

To better understand the dynamics of pDC commitment, we generated a heat map based on genes uniquely expressed at the DN stage (switch 1) and at the DN and SP stages (switch 2) through the mature pDC stage (switch 6) (Fig. 4c). Transcripts were also distributed according to shared expression patterns across two cell subsets, defined as peaks (Fig. 4c and Supplementary Table 1). The resulting developmental-expression heat map reflected the transcriptional landscape for pDC commitment and was used to evaluate switch-specific transcription factors and surface receptors (Fig. 4d,e and Supplementary Fig. 4a,b). *Spib* and *Irf7* were highly expressed only in mature pDCs (Fig. 4d), a result consistent with the inability of DN, SP and DP progenitors to produce IFN- α and with their requirement at later stages of development. The SP stage, which is the only one permissive for B cell development, was marked by the expression of B cell-specific transcription-factor transcripts, such as *Pax5* and *Ebf1* (Fig. 4d) as well as surface-receptor transcripts, such as *Cd19*, *Vpreb1* and *Vpreb2*, and *Cd79a* (Fig. 4e). Transcripts encoding transcription factors known to be essential during pDC development, particularly *Tcf4*, *Irf8*, *Zeb2* and *Bcl11a*, were expressed at the DP stage and were further upregulated after maturation (Fig. 4d), thus suggesting that pDC lineage specification was achieved at the DP stage. Importantly, whereas the *Il7r* transcript as well as IL-7R protein are expressed during development and on mature pDCs, the *Csf1r* transcript was detected on all progenitors,

in the absence of the protein at all stages (Fig. 4e and Fig. 2a). This result provides a potential explanation for the apparent conflict of lineage tracing in mice, in which pDCs were labeled in both *Il7r^{cre}* (ref. 34) and *Csf1r^{cre}* mice³⁵.

We next searched for differentially expressed genes between DP cells and all the other analyzed subsets (Supplementary Fig. 4d–f and Supplementary Table 1). Gene set enrichment analysis between DP progenitors and mature pDCs identified changes in three major pathways: E2F targets, the G2–M checkpoint and IFN- α production, thus suggesting that maturation was achieved through the downregulation of cell-cycle-associated genes and the upregulation of genes mediating functional properties (Fig. 4f, Supplementary Fig. 4c and Supplementary Table 2). Collectively, these data reveal that pDC lineage specification is already transcriptionally established at the DP stage.

Expression of IRF8 marks pDC lineage commitment on SP cells.

Given the sustained expression of CD135 and CD127 at all stages of pDC development and on mature pDCs, we examined the requirement of the corresponding ligands FLT3L and IL-7 during commitment. *Flt3l*^{-/-} mice showed impaired pDC development across all stages, with approximately tenfold-fewer total DN progenitors than those in wild-type control mice (Fig. 5a and Supplementary Fig. 5a,e). *Il7*^{-/-} mice, compared with wild-type controls, had unaltered numbers of DN and DP progenitors, as well as mature pDCs, but markedly lower numbers of SP progenitors and mature B cells (Fig. 5a and Supplementary Fig. 5a,e,f). This result correlated with the greater B cell-specific developmental and transcriptional bias of SP precursors and suggested that SP cells were heterogeneous and already committed to either the B or the pDC lineage. Quantitative PCR analysis validated the stage-specific expression of several transcription factors important for B, pDC and cDC development^{4,8,36} (Fig. 5b and Supplementary Fig. 5b). Transcripts for *Spib* and *Irf7* were low

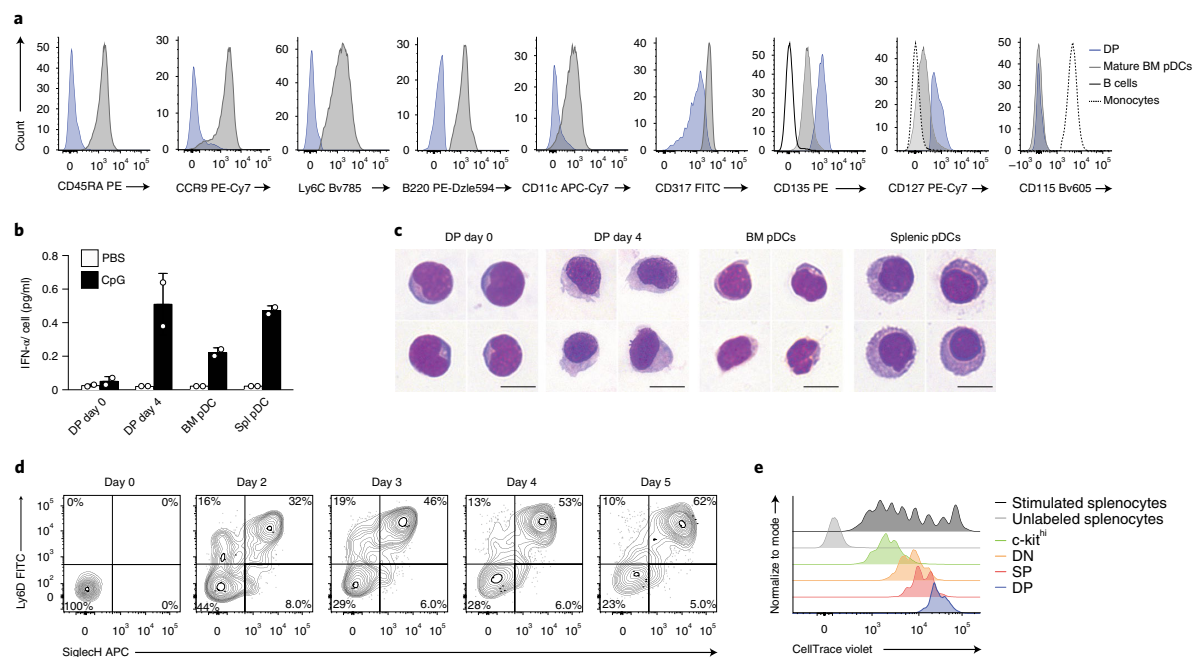


Fig. 3 | SiglecH⁺Ly6D⁺ DP cells are bona fide pDC progenitors. **a**, Representative single-color histograms for the indicated surface markers expressed by DP pre-pDCs (blue), mature pDCs (gray), B cells (black) and monocytes (broken line) ($n=3$ independent experiments). **b**, DP pre-pDC progenitors were cultured for 4 d in the presence of FLT3L. IFN- α was measured in the supernatants collected on day 0 and day 4, or on freshly plated mature pDCs 16 h after stimulation with CpG-A, as indicated ($n=3$ independent experiments, with one representative experiment shown; each dot represents a technical replicate, and thin lines represent the mean \pm s.d.). Spl, splenic. **c**, May-Gruenwald staining of sort-purified mature BM, splenic pDCs and DP progenitors at day 0 and after 4 d of culture ($n=4$ representative images taken from 3 independent experiments; scale bars, 10 μ m). **d**, DN progenitors, as defined in Fig. 2a, were cultured in the presence of FLT3L for 5 d. Shown are two-color histograms for the expression of Ly6D and SiglecH analyzed at the indicated time points ($n=3$ independent experiments, with representative data from one experiment shown). **e**, DP (blue), SP (red), DN (orange) and c-kit^{hi} (Lin⁻B220⁻Ly6C⁻CD117^{hi}) (green) progenitors were cultured for 4 d in the presence of FLT3L. Proliferation was assessed through CellTrace Violet dilution. Unlabeled (light gray) or labeled (dark gray) splenocytes were stimulated with anti-CD3 and anti-CD28 ($n=3$ independent experiments, with representative data from one experiment shown). Statistical analysis was done with one-way ANOVA with Tukey post-test. * $P < 0.05$, ** $P < 0.01$, *** $P < 0.001$, **** $P < 0.0001$.

or absent on progenitors but were induced in mature pDCs, whereas the expression of *Irf8*, *Tcf4* and *Runx2* was already established at the DP progenitor stage and further increased in mature pDCs (Fig. 5b). Notably, *Ebf1* expression was confined within the SP subset, in agreement with the exclusive ability of SP progenitors to generate B cells (Fig. 5b). To address whether SP progenitors were heterogeneous, we examined the expression of EBF1 and IRF8 on DN, SP and DP progenitors in wild-type, *Il7*^{-/-} and *Flt3l*^{-/-} mice. Indeed, SP progenitors could be split into EBF1⁺IRF8^{int} and EBF1⁻IRF8^{hi} cells, whereas DP cells were exclusively EBF1⁻IRF8^{hi} (Fig. 5c). Furthermore, induction of EBF1, but not IRF8 expression, was compromised at the SP stage in *Il7*^{-/-} mice compared with littermate controls, in agreement with fewer mature B cells³⁷ (Supplementary Fig. 5c,d).

Whereas FLT3L deficiency resulted in a partial decrease in DP progenitors, *Irf8*^{-/-} or *Irf8*^{R249C} mutant mice (Methods), in which an R249C mutation prevents the interaction with partner transcription factors such as PU.1, IRF2 and SpiB³⁸, completely lacked DP cells^{5,39} (Fig. 5d,e). SP cells accumulated in both *Irf8*^{-/-} and *Irf8*^{R249C} mice, a result indicative of a developmental block at the transition from SP to DP cells (Fig. 5d). In agreement with this finding, *Irf8*^{-/-} mice lacked mature SiglecH⁺B220⁺ pDCs in the BM and SiglecH^{hi}CD317^{hi} in the spleen (Fig. 5e-h). However, a population of SiglecH^{int}CD317^{int} pDC-like cells was detected and was even found to be elevated in the *Irf8*^{-/-} spleens (Fig. 5g,h). These results indicate that SP cells can

be subdivided into IRF8^{hi}, IL-7-independent pDC-committed and EBF1⁺, IL-7-dependent B cell-committed progenitors.

IRF8 and EBF1 define pDC and B cell lineage dichotomy. To dissect the heterogeneity of the SP compartment, we used IRF8-eGFP and EBF1-hCD2 reporter mice, which express a 3' IRES-GFP and an IRES-human CD2, respectively, thus allowing us to trace the genes and sort the expressing subsets. SP cells from IRF8-eGFP or EBF1-hCD2 mice could be sorted into IRF8-GFP^{int} (IRF8^{int} SP) or IRF8-GFP^{hi} (IRF8^{hi} SP) and into EBF1-hCD2⁻ (EBF1⁻ SP) and EBF1-hCD2⁺ SP (EBF1⁺ SP) cells (Supplementary Fig. 6a,c). We then assessed the pDC- and B cell-differentiation potential of each SP subset in vitro, as described above. IRF8^{hi} SP progenitors had almost exclusive pDC output and could not differentiate into B cells (Fig. 6a-d and Supplementary Fig. 6b,d), thus suggesting that the B cell potential was lost concomitant with the induction of high IRF8 expression at the SP precursor stage. Similarly, EBF1⁻ SP progenitors did not differentiate into B cells on OP9 stromal cells under B cell-polarizing conditions (Supplementary Fig. 6e-h), thus suggesting that EBF1 expression at the SP stage is necessary to promote B cell lineage commitment.

Expression of TCF4, specifically its long isoform (*Tcf4_L*), is required for pDC development, because pDCs do not develop in its absence^{25,27}. RT-qPCR analysis indicated comparable expression

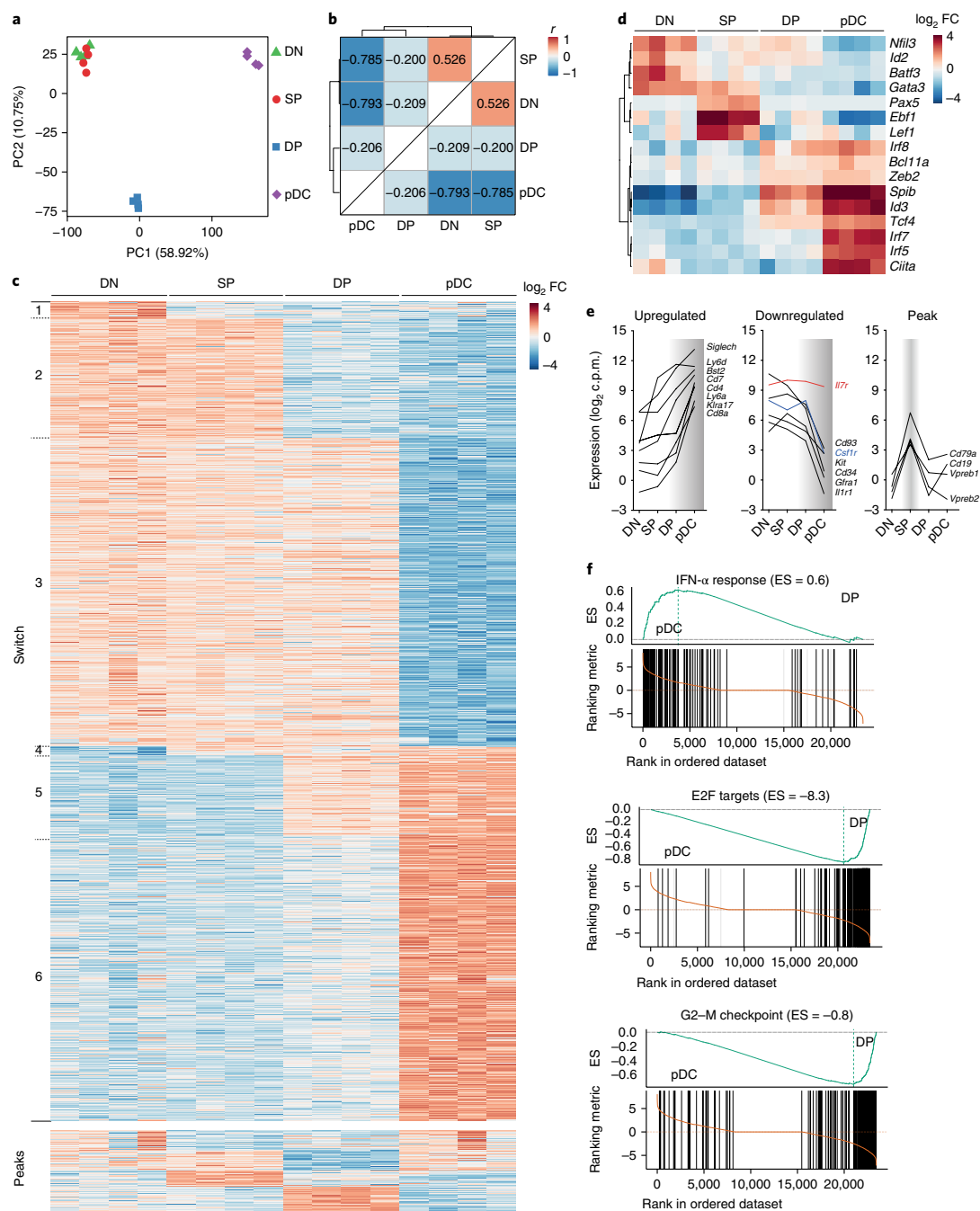


Fig. 4 | Stage-specific transcriptional signatures define pDC commitment. a-f. Bulk RNA sequencing was performed on cell-sorted DN, SP and DP progenitors, and mature pDCs (Methods). **a, b.** PCA (**a**) and hierarchical clustering (**b**) of the progenitor subsets and mature pDCs on the basis of Pearson's correlation coefficient calculated on the 25% of genes with the highest variance (calculated as interquartile range). PC, principal component. **c.** Heat map based on a developmental-stage model from DN to SP to DP and to mature pDCs, generated on selected genes (fold change (FC) >1 and $P < 0.05$; Methods). Genes were ordered in switches and peaks according to their expression profiles for the different subsets. **d.** Correlation heat map for selected transcription factors. **e.** Specific surface markers, plotted according to their expression profiles (upregulated, downregulated or peak) across the indicated developmental stages from DN to mature pDCs. Highlighted are the transcript levels as c.p.m. for *Irf7* (red) and *Csf1r* (blue). **f.** Gene set enrichment analysis, performed on the Molecular Signature Database (MSigDb v5.2) comparing the enrichment score (ES) for DP progenitors with mature pDCs, as depicted (IFN- α response, $P < 0.00358$; E2F targets, $P < 0.00146$; G2-M checkpoint, $P < 0.000946$). RNA was collected from sort-purified subsets in $n = 4$ independent experiments. For each experiment, all progenitors were obtained from one mouse.

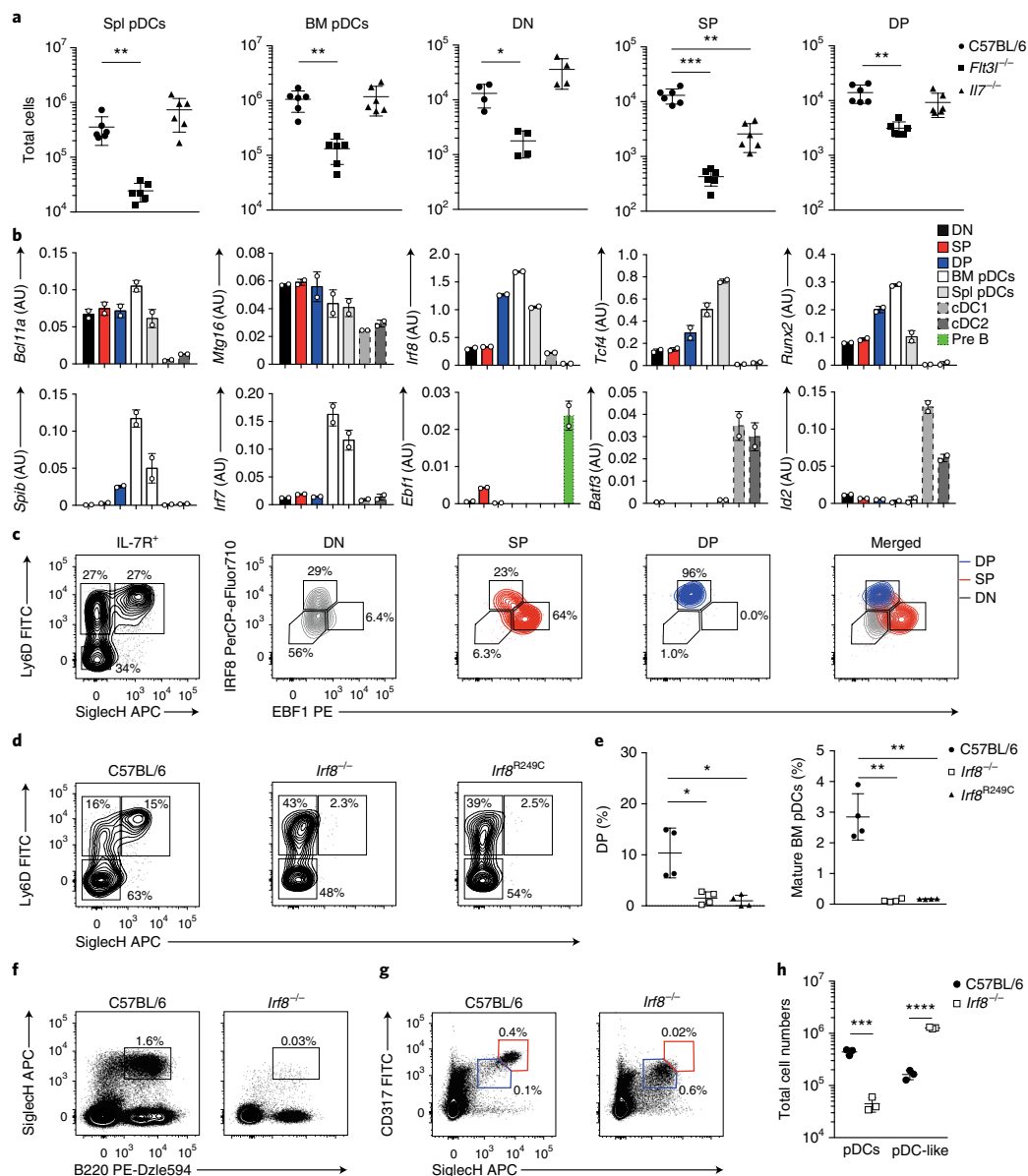


Fig. 5 | Expression of IRF8 marks pDC lineage commitment on SP cells. **a**, Total mature BM and splenic pDCs and DN, SP and DP progenitors in wild-type, *Flt3l*^{-/-} and *Il7*^{-/-} mice, as indicated ($n = 6$ independent experiments; each symbol represents a mouse, and thin lines represent the mean \pm s.d.). **b**, Expression of selected genes (arbitrary units (AU) relative to β -actin) on sort-purified DN, SP and DP BM progenitors, gated as in Fig. 2a, mature BM and splenic pDCs (SiglecH⁺CD317⁺), cDC1 (CD11c⁺MHCII^{hi}CD24⁺XCR1⁺) and cDC2 (CD11c⁺MHCII^{hi}CD11b⁺Sirp- α ⁺) were analyzed for the expression of selected genes ($n = 3$ independent experiments, with one representative experiment shown; each dot represents a technical replicate, and thin lines represent the mean \pm s.d.). **c**, Expression of IRF8 and EBF1, determined on DN (black), SP (red) and DP (blue) progenitors ($n = 6$ mice; representative experiment shown). **d, e**, DN, SP and DP subsets and mature pDCs were analyzed in *Irf8*^{-/-} and BXH2 (*IRF8*^{R249C}) mice. Shown are representative two-color histograms for the expression of Ly6D and SiglecH (**d**) and the percentage DP pre-pDCs and mature BM pDCs (**e**) ($n = 4$; each symbol represents a mouse, and thin lines represent the mean \pm s.d.). **f-h**, Splenic and BM pDCs analyzed in C57BL/6 and *Irf8*^{-/-} mice. Shown are representative two-color histograms for the expression of SiglecH and B220 on BM cells (**f**) and CD317 and SiglecH on splenocytes (**g**). CD317^{hi}SiglecH^{hi} pDCs (red) and CD317^{int}SiglecH^{int} pDC-like cells (blue), gated as in **g**, were quantified (**h**) ($n = 3$; each symbol represents a mouse, and thin lines represent the mean \pm s.d.). Statistical analysis was done with two-tailed Student's *t* test (**b, e, h**). * $P < 0.05$, ** $P < 0.01$, *** $P < 0.001$, **** $P < 0.0001$.

of *Tcf4*_L in DP cells and mature BM and splenic pDCs (Fig. 6e). The expression of *Irf8* in IRF8^{hi} SP cells was comparable to that observed in DP cells and mature pDCs, whereas the expression of *Tcf4*_L in

IRF8^{hi} SP cells was low, and similar to that in DN cells (Fig. 6e), thus suggesting that the expression of IRF8 but not *Tcf4*_L mirrored the acquisition of pDC-lineage specification.

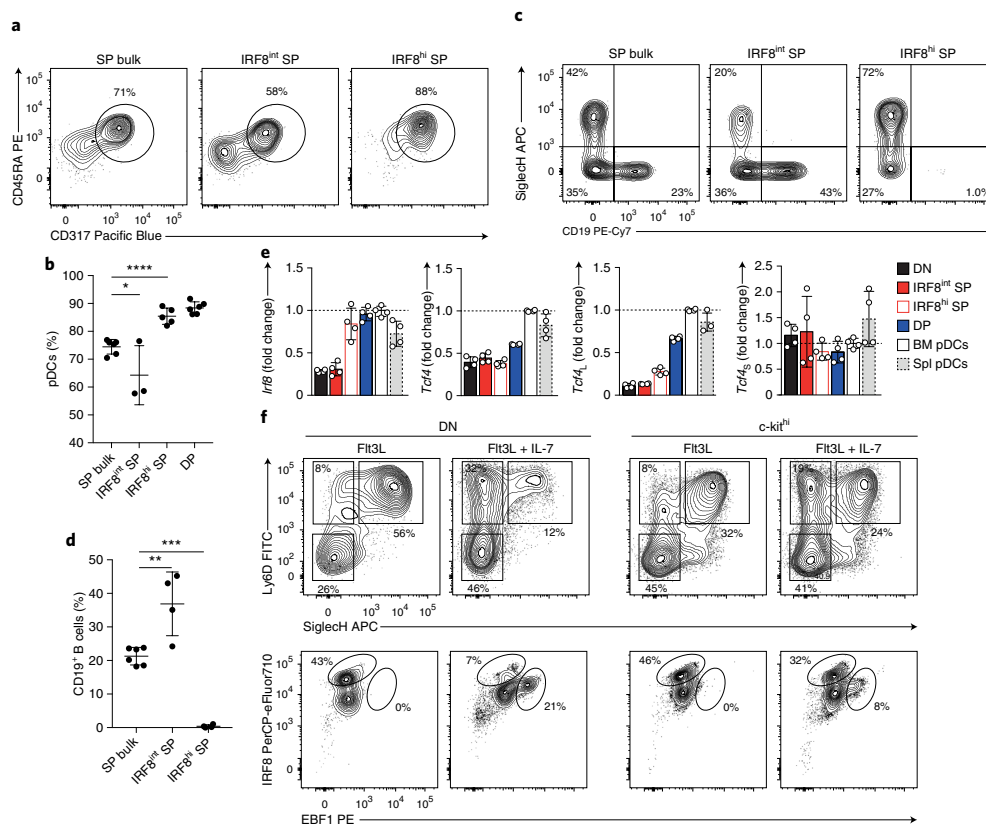


Fig. 6 | IRF8 and EBF1 define pDC and B cell lineage dichotomy. a–d, Progenitors from C57BL/6 (bulk) and *Irf8^{egfp}* reporter mice, as indicated and gated as in Supplementary Fig. 6a, were sort-purified and analyzed for pDC and B cell potential. Specifically, DP and unfractionated SP (SP bulk) and SP progenitors expressing intermediate (IRF8^{int} SP) or high (IRF8^{hi} SP) levels of IRF8 were sort-purified and cultured for 4 d in the presence of FLT3L (**a,b**) or FLT3L and OP9 stromal cells (**c,d**), as indicated. Shown are two-color histograms and percentages of CD45RA⁺CD317⁺ pDCs (**a,b**) and SiglecH⁺CD19⁺ (**c,d**) ($n=3$ independent experiments with 1 or 2 technical replicates; each symbol represents a sample, and thin lines represent the mean \pm s.d.). **e**, Expression of *Irf8*, *Tcf4* and its long (*Tcf4_L*) or short (*Tcf4_S*) isoforms, quantified in DN, SP IRF8^{int}, SP IRF8^{hi}, DP, BM and splenic pDCs from IRF8-eGFP reporter mice. Shown are the expression levels indicated as a ratio to BM pDCs ($n=2$ independent experiments with 2 technical replicates; data shown as mean \pm s.d.). **f**, DN and c-kit^{hi} progenitors were cultured for 5 d in the presence of FLT3L with or without IL-7 as indicated. Shown are two-color histograms for the expression of Ly6D/SiglecH (top) and IRF8/EBF1 (bottom) ($n=3$ independent experiments, with one representative experiment shown). Statistical analysis was done with one-way ANOVA with Tukey post-test. * $P < 0.05$, ** $P < 0.01$, *** $P < 0.001$, **** $P < 0.0001$.

BM niches are likely to influence progenitor lineage choice through the availability of cytokines and other cues. We simulated the contact and the exposure to the BM stromal environment by using a Transwell culture system, in which SP cells and DP cells were cultured in the presence of FLT3L, either in direct contact with OP9 stromal cells or exposed to soluble factors released by OP9 stromal cells. Differentiation of SP and DP cells toward CD317⁺ pDCs was significantly inhibited by direct contact with OP9 stromal cells, whereas differentiation of SP cells toward CD19⁺ B cells required direct contact (Supplementary Fig. 6i–l). To understand the role played by polarizing cytokines in pDC and B cell lineage specification, we examined the induction of IRF8 and EBF1 in uncommitted DN and c-kit^{hi} progenitors exposed to FLT3L and IL-7. Exposure of DN and c-kit^{hi} precursors to FLT3L resulted in a strong induction of IRF8 expression as well as accumulation of DP progenitors after 5 d of culture (Fig. 6f). The addition of IL-7 promoted the accumulation of SP progenitors and induced EBF1 expression in the absence of OP9 stromal cells (Fig. 6f). This result indicates that lineage specification toward pDCs or B cells occurs in SiglecH⁺Ly6D⁺

SP cells and is defined by the mutually exclusive, high expression of IRF8 or EBF1, which was in turn governed by the exposure to FLT3L or IL-7 and influenced by contact with stromal cells.

Single-cell analysis elucidates pDC heterogeneity. To understand how tissue imprinting as well as ontogeny might influence the transcriptional landscape of pDCs, we performed bulk as well as single-cell RNA sequencing. Bulk RNA sequencing was done on ex vivo-isolated mature pDCs from the BM and spleen, and on in vitro-generated CD317⁺SiglecH⁺ pDCs from IL-7R⁺ LPs and CDPs. A high correlation coefficient ranging from 0.8 to 0.95 was obtained across all pDC samples analyzed (Supplementary Fig. 7a). Through PCA, we were able to highlight differences related to in vitro-generated versus ex vivo-isolated pDCs (principal component 1, 49%), and differences associated with tissue imprinting, in splenic versus BM pDCs (principal component 2, 14%) (Fig. 7a). Further analysis of the sample was performed after filtering for the 25% most variable genes. By focusing on differences related to their ontogeny and using a stringent cutoff (\log_2 fold change > 2)

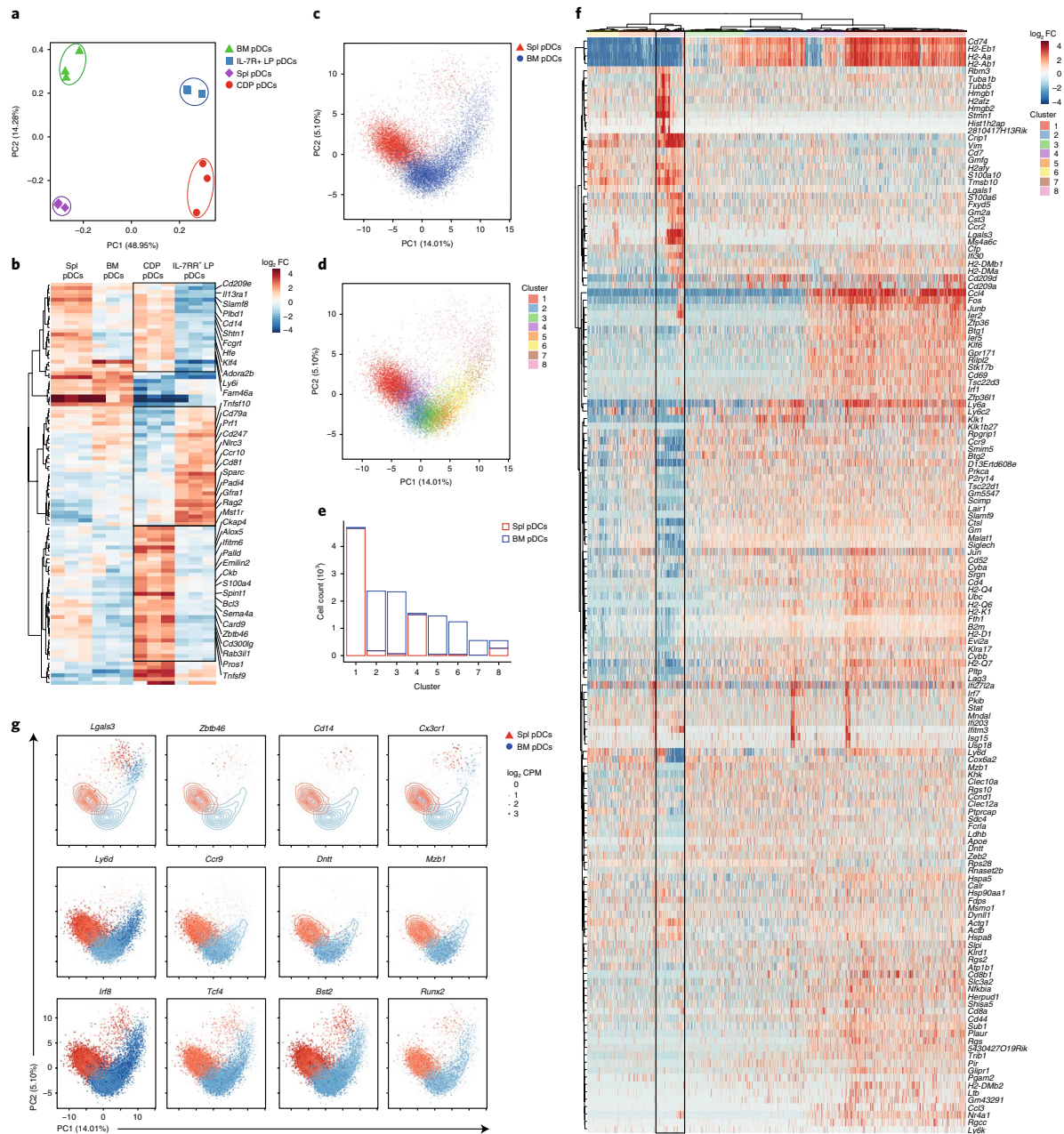


Fig. 7 | Single-cell analysis elucidates pDC heterogeneity. a, b, Bulk RNA sequencing on mature BM and splenic pDCs, and on IL-7R⁺ LP- and CDP-derived pDCs, performed as described in Methods. **a**, PCA performed on the 25% most variable genes. **b**, Heat map showing relative expression for differentially expressed genes (log₂ fold change >2.0) from IL-7R⁺ LPs versus CDP-derived pDCs. **c–g**, Single-cell RNA sequencing, performed as described in Methods, on sort-purified BM and splenic pDCs. **c, d**, PCA based on the 148 hypervariable genes (biological variation >0.1 and false discovery rate <0.05). Colors indicate the tissue of origin (**c**) or the identified clusters (**d**). **e**, Number of cells identified for each cluster in the BM and spleen. **f**, Heat map for 148 hypervariable genes across all 14,744 cells. At top, colors indicate the identified clusters as in **d**. **g**, Expression of the indicated genes from individual BM (blue) and splenic (red) pDCs. The size of each dot corresponds to the relative expression of a given gene for each cell. The contour lines indicate the density of the BM (blue) and splenic (red) cells in the PCA space. Cells for bulk and single-cell RNA sequencing were harvested from $n=3$ mice in 3 independent experiments.

we identified 107 genes differentially expressed in CDP- and IL-7R⁺ LP-derived pDCs (Fig. 7b and Supplementary Fig. 7c,d). Importantly, whereas pDC-related transcripts, such as *Irf8*, *Siglech*,

Tcf4 and *Bst2*, showed high expression, most of the genes expressed differentially between CDP and IL-7R⁺ LP-derived pDCs, such as *Rag2* and *Cd14*, were expressed at low levels (Supplementary Fig. 7b).

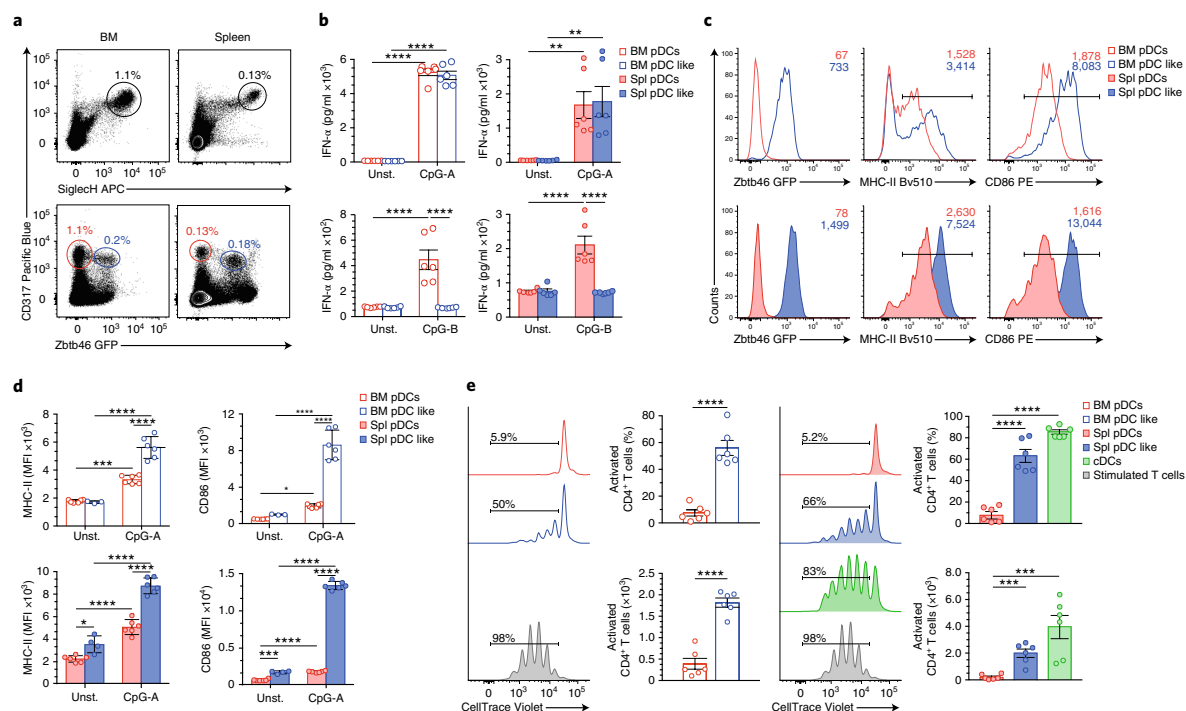


Fig. 8 | Functional heterogeneity of pDCs is developmentally encoded. a–e. BM and splenic pDCs and pDC-like cells, analyzed in *Zbtb46^{flp/+}* mice. **a**, Two-color histograms for the expression of CD317/SiglecH and CD317/Zbtb46-GFP on BM and splenic pDCs pregated on CD11c⁺MHCII⁺ cells. BM and splenic pDCs are labeled in red, and pDC-like cells are marked in blue ($n=6$ mice, with one representative experiment shown). **b**, IFN- α , measured from BM and splenic pDCs and pDC-like cells stimulated for 16 h with CpG-A or CpG-B, or left unstimulated (unst.), as indicated ($n=3$ independent experiments with 2 technical replicates; each symbol represents a sample, and thin lines represent the mean \pm s.e.m.). Expression of Zbtb46-GFP, MHC-II and CD86, determined in BM and splenic pDCs (red) and pDC-like cells (blue) 16 h after CpG-A stimulation. **c, d** Representative single-color histograms with mean fluorescence intensity (MFI) (**c**) and the compiled values from BM and splenic cells (**d**) ($n=3$ independent experiments with 2 technical replicates; each symbol represents a sample, and thin lines represent the mean \pm s.d.). **e**, Proliferation of OT-II T cells induced by sort-purified BM and splenic pDCs (red), pDC-like cells (blue) and splenic cDCs (green) (Methods). Cells were cultured in the presence of CpG-A, lipopolysaccharide and OVA-protein for 4 d. T cells stimulated with anti-CD3 and anti-CD28 (gray) were used as controls ($n=3$ independent experiments with 2 technical replicates; each symbol represents a sample, and thin lines represent the mean \pm s.e.m.). Statistical analysis was done with two-way ANOVA with Tukey post-test (**b, d, e**). * $P < 0.05$, ** $P < 0.01$, *** $P < 0.001$, **** $P < 0.0001$.

In line with their ontogeny, IL-7R⁺ LP-derived pDCs were enriched in expression of lymphoid-associated genes, such as *Rag2* and *Cd79*, whereas CDP-derived pDCs expressed several cDC- and myeloid-related genes, such as *Zbtb46*, *Cd14* and *Klf4* (Fig. 7b). To validate the ontogeny-based heterogeneity of mature pDCs, we performed single-cell RNA sequencing on approximately 8,000 BM and 7,000 splenic CD317⁺SiglecH⁺ pDCs, detecting approximately 2,000 genes per cell. PCA based on 148 hypervariable genes confirmed tissue-specific identity at the single-cell level. Each cell was plotted in two-dimensional PCA space, and whereas splenic pDCs split into two discrete subgroups, BM pDCs spread along a diagonal over principal components 1 and 2 (Fig. 7c). Clustering analysis (Methods) identified eight clusters (Fig. 7d–f), with splenic pDCs splitting into three major clusters (1, 4 and 8), and BM pDCs splitting into six clusters (2, 3, 5, 6, 7 and 8) (Fig. 7e and Supplementary Fig. 7e). The relative and absolute frequency of cells belonging to each cluster showed almost exclusive tissue specificity for each cluster except for cluster 8, which was equally represented in both tissues and accounted for approximately 5% of the total pDC population (Fig. 7e and Supplementary Fig. 7e). A pairwise comparison of the differentially expressed genes (absolute log₂ fold change > 1.5) across all clusters showed limited differences across clusters 1–6, and only clusters

7 and 8 diverged from the other clusters (Supplementary Fig. 7f). The numbers of detected genes per cluster and cell-cycle-associated genes indicated that BM cluster 7 was actively cycling and was probably an immediate precursor of cluster 8 (Supplementary Fig. 7g,h). Transcripts associated with cluster 8, i.e., *Lgals3*, *Zbtb46* and *Cd14*, were reminiscent of the CDP-derived pDCs. Clusters 1 to 6 showed expression of genes previously identified in IL-7R⁺ LP-derived pDCs (Fig. 7b,g and Supplementary Table 3), i.e., *Ly6d*, *Ccr9* and *Dnnt1*. All clusters expressed high amounts of pDC-specific transcripts, such as *Tcf4*, *Irf8* and *Bst2* (Fig. 7g), thus ruling out contamination of cluster 8 with other myeloid lineages. As such, single-cell analysis revealed heterogeneity of the pDC compartment and validated the segregation of lymphoid and myeloid signatures in two distinct subsets: the conventional pDCs and cluster 8, referred to as pDC-like cells.

The functional heterogeneity of pDCs is developmentally encoded. A prerequisite for performing a functional analysis of pDC-like cells was the identification of specific markers and the establishment of a gating strategy, which would enable us to sort and directly compare pDCs and pDC-like cells. We used *Zbtb46^{flp/wt}* mice to sort Zbtb46-GFP⁺SiglecH^{hi}CD317⁺ pDCs and Zbtb46-GFP⁺SiglecH^{int}CD317⁺ pDC-like cells (Fig. 8a and Supplementary

Fig. 8a). We extended our phenotypic analysis of pDCs and pDC-like cells by comparing the transcript expression and, when possible, the protein expression of several pDC- and cDC-related genes. Both subsets expressed similar levels of pDC- and cDC-specific transcripts, such as *Siglech*, *Bst2*, *Ly6c*, *H2-Aa*, *Ilgax*, *Runx2* and *Irf8*. In addition, the protein expression of SiglecH, Bst2, MHC-II, CD11c and Ly6C was comparable between the two subsets, and only slight differences were detected (Supplementary Fig. 8b–f). However, CX3CR1 was expressed exclusively on pDC-like cells (Supplementary Fig. 8d,e), a result reminiscent of nonconventional CX3CR1⁺CD8 α ⁺ DCs previously identified⁴⁰, with the exception that pDC-like cells were CD8 α ⁻ (data not shown). Both subsets produced IFN- α when stimulated with CpG-A (Fig. 8b). However, unlike conventional pDCs, pDC-like cells did not respond to CpG-B stimulation (Fig. 8b), thus suggesting different signal regulation. Furthermore, when stimulated with CpG-A, pDC-like cells had higher surface expression of MHC-II and the co-stimulatory molecule CD86 than did conventional pDCs (Fig. 8c,d). Importantly, in contrast to conventional pDCs, pDC-like cells from BM and spleen were efficient at taking up, processing and presenting protein and induced strong proliferation of OT2 T cells, at levels comparable to those observed in cDCs⁴¹ (Fig. 8e) and consistent with their expression of cDC transcripts. In summary, pDC-like cells were phenotypically and transcriptionally similar to conventional pDCs but also exhibited several cDC features, including efficient antigen processing and presentation.

Discussion

Here we demonstrated that pDC development predominantly occurred from IL-7R⁺ LPs rather than from CDPs or the previously identified CSF1R-IL-7R⁻ NPs^{2,23}. Within the IL-7R⁺ LPs, Ly6D⁺SiglecH⁺ DP precursors gave rise almost exclusively to pDCs when cultured in the presence of FLT3L, thus suggesting that they might represent committed pre-pDCs that depend on the expression of IRF8 and are only two divisions away from maturity. Whereas Ly6D⁺SiglecH⁻ DN progenitors were still uncommitted and showed the broadest lineage potential, Ly6D⁺SiglecH⁻ SP cells were able to differentiate into pDCs and B cells, depending on the expression of IRF8 or EBF1, respectively. High expression of IRF8 within the SP cells determined loss of B cell potential and pDC lineage specification, which already occurred in the absence of TCF4_L, thus suggesting that the amount of IRF8 is key for pDC commitment.

How IRF8 is induced and regulated during pDC development remains an open question. Proliferation may be a key factor determining accumulation or dilution rates, as has been suggested for PU.1 during macrophage versus B cell differentiation⁴². BM niches rich in IL-7 would promote high proliferation of precursors, maintain low levels of IRF8 and allow for the induction of Pax5 by EBF1, thus leading to efficient B cell differentiation. Progressive expansion of the progenitor pool would also separate distal cells from the IL-7-rich BM niches, thereby limiting their proliferation and consequently leading to the accumulation of a specific IRF8 threshold promoting pDC development. A transcriptional mechanism may conceivably result in autoregulatory induction of IRF8 acting during pDC lineage specification, similarly to the one described for cDC1 (ref. 17). Beside the induction of IRF8 at the SP stage, transition to DP cells was characterized by the progressive expression of lineage-specific genes, including TCF4_L, IRF7 and SpiB, concomitant with the downregulation of cell-cycle-associated genes. Further studies will be necessary to characterize the intrinsic and extrinsic players acting in the context of pDC development, given that different mechanisms are likely to shape differentiation along the lymphoid and the myeloid branch. Although the levels of ID2 and TCF4 were shown to be critical for the commitment toward cDC1 and pDCs along the myeloid differentiation pathway, repression of ID2 and cDC1 commitment may not be necessary along the lymphoid,

IL-7R⁺ LP-derived developmental pathway, in which B cell potential instead must be prevented.

Neither DP cells nor conventional type 1 IFN-producing pDCs develop in mice lacking IRF8 or carrying the IRF8^{R249C} mutation. In these mice, we observed the expansion of an alternative type of pDCs, which were unable to produce type 1 IFNs in response to CpG-B³⁹, a pDC-defining hallmark^{39–41}, and which expressed several features reminiscent of cDCs, including the ability to process and present antigens to T cells³⁹. Nevertheless, caution is necessary when interpreting data from knockout mice. Although most pDCs arose from IL-7R⁺ LPs, they also developed from myeloid CDPs. In agreement with the greater contribution of lymphocyte progenitors than CDPs to the mature pDC pool, pDCs have a slower turnover rate than cDCs. Approximately 10% of mature pDCs are replaced within 2 d, a rate similar to that of T cells, whereas the turnover of cDCs is much faster, such that approximately 50% of the mature pool is replaced within the same timeframe⁴³. These results support either a different number of cell divisions necessary for pDCs and cDCs to acquire maturity from CDPs, or, as is more likely and is supported by our data, for a different ontogeny of most pDCs and cDCs. Further supporting a major lymphoid developmental path of pDCs, a novel computational fate-mapping analysis performed on hematopoietic cells (FateID) revealed the presence of a common early progenitor shared by B cells and pDCs⁴⁴.

The dual origin of pDCs may suggest a heterogeneous pool of mature cells able to perform the variety of functions ascribed to pDCs⁴⁵. Our data on CDP- and IL-7R⁺ LP-derived pDCs as well as single-cell RNA sequencing highlighted this heterogeneity, revealing at least two subsets of mature pDCs: conventional pDCs and a small subset of pDC-like cells. pDC-like cells, which account for approximately 5–10% of the mature pDCs in the BM and spleen, were characterized by the concomitant expression of pDC-specific and cDC-associated transcripts. A small subset of peripheral blood mononuclear cells that combine features of pDCs and cDCs has recently also been identified in humans^{46,47}. The use of Zbtb46^{flp} (ref. 48) mice was key in enabling us to identify and purify pDCs and pDC-like cells to perform a direct comparison of the two pDC subsets. Beyond phenotypic differences, conventional pDCs and pDC-like cells were functionally distinct. Although both subsets secreted type 1 IFNs in response to CpG-A stimulation, pDC-like cells were unable to do so when stimulated with CpG-B. Similarly to cDCs, pDC-like cells were better than conventional pDCs at antigen processing and presentation. This feature, which is atypical for pDCs⁴¹, may explain the ability of mature pDCs, including pDC-like cells, to induce antitumor responses in clinical trials on patients with melanoma⁴⁹. In summary, our investigation of the developmental trajectory of pDCs led to the identification and characterization of a novel subset of antigen-presenting cells, pDC-like cells, which share transcriptional and functional features with both pDCs and cDCs.

Methods

Methods, including statements of data availability and any associated accession codes and references, are available at <https://doi.org/10.1038/s41590-018-0136-9>.

Received: 10 April 2017; Accepted: 15 May 2018;

Published online: 20 June 2018

References

- Banchereau, J. & Steinman, R. M. Dendritic cells and the control of immunity. *Nature* **392**, 245–252 (1998).
- Guilliams, M. et al. Dendritic cells, monocytes and macrophages: a unified nomenclature based on ontogeny. *Nat. Rev. Immunol.* **14**, 571–578 (2014).
- Colonna, M., Trinchieri, G. & Liu, Y. J. Plasmacytoid dendritic cells in immunity. *Nat. Immunol.* **5**, 1219–1226 (2004).
- Murphy, T. L. et al. Transcriptional control of dendritic cell development. *Annu. Rev. Immunol.* **34**, 93–119 (2016).

5. Mildner, A. & Jung, S. Development and function of dendritic cell subsets. *Immunity* **40**, 642–656 (2014).
6. Tamura, T. et al. IFN regulatory factor-4 and -8 govern dendritic cell subset development and their functional diversity. *J. Immunol.* **174**, 2573–2581 (2005).
7. Suzuki, S. et al. Critical roles of interferon regulatory factor 4 in CD11b^{hi}CD8α^{hi} dendritic cell development. *Proc. Natl Acad. Sci. USA* **101**, 8981–8986 (2004).
8. Belz, G. T. & Nutt, S. L. Transcriptional programming of the dendritic cell network. *Nat. Rev. Immunol.* **12**, 101–113 (2012).
9. Perussia, B., Fanning, V. & Trinchieri, G. A leukocyte subset bearing HLA-DR antigens is responsible for in vitro alpha interferon production in response to viruses. *Nat. Immun. Cell. Growth Regul.* **4**, 120–137 (1985).
10. Siegal, F. P. et al. The nature of the principal type 1 interferon-producing cells in human blood. *Science* **284**, 1835–1837 (1999).
11. Cella, M. et al. Plasmacytoid monocytes migrate to inflamed lymph nodes and produce large amounts of type I interferon. *Nat. Med.* **5**, 919–923 (1999).
12. Naik, S. H. et al. Development of plasmacytoid and conventional dendritic cell subtypes from single precursor cells derived in vitro and in vivo. *Nat. Immunol.* **8**, 1217–1226 (2007).
13. Liu, K. et al. In vivo analysis of dendritic cell development and homeostasis. *Science* **324**, 392–397 (2009).
14. Karsunky, H., Merad, M., Cozzio, A., Weissman, I. L. & Manz, M. G. Flt3 ligand regulates dendritic cell development from Flt3⁺ lymphoid and myeloid-committed progenitors to Flt3⁺ dendritic cells in vivo. *J. Exp. Med.* **198**, 305–313 (2003).
15. D'Amico, A. & Wu, L. The early progenitors of mouse dendritic cells and plasmacytoid dendritic cells are within the bone marrow hemopoietic precursors expressing Flt3. *J. Exp. Med.* **198**, 293–303 (2003).
16. Sathe, P., Vremec, D., Wu, L., Corcoran, L. & Shortman, K. Convergent differentiation: myeloid and lymphoid pathways to murine plasmacytoid dendritic cells. *Blood* **121**, 11–19 (2013).
17. Grajales-Reyes, G. E. et al. Batf3 maintains autoactivation of Irf8 for commitment of a CD8⁺ conventional DC clonogenic progenitor. *Nat. Immunol.* **16**, 708–717 (2015).
18. Tussiwand, R. et al. Klf4 expression in conventional dendritic cells is required for T helper 2 cell responses. *Immunity* **42**, 916–928 (2015).
19. Miller, J. C. et al. Deciphering the transcriptional network of the dendritic cell lineage. *Nat. Immunol.* **13**, 888–899 (2012).
20. Shigematsu, H. et al. Plasmacytoid dendritic cells activate lymphoid-specific genetic programs irrespective of their cellular origin. *Immunity* **21**, 43–53 (2004).
21. Pelayo, R. et al. Derivation of 2 categories of plasmacytoid dendritic cells in murine bone marrow. *Blood* **105**, 4407–4415 (2005).
22. Schlitzer, A. et al. Identification of CCR9⁺ murine plasmacytoid DC precursors with plasticity to differentiate into conventional DCs. *Blood* **117**, 6562–6570 (2011).
23. Onai, N. et al. A clonogenic progenitor with prominent plasmacytoid dendritic cell developmental potential. *Immunity* **38**, 943–957 (2013).
24. Schlitzer, A. et al. Tissue-specific differentiation of a circulating CCR9⁺ pDC-like common dendritic cell precursor. *Blood* **119**, 6063–6071 (2012).
25. Cisse, B. et al. Transcription factor E2-2 is an essential and specific regulator of plasmacytoid dendritic cell development. *Cell* **135**, 37–48 (2008).
26. Ghosh, H. S., Cisse, B., Bunin, A., Lewis, K. L. & Reizis, B. Continuous expression of the transcription factor e2-2 maintains the cell fate of mature plasmacytoid dendritic cells. *Immunity* **33**, 905–916 (2010).
27. Grajkowska, L. T. et al. Isoform-specific expression and feedback regulation of E protein TCF4 control dendritic cell lineage specification. *Immunity* **46**, 65–77 (2017).
28. Ghosh, H. S. et al. ETO family protein Mtg16 regulates the balance of dendritic cell subsets by repressing Id2. *J. Exp. Med.* **211**, 1623–1635 (2014).
29. Scott, C. L. et al. The transcription factor Zeb2 regulates development of conventional and plasmacytoid DCs by repressing Id2. *J. Exp. Med.* **213**, 897–911 (2016).
30. Wu, X. et al. Transcription factor Zeb2 regulates commitment to plasmacytoid dendritic cell and monocyte fate. *Proc. Natl Acad. Sci. USA* **113**, 14775–14780 (2016).
31. Kondo, M., Weissman, I. L. & Akashi, K. Identification of clonogenic common lymphoid progenitors in mouse bone marrow. *Cell* **91**, 661–672 (1997).
32. Swiecki, M. et al. Type I interferon negatively controls plasmacytoid dendritic cell numbers in vivo. *J. Exp. Med.* **208**, 2367–2374 (2011).
33. Blasius, A. L. et al. Bone marrow stromal cell antigen 2 is a specific marker of type I IFN-producing cells in the naive mouse, but a promiscuous cell surface antigen following IFN stimulation. *J. Immunol.* **177**, 3260–3265 (2006).
34. Schlenner, S. M. et al. Fate mapping reveals separate origins of T cells and myeloid lineages in the thymus. *Immunity* **32**, 426–436 (2010).
35. Loschko, J. et al. Inducible targeting of cDCs and their subsets in vivo. *J. Immunol. Methods* **434**, 32–38 (2016).
36. Nutt, S. L. & Kee, B. L. The transcriptional regulation of B cell lineage commitment. *Immunity* **26**, 715–725 (2007).
37. Kikuchi, K., Lai, A. Y., Hsu, C. L. & Kondo, M. IL-7 receptor signaling is necessary for stage transition in adult B cell development through up-regulation of EBF. *J. Exp. Med.* **201**, 1197–1203 (2005).
38. Tailor, P., Tamura, T., Morse, H. C. III & Ozato, K. The BXH2 mutation in IRF8 differentially impairs dendritic cell subset development in the mouse. *Blood* **111**, 1942–1945 (2008).
39. Sichien, D. et al. IRF8 transcription factor controls survival and function of terminally differentiated conventional and plasmacytoid dendritic cells, respectively. *Immunity* **45**, 626–640 (2016).
40. Bar-On, L. et al. CX3CR1⁺ CD8α⁺ dendritic cells are a steady-state population related to plasmacytoid dendritic cells. *Proc. Natl Acad. Sci. USA* **107**, 14745–14750 (2010).
41. Krug, A. et al. Interferon-producing cells fail to induce proliferation of naive T cells but can promote expansion and T helper 1 differentiation of antigen-experienced unpolarized T cells. *J. Exp. Med.* **197**, 899–906 (2003).
42. Kueh, H. Y., Champhekar, A., Nutt, S. L., Elowitz, M. B. & Rothenberg, E. V. Positive feedback between PU.1 and the cell cycle controls myeloid differentiation. *Science* **341**, 670–673 (2013).
43. Chen, M., Huang, L., Shabier, Z. & Wang, J. Regulation of the lifespan in dendritic cell subsets. *Mol. Immunol.* **44**, 2558–2565 (2007).
44. Herman, J. S., Sagar & Grün, D. FateID infers cell fate bias in multipotent progenitors from single-cell RNA-seq data. *Nat. Methods* **15**, 379–386 (2018).
45. Swiecki, M. & Colonna, M. The multifaceted biology of plasmacytoid dendritic cells. *Nat. Rev. Immunol.* **15**, 471–485 (2015).
46. See, P. et al. Mapping the human DC lineage through the integration of high-dimensional techniques. *Science* **356**, eaag3009 (2017).
47. Villani, A. C. et al. Single-cell RNA-seq reveals new types of human blood dendritic cells, monocytes, and progenitors. *Science* **356**, eaah4573 (2017).
48. Satpathy, A. T. et al. Zbtb46 expression distinguishes classical dendritic cells and their committed progenitors from other immune lineages. *J. Exp. Med.* **209**, 1135–1152 (2012).
49. Tel, J. et al. Natural human plasmacytoid dendritic cells induce antigen-specific T-cell responses in melanoma patients. *Cancer Res.* **73**, 1063–1075 (2013).

Acknowledgements

We thank A. G. Rolink (DBM University of Basel), K. M. Murphy (Washington University in St. Louis), and P. Tsapogas (DBM University of Basel) for sharing reagents, expertise and discussions; B. Lambrecht and M. Guillemins (VIB-Ugent Center for Inflammation Research) for sharing data and reagents; M. Busslinger (Research Institute of Molecular Pathology IMP, Vienna) for kindly providing us with *Ebf1*^{βCD2} reporter mice; D. Schreiner and C. King for constant input and critical reading of the manuscript; D. Labes (DBM University of Basel), K. Eschbach and C. Beisel (Department of Biosystems Science and Engineering (D-BSE) University of Zurich, Basel) for excellent technical support; the DBM-Microscopy Core Facility; A. Brühlhart and all the animal caretakers of WRO1060; and C. Cannavo for IT support. This study was supported by SNF project number PP00P3_150714 and by the Novartis Foundation for medical-biological research n.16A052. This work is dedicated to the memory of Ton Rolink.

Author contributions

P.R.F. and R.T. designed the project, performed experiments, interpreted the data and wrote the manuscript. L.A.-S. and R.I. analyzed the RNA-sequencing data and contributed to writing the paper. A.E. and G.E.G.-R. performed experiments. All authors agreed to the submission of the manuscript for publication.

Competing interests

The authors declare no competing interests.

Additional information

Supplementary information is available for this paper at <https://doi.org/10.1038/s41590-018-0136-9>.

Reprints and permissions information is available at www.nature.com/reprints.

Correspondence and requests for materials should be addressed to R.T.

Publisher's note: Springer Nature remains neutral with regard to jurisdictional claims in published maps and institutional affiliations.

Methods

Mice. All animals were bred and maintained in a specific-pathogen-free animal facility according to institutional guidelines (Veterinäramt BS, license number 2786_26606). Mice of the following genotypes were purchased from Jackson Laboratories: C57BL/6J, CD11c-cre⁵⁶, IRF8^{8249C} (ref. 39) and *Irf8*⁶⁰¹ (ref. 51). *Irf8*^{-/-} mice were generated by crossing *Irf8*⁶⁰¹ mice with CMV-Cre mice⁵². *Il7*^{-/-} (ref. 53), *Flt3*^{-/-} (ref. 54), *Ebf1*^{hCD2} (ref. 55), *Irf8*^{88P} (ref. 36) and *Zbtb46*^{ep48} were bred in house. For BM chimera experiments, B6.SJL⁵⁷ mice were purchased from Jackson Laboratories. Unless otherwise indicated, experiments used sex- and age-matched littermates between 6 and 14 weeks of age.

Progenitor-cell harvest. BM was collected from femurs, tibia and pelvic bones. Bones were fragmented with a mortar and pestle, and debris was removed by filtration through a 70- μ m strainer. Red blood cells were lysed with ACK lysis buffer. Cells were counted, then stained for analysis or cell sorting. c-kit^{hi} progenitors were identified as Lin⁻B220⁻Ly6C⁻CD16/32⁻CD117^{int/lo}CD135⁺ cells; CDPs were identified as Lin⁻CD16/32⁻B220⁻Ly6C⁻CD117^{int/lo}CD135⁺CD115⁺CD127⁻ cells¹³; pDC progenitors were gated as Lin⁻CD16/32⁻B220⁻Ly6C⁻CD117^{int/lo}CD135⁺CD115⁺CD127⁻ (CSF1R-IL-7R-NP)²³ and CD317⁺B220⁻CD11c⁺CCR2⁺ (CCR9⁻) cells²⁵; IL-7R⁺ LPs were identified as Lin⁻CD16/32⁻B220⁻Ly6C⁻CD117^{int/lo}CD135⁺CD115⁺CD127⁺ cells; DN, SP and DP progenitors were included within the IL-7R⁺ LP gate and were defined by the expression of SiglecH, and Ly6D, as indicated in Fig. 2a (lineage markers CD3, CD19, Ter119, CD105 and NK1.1). The following gating strategy was used for bulk RNA sequencing: mature BM pDCs were gated as Lin⁻CD11c⁺SiglecH⁺Ly6C⁺Ly6D⁺, whereas mature splenic pDCs were characterized and sorted as Lin⁻SiglecH⁺B220⁻Ly6C⁺. For single-cell RNA sequencing, pDCs from the BM and spleen were sorted as Lin⁻CD11c⁺B220⁻SiglecH⁺. For cell sorting, a BD FACSAria II instrument with a custom built-in violet laser was used. Cells were sorted into PBS supplemented with 0.5% BSA and 2.5 mM EDTA. Cell purities of at least 95% were confirmed by post-sort analysis.

In vivo transfer. 3 \times 10⁴ to 6 \times 10⁴ sort-purified CD45.1 or CD45.2 progenitors were co-injected intravenously at a 1:1 ratio into sublethally irradiated CD45.1/2 mice. The reconstitution ability of progenitors was assessed 4 d after injection, through flow cytometry.

Cell culture. 5 \times 10² to 5 \times 10³ sort-purified progenitors were cultured for 4 d in IMDM (Gibco) supplemented with 10% FCS (MPbio). To induce pDC or cDC development, cells were cultured in the presence of 100 ng/ml recombinant hFLT3L. To induce B cell differentiation, cells were cultured on irradiated OP9 stromal cells in the presence of 100 ng/ml recombinant hFLT3L (Peprotech), as previously described^{38,39}. In some experiments, as indicated, 100 ng/ml recombinant mIL-7 was added. For Transwell experiments (Corning), 5.6 \times 10³ irradiated OP9 stromal cells were plated in the lower compartment, and 2 \times 10³ sort-purified progenitors were cultured either over stromal cells (lower chamber) or in the upper chamber.

Type 1 IFN ELISA. 2 \times 10⁴ mature pDCs and 2 \times 10³ progenitor cells were sort-purified and stimulated with CpG-A 2216 (6 μ g/ml) or CpG-B 1826 (6 μ g/ml) for 16 h at day 0 or after 4 d of culture. Supernatants were analyzed with a Mouse IFN alpha Platinum ELISA Kit (eBioscience).

May-Gruenwald Giemsa staining. Cytospins of 5 \times 10³ sort-purified cells were stained with May-Gruenwald Giemsa (Sigma Aldrich), according to the manufacturer's instructions. Slides were air-dried and sealed with Eukit quick-hardening mounting medium (Sigma Aldrich), and images were taken with a Leica DMI 4000 microscope.

In vitro proliferation assays. Total splenocytes or sort-purified progenitors were stained with CellTrace Violet (Invitrogen), according to the manufacturer's guidelines. Total splenocytes were cultured on dishes coated with anti-CD3 and anti-CD28 (0.5 mg/ml) and were used as a positive control. Dilution of the cell dye was determined by flow cytometry.

OT-II proliferation assays. 2 \times 10³ sort-purified conventional pDCs, pDC-like cells and splenic cDCs were co-cultured with 1 \times 10⁴ labeled OT-II CD4⁺ T cells in the presence of OVA protein (1 μ g/ml) and stimulated with LPS and CpG-A (both at 6 μ g/ml) or left unstimulated. OT-II T cells were labeled with CellTrace Violet (Thermo Fisher Scientific) according to the manufacturer's instructions. Proliferation rates were measured after 4 d in culture. As controls, labeled and unlabeled OT-II T cells were cultured on anti-CD3 (1 μ g/ml) and anti-CD28 (0.5 μ g/ml) precoated wells.

Antibodies and flow cytometry. Cells were stained as previously described¹⁸ with the antibodies listed in the Supplementary Information Note. Cells were analyzed on a BD LSR Fortessa instrument, and data were analyzed with FlowJo X software (TreeStar).

Intracellular cytokine staining. For intracellular cytokine staining, cells were surface stained and subsequently fixed and permeabilized with a BD Cytotfix/Cytoperm Kit.

Quantitative PCR. RNA of sort-purified progenitors was extracted, and cDNA was generated as previously described¹⁸. A KAPA SYBR Fast universal qPCR kit (KapaBiosystems) was used, and samples were run on an Applied Biosystems StepOnePlus qPCR machine. Primers are listed in the Supplementary Information Note.

Statistical analysis. Analysis of all data was done with paired two-tailed Student's *t* test or one-way ANOVA with Tukey post-test with a 95% confidence interval (Prism, GraphPad Software). *P* < 0.05 was considered significant. *0.01 < *P* < 0.05; **0.001 < *P* < 0.01; ****P* < 0.001; *****P* < 0.0001.

RNA-seq analysis. Bulk RNA-seq. Total RNA was isolated from cells with an Ambion RNAqueous Micro Kit. RNA quality was assessed with a Fragment Analyzer. cDNA was prepared with a SMART-Seq v4 Ultra Low Input RNA Kit (Clontech). RNA libraries were prepared with a Nextera XT DNA Library Preparation Kit (Illumina). Indexed cDNA libraries were sequenced on an Illumina HiSeq 2500 machine and Illumina NexSeq 500. The sequence quality of the obtained single end reads (SR51) was assessed with the FastQC tool (version 0.11.3). Reads were mapped to the mouse genome assembly, version mm10 (<http://genome.ucsc.edu/>), with RNA-STAR (version 2.5.2a)⁶⁰ with default parameters. As an exception, reporting for multimappers comprised only one hit in the final alignment files (outSAMmultNmax = 1) and filtering reads without evidence in the spliced junction table (outFilterType = "BySJout"). All subsequent gene expression data analysis was done in the R software package (R Foundation for Statistical Computing). With RefSeq mRNA coordinates from UCSC (<http://genome.ucsc.edu/>, downloaded in December 2015) and the qCount function from the QuasR package (version 1.16.0)⁶¹, we quantified gene expression as the number of reads that started within any annotated exon of a gene. The differentially expressed genes were identified with the Generalized Linear Model (GLM) framework in the edgeR package (version 3.18.1)⁶². Factors indicating mouse IDs were included in the model as covariates. Genes with a false discovery rate < 0.05 and a minimum log₂ FC of 1 were considered differentially expressed genes. Gene set enrichment analysis was performed with the function 'camera' from the edgeR package and with all gene sets from the Molecular Signature Database (MSigDB v5.2). We considered only sets containing more than ten genes and used later implementations of camera, in which correlations of genes within gene sets were set to a fixed value of 0.01. Data were corrected for batch effects (mouse ID) for visualization purposes. A linear model with a single factor indicating mouse ID was fitted to the log-transformed data (The 'voom' function from the edgeR package was used to transform the data, and the lmf function from the limma package (version 3.32.10) was used to fit the model). The residuals from this model were used for PCA and heat-map figures. The developmental heat map was generated as follows: the samples were first ordered according to their developmental stages, and all possible combinations of peak/switch models were fitted to the expression of individual genes with the GLM framework in the edgeR package, with mouse ID used as a covariate. For each gene, the best-fitting model was selected, and the gene was assigned to the corresponding category. All genes with a false discovery rate < 0.05 and a FC > 1 were selected and plotted in Fig. 4c and are listed in Supplementary Table 1. Subsequently, the generated list was filtered for transcription-factor log₂ FC > 1.5 (TF; GO 0003677) and cell-surface-marker log₂ FC > 3 (CS; GO:0009986), both filtered for log₂ CPM > 1 in at least one set of replicates, and log₂ FC > 1.5 values were individually plotted (Supplementary Fig. 4c,d). Each identified set of genes was tested for an enrichment in biological processes (package GO.db version 3.4.1) with the hypergeometric test implemented in the GOSTats package (version 2.42.0).

Single-cell RNA-seq. BM and splenic pDCs were sorted from three mice and counted with a Countess II FL instrument (Life Technologies). 3,000 cells from each sample were loaded on a 10 \times Genomics Chromium Single Cell Controller. Single-cell capture and cDNA and library preparation were performed with a Single Cell 3' v2 Reagent Kit (10 \times Genomics) according to the manufacturer's instructions. Sequencing libraries were loaded on an Illumina NextSeq 500 instrument with high-output 75-cycle kits and paired-end sequenced with the following read lengths: read 1, 26 cycles; read 2, 8 cycles; read 3, 58 cycles. Single-cell sequencing files (basecalls) were processed with the Cell Ranger Single Cell Software Suite (version 2.0.0) to perform quality control, sample demultiplexing, barcode processing and single-cell 3' gene counting (<https://support.10xgenomics.com/single-cell-gene-expression/software/overview/welcome/>). Samples were first demultiplexed and then were aligned to the UCSC mouse (mm10) transcriptome and genome with 'cellranger' with default parameters for all six samples. UMI were counted with 'cellranger count'. Samples were merged with the 'cellranger aggregate' procedure without downscaling. Further analysis was performed in R (version 3.4.0) with the scran (1.4.5) and scatter (1.4.0) packages by following the Bioconductor workflow (for version 3.5). Cells with log library sizes (or log total features) more than three median absolute deviations (MADs) below the median

log library size (or log total features) were filtered out. Similarly, cells with a proportion of reads mapping to the mitochondrial genome more than three MADs above the median percentage of reads mapping to the mitochondrial genome were removed. Low-abundance genes with average \log_2 CPM counts <0.0023 were filtered out. This threshold was estimated from the distribution of average \log_2 CPM counts after fitting two normal distributions (assuming two populations of genes: not expressed – background, and expressed) with Mclust function (mclust version 5.3) and choosing a threshold of $P=0.05$ for background population. Expression values of 11,753 genes for 14,744 cells were kept. The raw UMI counts were normalized with the size factors estimated from pools of cells to avoid dominance of zeros in the matrix⁶³. A mean-dependent trend was fitted to the variances of the log expression values of endogenous genes to distinguish between genuine biological variability and technical noise, under the assumption that most genes are not differentially expressed across cells, and their variance is mainly technical (trendVar function with 'loess' trend and span of 0.01 to better fit the sparse data). Afterward, the fitted technical noise was subtracted, the genes were sorted on the basis of the biological components of their variance, and those with a variance larger than 0.1 were used for clustering of cells and PCA ($n=148$). The clustering of cells into putative subpopulations was done on log expression values (hierarchical clustering on the Euclidean distances between cells, with Ward's criterion to minimize the total variance within each cluster). The clusters of cells were identified by applying a dynamic tree cut⁶⁴, which resulted in eight putative subpopulations. Afterward, the marker genes specific for each cluster were identified with the findMarkers function (scrn package), which fits a linear model to the log-transformed expression values for each gene with the imma framework⁶⁵. The expression profiles of individual clusters were also compared in a pairwise analysis (P values in those analyses were considered only as ranks, because the same data were used for cluster identification and statistical testing).

Reporting Summary. Further information on experimental design is available in the Nature Research Reporting Summary linked to this article.



Data availability. The RNA-seq data generated in the current study are available in the Gene Expression Omnibus database under accession code GSE114315.

References

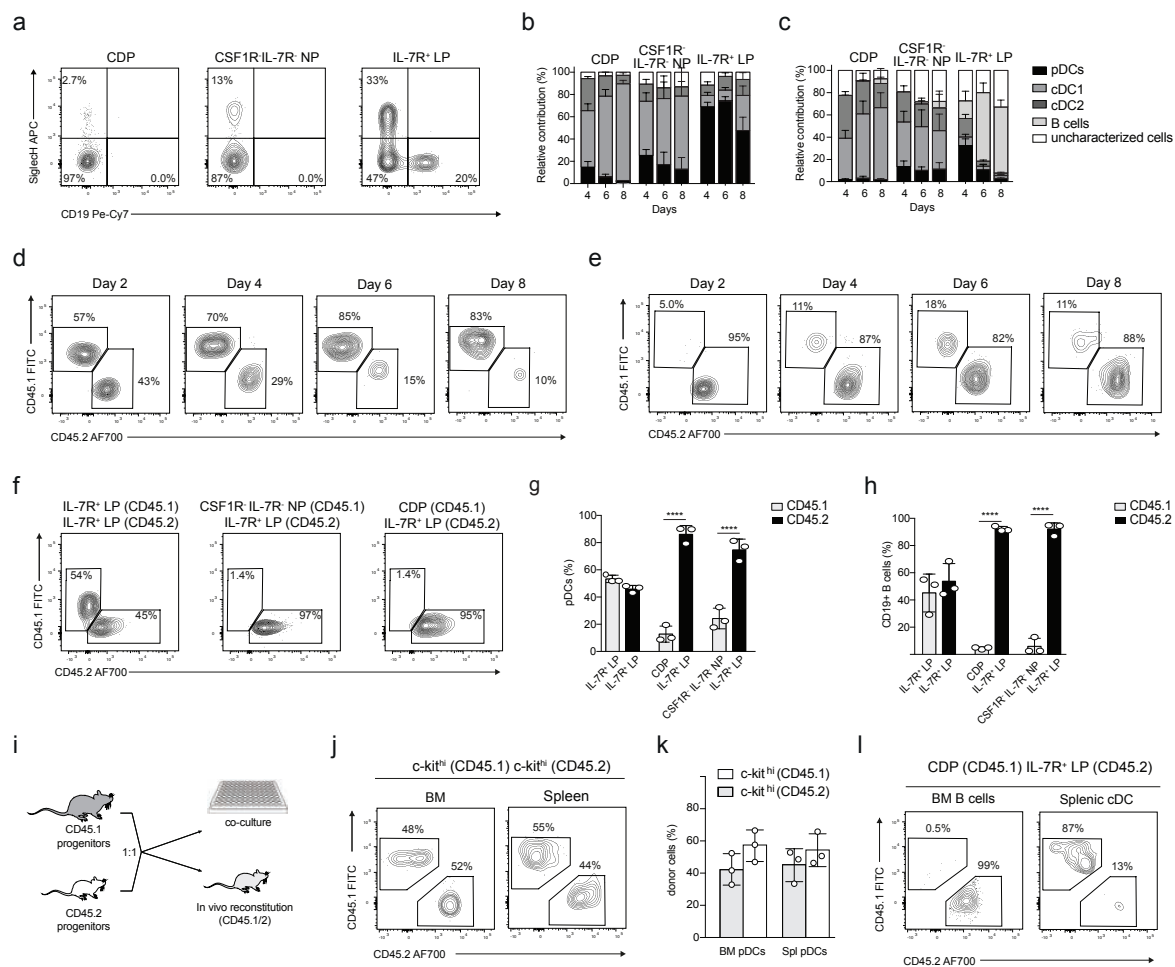
- Caton, M. L., Smith-Raska, M. R. & Reizis, B. Notch-RBP-J signaling controls the homeostasis of CD8⁺ dendritic cells in the spleen. *J. Exp. Med.* **204**, 1653–1664 (2007).
- Feng, J. et al. IFN regulatory factor 8 restricts the size of the marginal zone and follicular B cell pools. *J. Immunol.* **186**, 1458–1466 (2011).
- Schwenk, F., Baron, U. & Rajewsky, K. A cre-transgenic mouse strain for the ubiquitous deletion of loxP-flanked gene segments including deletion in germ cells. *Nucleic Acids Res.* **23**, 5080–5081 (1995).
- von Freeden-Jeffry, U. et al. Lymphopenia in interleukin (IL)-7 gene-deleted mice identifies IL-7 as a nonredundant cytokine. *J. Exp. Med.* **181**, 1519–1526 (1995).
- McKenna, H. J. et al. Mice lacking flt3 ligand have deficient hematopoiesis affecting hematopoietic progenitor cells, dendritic cells, and natural killer cells. *Blood* **95**, 3489–3497 (2000).
- Vilagos, B. et al. Essential role of EBF1 in the generation and function of distinct mature B cell types. *J. Exp. Med.* **209**, 775–792 (2012).
- Wang, H. et al. IRF8 regulates B-cell lineage specification, commitment, and differentiation. *Blood* **112**, 4028–4038 (2008).
- Janowska-Wieczorek, A. et al. Platelet-derived microparticles bind to hematopoietic stem/progenitor cells and enhance their engraftment. *Blood* **98**, 3143–3149 (2001).
- Nakano, T., Kodama, H. & Honjo, T. Generation of lymphohematopoietic cells from embryonic stem cells in culture. *Science* **265**, 1098–1101 (1994).
- Balciunaite, G., Ceredig, R., Massa, S. & Rolink, A. G. A B220⁺ CD117⁺ CD19⁺ hematopoietic progenitor with potent lymphoid and myeloid developmental potential. *Eur. J. Immunol.* **35**, 2019–2030 (2005).
- Dobin, A. et al. STAR: ultrafast universal RNA-seq aligner. *Bioinformatics* **29**, 15–21 (2013).
- Gaidatzis, D., Lerch, A., Hahne, F. & Stadler, M. B. QuasR: quantification and annotation of short reads in R. *Bioinformatics* **31**, 1130–1132 (2015).
- Robinson, M. D., McCarthy, D. J. & Smyth, G. K. edgeR: a Bioconductor package for differential expression analysis of digital gene expression data. *Bioinformatics* **26**, 139–140 (2010).
- Lun, A. T., Bach, K. & Marioni, J. C. Pooling across cells to normalize single-cell RNA sequencing data with many zero counts. *Genome Biol.* **17**, 75 (2016).
- Langfelder, P., Zhang, B. & Horvath, S. Defining clusters from a hierarchical cluster tree: the Dynamic Tree Cut package for R. *Bioinformatics* **24**, 719–720 (2008).
- Ritchie, M. E. et al. limma powers differential expression analyses for RNA-sequencing and microarray studies. *Nucleic Acids Res.* **43**, e47 (2015).

In the format provided by the authors and unedited.

Distinct progenitor lineages contribute to the heterogeneity of plasmacytoid dendritic cells

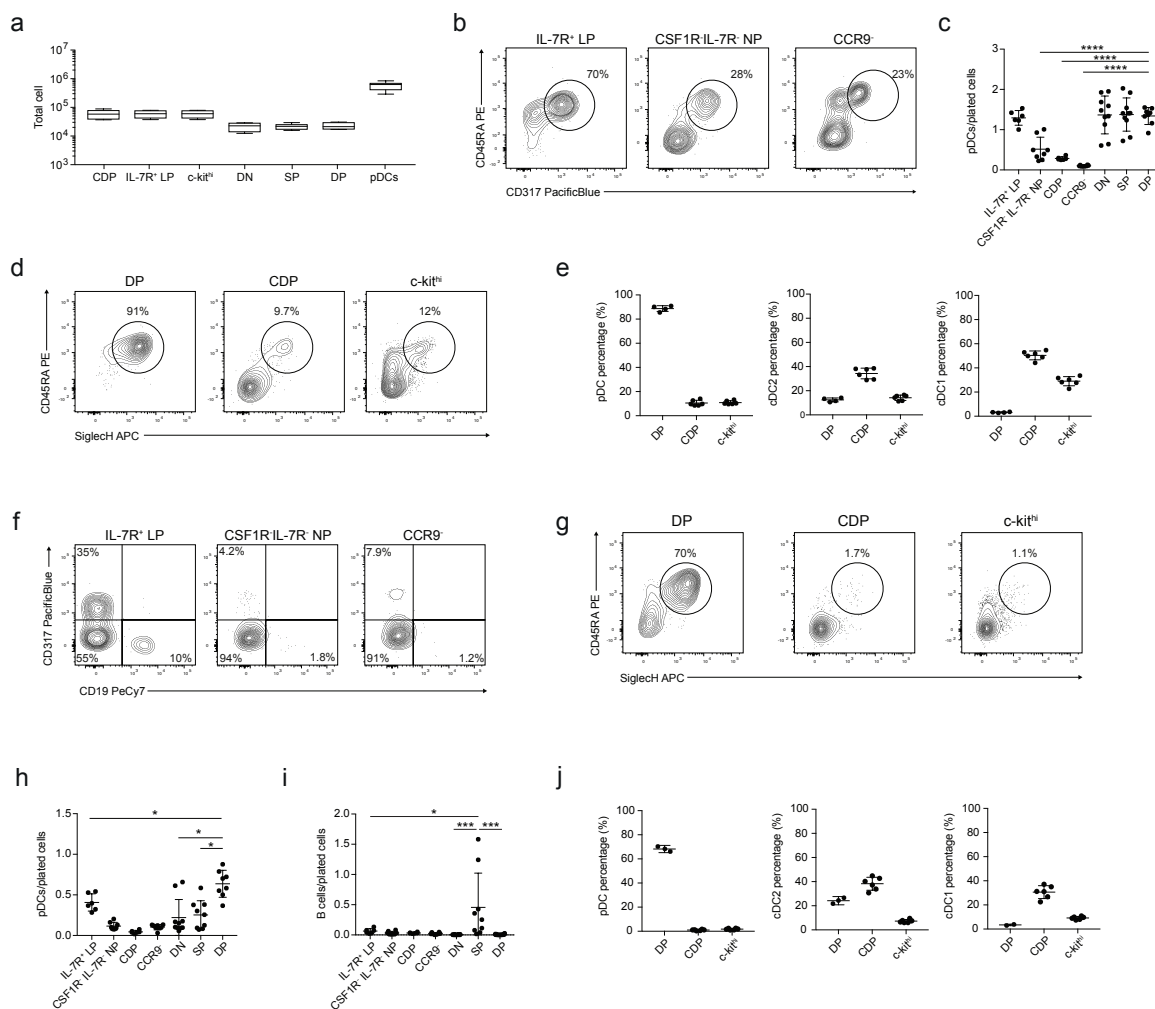
Patrick Fernandes Rodrigues¹, Llucia Alberti-Servera^{1,2}, Anna Eremin¹, Gary E. Grajales-Reyes³, Robert Ivanek^{1,4}  and Roxane Tussiwand¹ *

¹Department of Biomedicine, University of Basel, Basel, Switzerland. ²Department of Human Genetics and VIB Center for the Biology of Disease, Leuven, Belgium. ³Department of Pathology and Immunology, Washington University School of Medicine, St. Louis, MO, USA. ⁴Swiss Institute of Bioinformatics, Basel, Switzerland. *e-mail: rtussiwand@unibas.ch



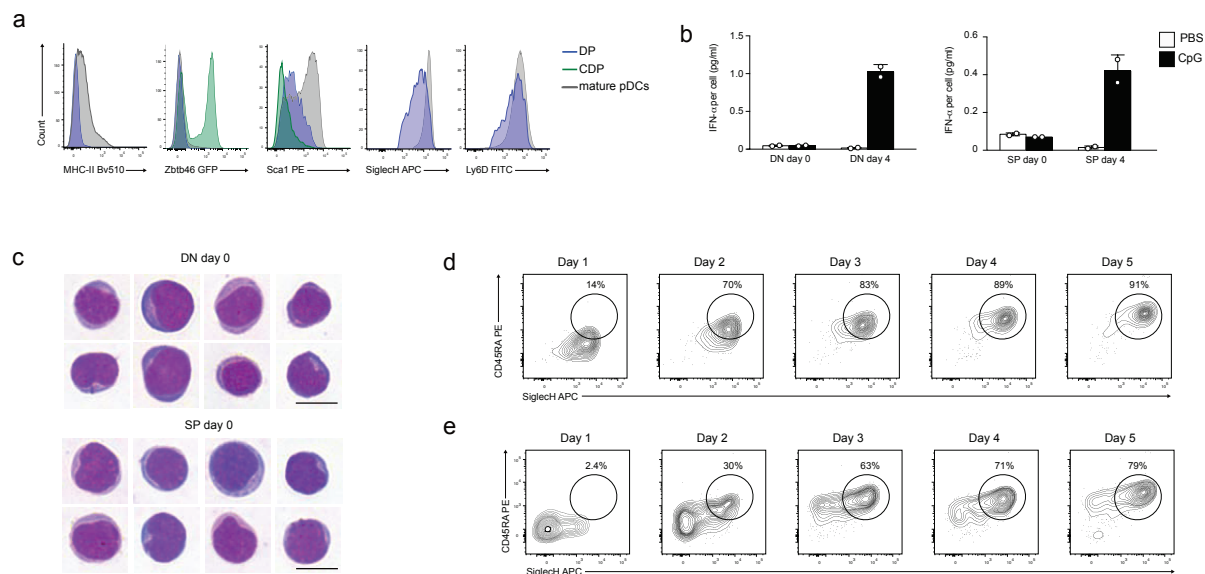
Supplementary Figure 1: pDCs develop primarily from IL-7R⁺ lymphoid progenitors.

(a-c) CDPs, IL-7R⁺ LP and CSF1R⁺IL-7R⁻ NP progenitors as gated in Fig. 1a were cultured over 8 days in the presence of FLT3L (b) or FLT3L and OP9 stromal cells (a,c). Shown are two color histograms for the expression of SiglecH and CD19 at day 4 of culture (a). Relative cell output for pDCs (SiglecH⁺ CD317⁺CD19), cDC1 (SiglecH⁻CD317⁺CD19⁻CD11c⁺MHCII⁺CD24⁺CD11b⁻), cDC2 (SiglecH⁻ CD317⁺CD19⁻CD11c⁺MHCII⁺CD24⁻CD11b⁺) and B cells (CD19⁺) was determined at day 4, 6 and 8 as indicated (n=6 independent experiments, thin line represents the mean +/-s.d.). (d-l) Sort purified progenitors as defined in methods were isolated from CD45.1 and CD45.2 mice and used in a 1:1 ratio for *in vitro* or *in vivo* experiments as explained in Supplementary Fig. 1i. (d,e) Shown are representative two-color histograms pre-gated on SiglecH⁺CD11c⁺ pDCs (d) or pre-gated on SiglecH⁻CD11c⁺MHCII⁺ cDCs (e) of IL-7R⁺ LP (CD45.1) and CDPs (CD45.2) cultured over 8 days in the presence of FLT3L. (n=3 independent experiments). (f) Shown are representative two-color histograms for the expression of CD45.1 and CD45.2 pre-gated on CD19⁺ B cells of progenitor subsets, as indicated co-cultured for 4 days in the presence of FLT3L and OP9 stromal cells. (g,h) Percent output of CD45.1⁺ SiglecH⁺ pDCs (g) and CD19⁺ B cells (h) of progenitors cultured as in (f) (n=3 independent experiments, each dot represents a mouse, thin line represents the mean +/-s.d.). (j-k) Bone marrow and splenic SiglecH⁺CD317⁺ pDC output was determined 4 days after *in vivo* i.v. co-transfer of CD45.1 and CD45.2 Lin⁻B220⁻Ly6C⁻CD117^{hi}CD135⁺ (c-kit^{hi}) progenitors. Shown are representative two-color histograms for the expression of CD45.1 and CD45.2 (j) or percent donor derived pDCs in BM and spleen (k) (n=3 independent experiments). (l) CD19⁺ BM B cells and splenic SiglecH⁻CD317⁺CD19⁻CD11c⁺MHCII⁺ cDC output was determined 4 days after *in vivo* i.v. co-transfer of CD45.1 CDPs and CD45.2 IL-7R⁺ LP (n=6 independent experiments). Shown are representative two-color histograms for the expression of CD45.1 and CD45.2. Statistical analysis was done using two-way ANOVA with Tukey post-test (g,h,k) (* = p < 0.05, ** = p < 0.01, *** = p < 0.001, **** = p < 0.0001).



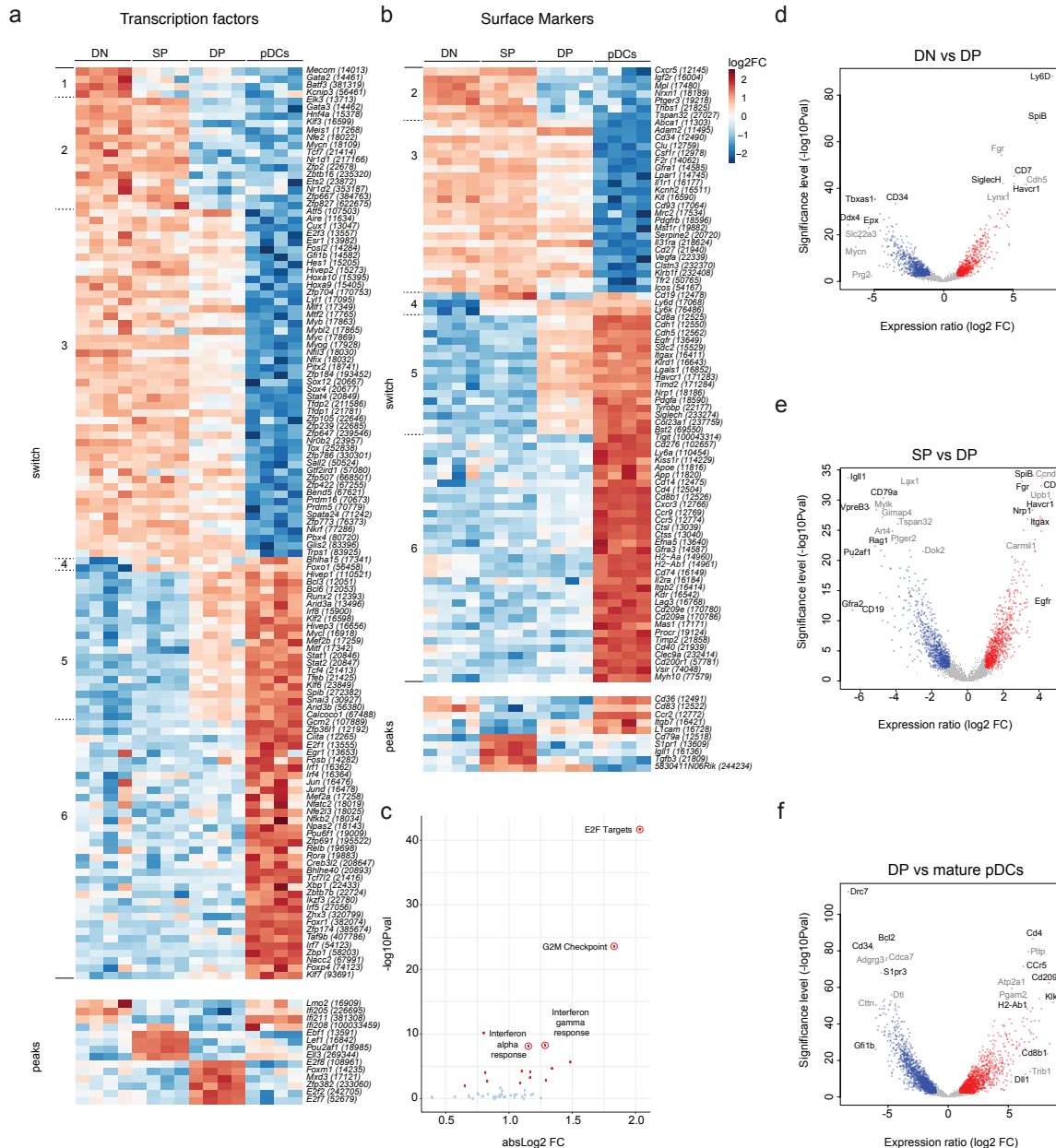
Supplementary Figure 2: SigleCH⁺Ly6D⁺ IL-7R⁺ LPs have exclusive pDC potential.

(a) Shown are box plots (median, range and 25th/75th percentile) for the frequency in the bone marrow of C57BL/6 mice of progenitors and mature CD45RA⁺CD317⁺ pDCs as indicated (n=6 independent experiments). (b-j) Sort-purified CD317⁺B220⁺CD11c⁺CCR9⁻ (CCR9⁺), Lin⁻B220⁻Ly6C⁻CD117^{high}CD135⁺ (c-kit^{hi}), CDPs, CSF1R/IL-7R NP, IL-7R⁺ LP and DP precursors, as defined in Methods, were cultured for 4 days in the presence of FLT3L (b-e) or in the presence of FLT3L and OP9 stromal cells (f-j). Shown are representative two-color histograms for the indicated markers (b,d,f,g), the total output (c,h,i) and the percent (e,j) mature CD45RA⁺CD317⁺ pDCs, SigleCH⁺CD317⁺CD19⁻CD11c⁺MHCII⁺CD24⁺CD11b⁻ cDC1, SigleCH⁺CD317⁺CD19⁻CD11c⁺MHCII⁺CD24⁺CD11b⁺ cDC2 and CD19⁺ B cells derived from the indicated progenitors (n=3 (d,e,g,j) n=5 (b,c,f,h,i) independent experiments, thin line represents the mean +/-s.d.). Statistical analysis was done using one-way ANOVA with Tukey post-test (c,h,i) (* = p < 0.05, ** = p < 0.01, *** = p < 0.001, **** = p < 0.0001).



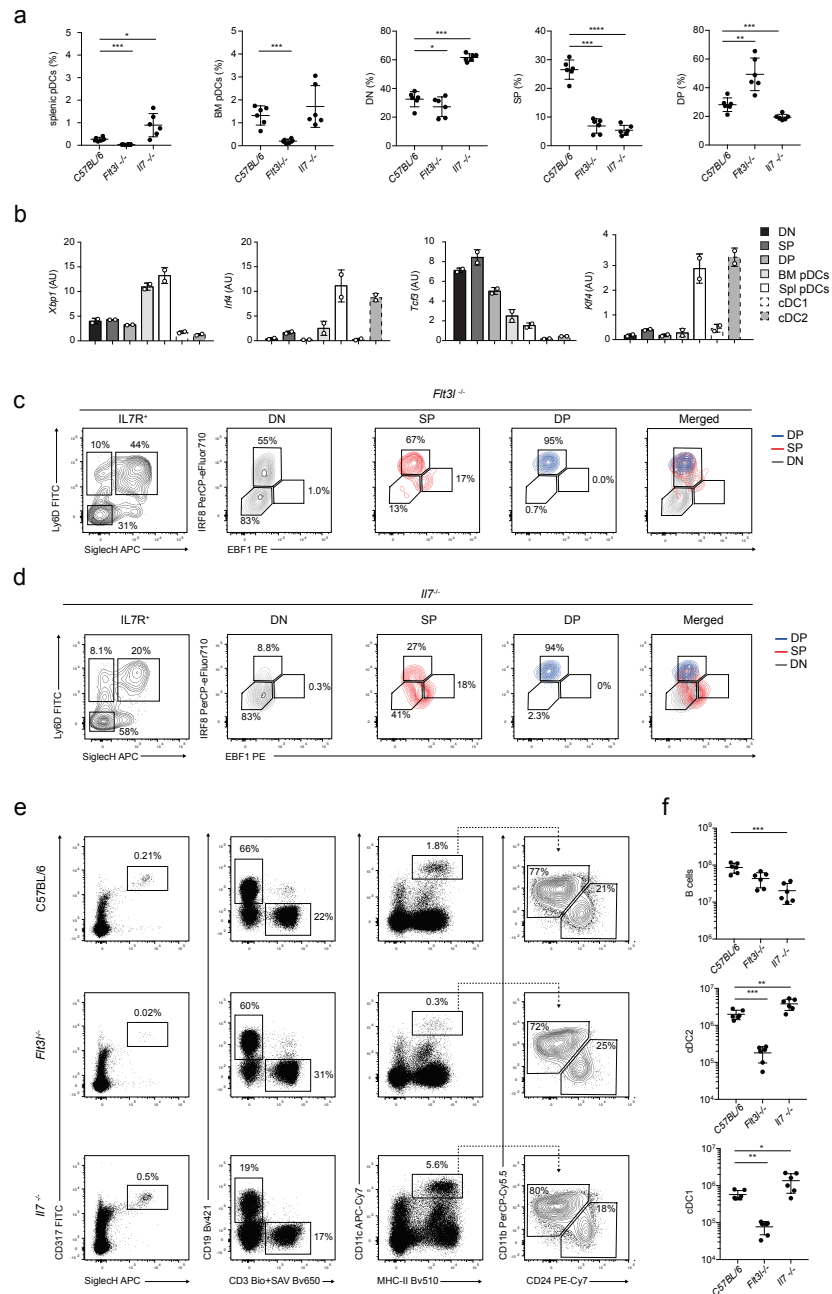
Supplementary Figure 3: SiglecH⁺Ly6D⁺ DP cells are bona fide pDC progenitors.

(a) Shown are single-color histograms for the indicated markers expressed by DP progenitors (blue), CDPs (green), mature pDCs (gray) ($n=3$ independent experiments). (b) IFN- γ was measured on supernatant collected 16h after stimulation with CpG-A from DN or SP progenitor cultured over-night (day 0) or after 4 days in the presence of FLT3L, as indicated ($n=3$ independent experiments, shown is a representative experiment). Each dot represents a technical replicate, thin line represents the mean \pm s.d.). (c) May-Gruenwald staining on cytopins of *ex-vivo* sort-purified DN and SP progenitors as described in Methods (8 representative images taken from 3 independent experiments, scale=10 μ m). (d,e) DP (d) and SP (e) progenitors were sorted as described in Methods and cultured over 5 days in the presence of FLT3L. Shown are representative two-color histograms for the expression of CD45RA and SiglecH at the indicated time points ($n=3$ independent experiments).



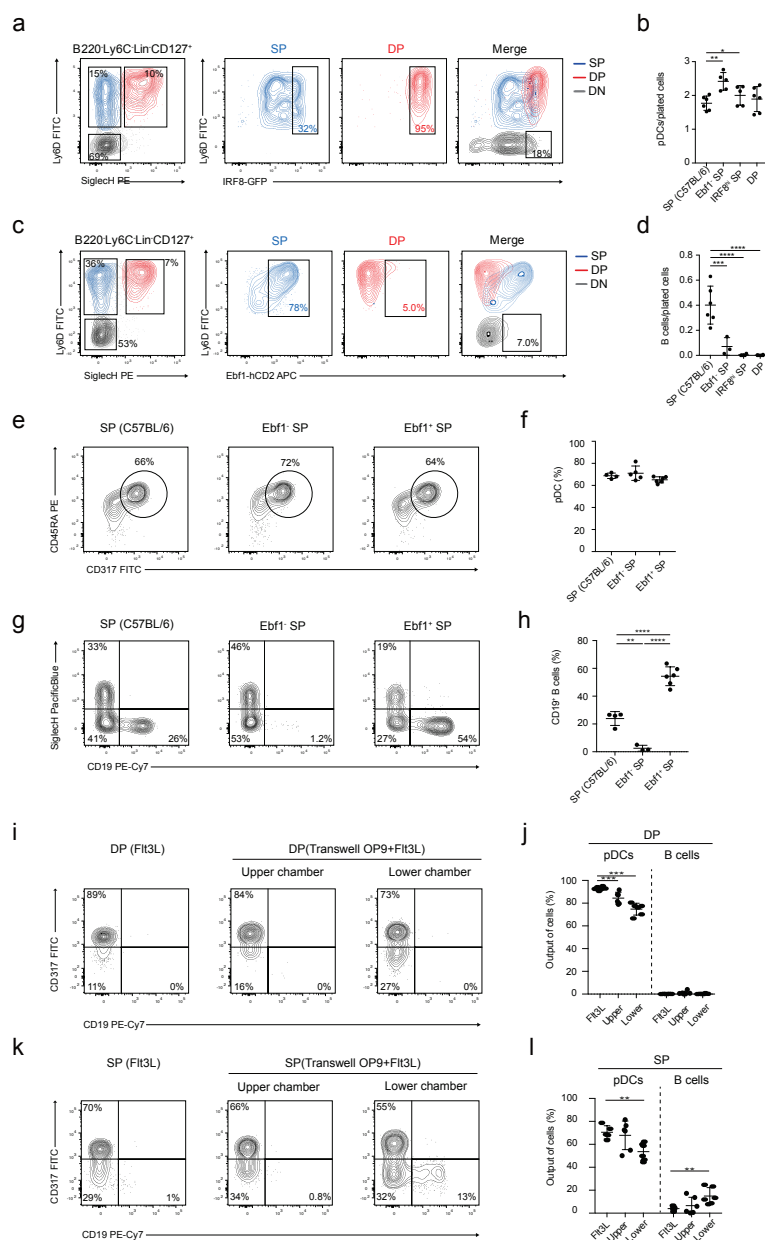
Supplementary Figure 4: Stage-specific transcriptional signatures define pDC commitment.

(a-f) RNASeq was performed on sort purified DN, SP, DP and mature BM pDCs as described in Methods. (a,b) Shown are developmental heatmaps, as described in Fig 4c, for transcription factors with expression values $\log_2FC > 1.5$ (a), or cell-surface markers with expression values $\log_2FC > 3$ (b). (c) Shown is Gene-Set Enrichment Analysis (GSEA) performed on Hallmark Signatures comparing DP pre-pDC progenitors with mature pDCs. (d-f) Volcano plots showing pair-wise comparisons of DP pre-pDC against DN, SP and mature pDC transcripts as indicated. Depicted in red are up-regulated transcripts ($\log_2FC > 1$), in blue down-regulated transcripts ($\log_2FC < -1$). (n=4 independent experiments. For each experiment, all progenitors were obtained from one mouse).



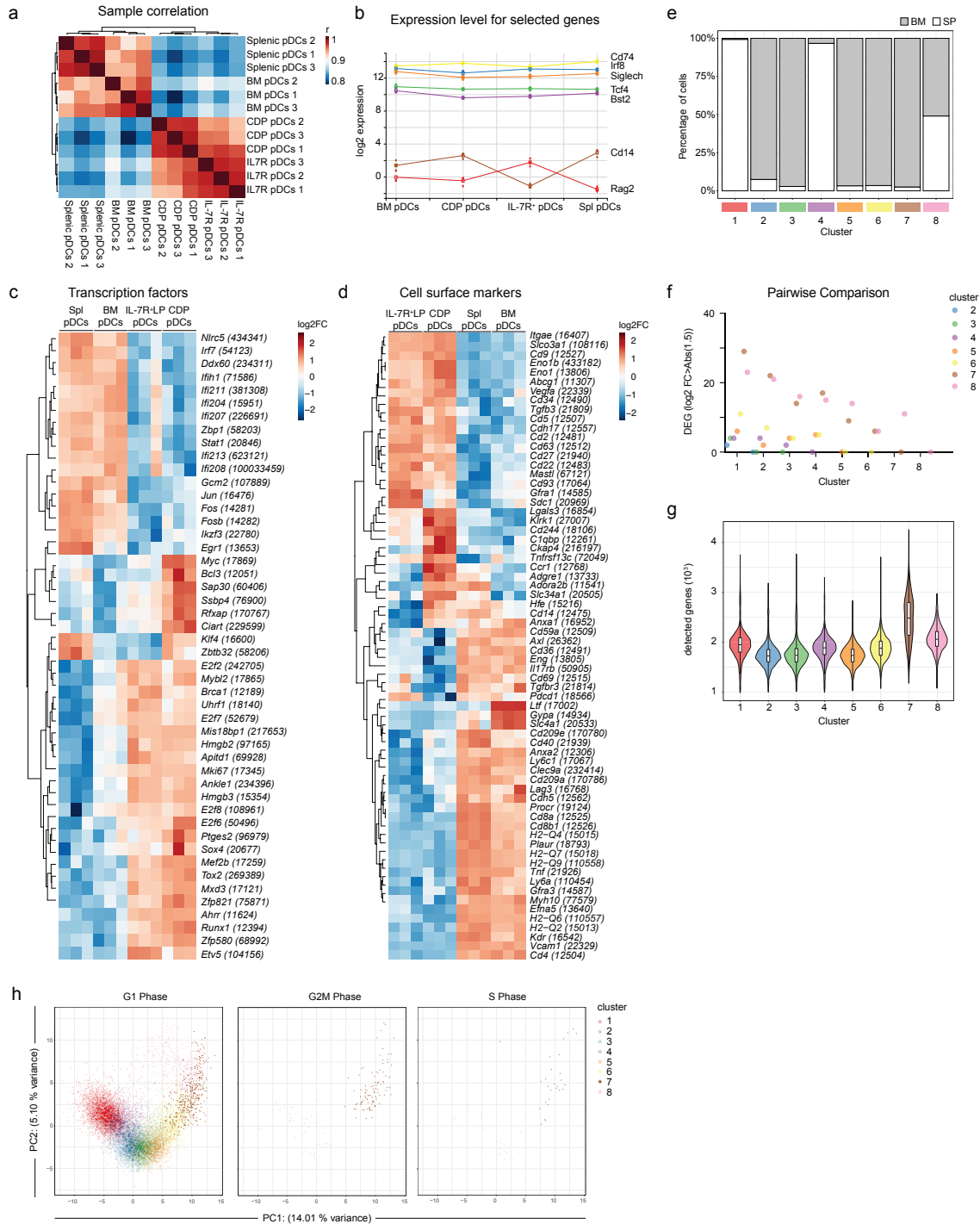
Supplementary Figure 5: Expression of IRF8 at the SP stage marks pDC lineage commitment.

(a) Shown are percent mature BM and splenic pDCs, DN, SP and DP progenitors, gated as described in Methods present in C57BL/6, *Flt3L*^{-/-} and *IL-7*^{-/-} mice. (b) QRT-PCR of the indicated genes on sort purified DN, SP and DP progenitors, gated as described in Methods, SiglecH⁺B220⁺Ly6D⁺Ly6C⁺ BM mature and SiglecH⁺CD317⁺CD11c⁺ splenic mature pDCs, splenic CD11c⁺MHCII^{hi}CD24⁺XCR1⁺cDC1 and CD11c⁺MHCII^{hi}CD11b⁺Sirp-a⁺cDC2. (n=3 independent experiments, shown are mean values of representative results, dots represent technical replicates +/-s.d.). (c-f) C57BL/6, *Flt3L*^{-/-} and *IL-7*^{-/-} mice were analyzed. Shown are representative two-color histograms (c-e) for the indicated markers and total splenic CD19⁺ B cells, CD11c⁺MHCII^{hi}CD24⁺CD11b⁺cDC1, and CD11c⁺MHCII^{hi}CD24⁺CD11b⁺cDC2 (f) of mice of the indicated genotype. (c-d) DN (black), SP (red) and DP (blue) progenitors, pre-gated as described in Methods were analyzed for the expression of IRF8 and EBF1 (right panels) in *Flt3L*^{-/-} (c) and *IL-7*^{-/-} (d). ((a,c-f) n=6 independent experiments. (f) Individual mice are plotted, mean +/- s.d). Statistical analysis was done using two-tailed Student's t test (f) (* = p < 0.05, ** = p < 0.01, *** = p < 0.001, **** = p < 0.0001).



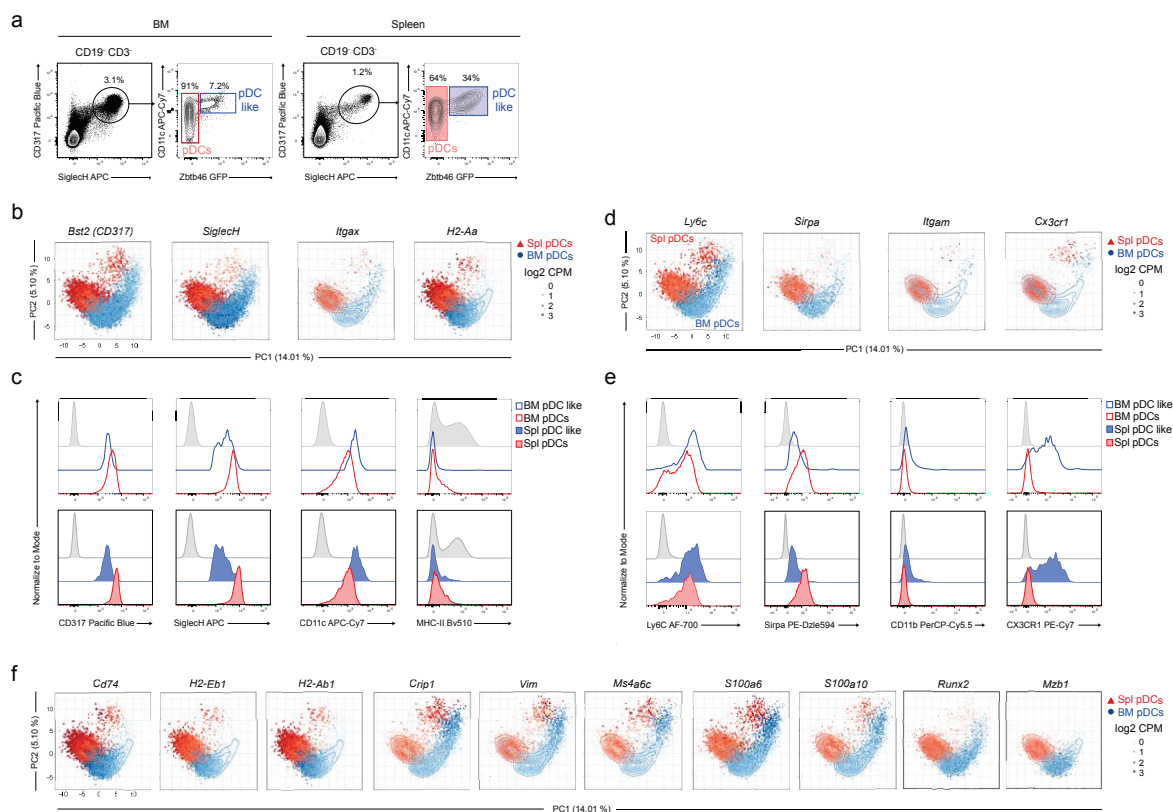
Supplementary Figure 6: IRF8 and EBF1 define pDC and B cell lineage dichotomy.

(a,c) Shown are gating strategies for DN, SP and DP progenitors in IRF8-eGFP (a) and Ebf1-hCD2 (c) reporter mice (n=3 independent experiments, shown is a representative experiment). (b,d) Shown is the total output of CD45RA⁺CD317⁺ pDCs (b) or CD19⁺ B cells (d) per plated progenitor cell cultured in the presence of FLT3L (b) or FLT3L and OP9 stromal cells (d) (n=3 independent experiments, shown is mean +/-s.d.). (e-h) Shown are two color histograms (e,g) for the expression of CD45RA/CD317 (e) and Siglech/CD19 (g) of sort-purified SP progenitors from C57BL/6, Ebf1⁻ SP and Ebf1⁺ SP progenitors, from Ebf1-hCD2 reporter mice as indicated culture for 4 days in the presence of FLT3L (e,f) or FLT3L with OP9 stromal cells. (g,h) Shown are mean +/-s.d. for percent CD45RA⁺CD317⁺ pDCs (f) and CD19⁺ B cells (h) obtained as described in e and g (n=3 independent experiments). (i-l) Shown are two color histograms for the expression of CD317/CD19 (i, k), and percent CD317⁺CD45RA⁺ pDCs and CD19⁺ B cells (j, l) of DP (i,j) and SP (k,l) progenitors isolated as described in Methods from C57BL/6 mice and cultured for 4 days in regular (left panels) or transwell® culture plates (middle and right panels). Progenitors cultured in transwell® were plated either in direct contact with OP9 stromal cells (lower chamber) or on the upper chamber, as indicated. (n=5 independent experiments. Shown are mean +/-s.d.). Statistical analysis was done using one-way ANOVA with Tukey post-test (b,d,h) or two-tailed Student's t test (j,l) (* = p < 0.05, ** = p < 0.01, *** = p < 0.001, **** = p < 0.0001).



Supplementary Figure 7: Single-cell analysis unravels pDC heterogeneity.

Single cell RNA sequencing delineates heterogeneous clusters within mature pDCs. **(a-d)** RNA Sequencing was performed as described in Methods on mature BM and splenic pDCs, and on in vitro generated pDCs from IL-7R⁺ LPs and CDPs. **(a)** Hierarchical clustering of all samples based on Pearson's correlation coefficient calculated on 25% of genes with highest variance (calculated as inter-quartile range). **(b)** Shown is the average expression level across all samples for the indicated genes. **(c-d)** Shown are relative expression levels for differentially expressed transcription factors **(c)** or cell-surface genes **(d)** (log₂FC > 1.5). **(e)** The 8 clusters, identified from the single cell RNA sequencing analysis (Fig. 7d and 7e) are plotted as percentage. **(f)** Shown is the number differentially expressed genes (DEG) (Log₂FC > abs(1.5)) of the identified clusters as a pairwise comparison. **(g)** The total number of detected genes is plotted for each cluster as a violin plot (median, range and 25th/75th percentile). **(h)** PCA analysis for the identified clusters for genes related to G1/G0, G2 and S phase. Cells for bulk and single cell RNASeq were harvested from 3 mice on three independent experiments.



Supplementary Figure 8: Phenotypic characterization of pDC-like cells.

(a-f) (a) Shown are the gating strategies for CD317⁺Siglech⁺Zbtb46-GFP⁻pDCs (red) and CD317⁺Siglech⁺Zbtb46-GFP⁺pDC like cells (blue) pre-gated on CD3⁻CD19⁺ cells (n=5). (b,d,f) Single cell analysis of BM and splenic pDCs as described in Fig. 7. Shown is the relative expression level for the indicated genes. The size of each dot corresponds to the relative expression of a given gene for each cell. Contour lines indicate density of the BM (blue) and splenic (red) cells in the PCA space. (c,e) Single-color histograms for the indicated surface markers expressed by BM (empty) or splenic (full) pDCs (red) and pDC like cells (blue) gated as in a. (n=3).

Supplementary Methods

Supplementary Tables

All supplementary tables can be downloaded online under following link:

<https://www.nature.com/articles/s41590-018-0136-9#Sec32>

Supplementary Table 1: Stage-specific transcriptional signatures

Listed are all genes shown in Fig. 4c with a fold change >1 and p-value < 0.05 . A generalized linear model (GLM framework of "edgeR" package) was used to generate the selection of the genes listed.

Supplementary Table 2: Stage-specific Gene Ontology (GO) enrichment analysis

Listed are GO enriched biological processes within the indicated switch and peak regions. The "Size" corresponds to the total number of genes in the process (from the universe), whereas the "Count" values stand for the number of genes in the peak/switch regions, which are members of this process. The "ExpCount" describes the expected number of genes in the process, given the number of genes in process and size of the peak/switch set. The "OddsRatio" is the ratio between the "Count" and the "ExpCount". Only sets containing more than 10 genes were considered. Universe: all genes from mouse genome version mm10 having at least 1 count in the dataset (16,200 genes).

Supplementary Table 3: Top hit genes for each cluster

Listed are all genes sorted by the „Top“ value, which specifies the size of the candidate marker set from each pairwise comparison. This set allows the cluster to be distinguished from the others based on the expression of at least one gene.

Antibodies:

Antibody	Clone	Supplier	Fluorophor	Dilution	Catalog Nr.
CD3	17A2	Biologend	Bio	1/1600	100244
CD3	17A2	Biologend	Pacific Blue	1/200	100214
CD11b	M1/70	Biologend	PerCP-Cy5.5	1/800	101228
CD11c	N418	Biologend	APC-Cy7	1/400	117324
CD19	6D6	Biologend	Pe-Cy7	1/400	115520
CD19	6D5	Biologend	Pacific Blue	1/1600	115523
CD24	M1/69	Biologend	Pe-Cy7	1/1600	101822
CD45.1	A20	Homemade	FITC	1/800	-
CD45.2	104	Biologend	AF700	1/400	109822
CD45R	RA3-6B2	Biologend	PeDazzle 594	1/1000	103257
CD45RA	14.8	Miltenyi	PE	1/200	130-102-526
CD86	GL-1	Biologend	PE	1/800	105007
CD103	2E7	eBioscience	PE	1/100	12-1031-82
CD115	AFS98	eBioscience	Pe efluor610	1/800	61-1152-80
CD115	AF298	Biologend	Bv605	1/800	135517
CD117	2B8	Biologend	APC-Cy7	1/200	105825
CD117	2B8	Biologend	Bv711	1/800	105835
CD127	eBioSB/199	eBioscience	Pe-Cy7	1/100	25-1273-82
CD135	A2F10	eBioscience	PerCP eFluor710	1/100	46-1351-82
CD135	A2F10	eBioscience	PE	1/100	12-1351-83
CD172 α	P84	Biologend	Pe/Dazzle 594	1/500	144016
CD317	927	Biologend	AF488	1/200	127012
CD317	927	Homemade	Pacific Blue	1/400	-
Ebf1	T26-818	BD	PE	1/200	565494
hCD2	RPA-2.10	Biologend	APC	1/200	300213
Irf8	V3GYWCH	eBioscience	PerCP-eFluor 710	1/200	46-9852-80
Ly6C	HK1.4	Biologend	AlexaFluor700	1/200	128024
Ly6D	49-H4	Biologend	FITC	1/400	138606
Ly6D	49-H4	Biologend	PE	1/1600	138604
MHCII	M5/114.15.2	Biologend	BV 510	1/400	107635
NK1.1	PK136	Biologend	BV421	1/1000	108732
SiglecH	551	Homemade	APC	1/1000	-
Ter119	Ter119	Biologend	Pacific Blue	1/200	116232

Primer Sequences:

Bcl11a FW	GATAAGCCGCCTTCCCCTTC
Bcl11a RW	GGGGATTAGAGCTCCGTGTG
Mtg16 FW	CAGCAGTTTGGCAGTGACATC
Mtg16 RW	GCACAGTGCAGGAGCTCAC
Irf8 FW	AAGGGCGTGTTTCGTGAAG
Irf8 RW	GGTGGCGTAGAATTGCTG
Tcf4 FW	TGAGATCAAATCCGACGA
Tcf4 RW	CGTTATTGCTAGATCTTGACCT
Tcf4 common RW	TGCTGGCTGCTGGCTTGAGGAA
Tcf4L FW	CCAGGAACCCTTTCGCCACCAAAC
Tcf4S FW	ATCCCGGGCATGGGCGGCAACTC
Runx2 FW	CAACTTCCTGTGCTCCGTG
Runx2 RW	CGGCCACAAATCTCAGATC
SpiB FW	CACTCCCAAACCTGTTTCAGC
SpiB RW	TGGGGTACGGAGCATAAG
IRF7 FW	TGGAGTTAACCTGCCACCC
IRF7 RW	CTGAGGCTCACTTCTTCCCT
Ebf1 FW	CAGGAAACCCACGTGACAT
Ebf1 RW	CCACGTTGACTGTGGTAGACA
Batf3 FW	AGACCCAGAAGGCTGACAA
Batf3 RW	CTGCACAAAGTTCATAGGACAC
Id2 FW RT	CATGAACGACTGCTACTCCAA
Id2 RW RT	GTGATGCAGGCTGACGATAGT
Xbp1 FW	GCGCAGACTGCTCGAGATAG
Xbp1 RW	CACCTCTGGAACCTCGTCAG

IRF4 FW	CGGCCCAACAAGCTAGAAAG
IRF4 RW	TCTGTCTCTGAGGGTCTGGA
Tcf3 FW	TTCCACGTTCCCTAGGAGCTG
Tcf3 RW	GCTGGGGAATGAGGGGTAAT
Klf4 FW	GAAGGGAGAAGACACTGCGT
Klf4 RW	TCGTTGAACTCCTCGGTCTC
B-actin FW	CTGTCGAGTCGCGTCCACC
B-actin RW	CGCAGCGATATCGTCATCCA

Discussion:

The origin of pDCs has long been controversial and committed progenitors to this lineage have never been described. Here we show that pDC development occurs predominantly from an IL-7R expressing lymphoid progenitor and not from CDPs or the previously identified CSF1R⁺IL-7R⁻ NP precursors^{56,60}. The expression of Ly6D and SiglecH within the IL-7R LPs marks a specification to the pDC lineage *in vitro*. We could further show that this developmental stage is dependent on high expression of IRF8 and still requires two rounds of proliferations until achieving complete maturation into pDCs. Specification towards the pDC lineage in IL-7R LPs starts at the Ly6D⁻SiglecH⁻ DN stage, which shows the broadest lineage differentiation potential, proceeds to the Ly6D⁺SiglecH⁻ SP stage, which can differentiate towards B- or pDCs depending on the expression of either EBF1 or IRF8, respectively, and is completed at the DP stage.

Additionally, we were able to show that high expression of IRF8 within the SP progenitors marks pDC lineage commitment concomitant with the loss of B cells potential. At this stage of development, besides high expression of IRF8, none of master regulators for pDC development are present, such as TCF4_L, suggesting that pDC lineage specification is TCF4 independent but IRF8 dependent. However, how the dichotomy of pDC versus B cell choice is induced and regulated by *Irf8* and *Ebf1* is still unresolved and matter of investigation. A possible candidate factor which could poise the balance between EBF1 and IRF8 is the transcription factor Zinc Finger Protein 521 (Zfp521). Zfp521 is a DNA binding protein that contains 30 Krüppel-like zinc fingers and has been implicated in the differentiation of multiple cell subsets, including HSCs and B lymphocytes^{271, 272}. Zfp521 showed up in our RNA sequencing analysis as progressively increased during pDC lineage commitment. It is expressed at low levels already on DN and SP progenitors and its expression gradually increases on DP pre-pDCs, peaking on mature pDCs. It has been reported that *Ebf1* expression and B cell specification are inhibited by Zfp521, through active binding of the *Ebf1* carboxyl-terminal region²⁷¹. In support to their hypothesis, the authors further showed that B cell development is strongly enhanced in Zfp521 knockdown experiments²⁷¹. Taken together, it is possible that increased Zfp521 expression levels might induce the inhibition of *Ebf1* and therefore mediate pDC commitment by preventing the specification towards the B cell lineage. Nevertheless, how this is achieved and the role of IRF8, *Ebf1* or Zfp521 is still unclear. Zfp521 deficient mice were recently generated and characterized, revealing an unexpected defect in

CLPs as well as B and T cell precursors²⁷³, arguing for a more complex transcriptional network, than previously hypothesized. The observed findings could be explained by either cell extrinsic mediated changes of the bone marrow microenvironment which then affects lymphoid development, or cell intrinsic processes, which would alter early hematopoietic progenitors impairing lymphoid lineage specification. To be able to understand the function of *Zfp521* during lymphopoiesis the generation of conditional mice is necessary, where *Zfp521* can be specifically ablated at different stages of development and within specific subsets.

Other questions such as how IRF8 shapes pDC development and which intrinsic or extrinsic cell signals mediate the development and specification towards the pDC lineage, still remain unclear. The fact that pDC commitment in lymphoid progenitors goes along with high expression levels of IRF8, additionally opens up the question about the transcriptional role of IRF8 in pDC development. It could well be that an autoregulatory induction of IRF8 mediates pDC lineage specification, similarly to the one described for cDC1³⁷. This autoregulatory loop might result in the accumulation of IRF8 within progenitors which would ultimately promote the expression of pDC lineage specific genes such as *Tcf4_L*, *Zeb2*, *IRF7* and *SpiB* and mediate the commitment towards pDC lineage.

The proliferation rate of progenitors within a specific niche might also be a key factor determining the accumulation or dilution of transcription factors such as IRF8, as it has been suggested for PU.1 during B cell versus macrophages lineage choice²⁷⁴. The close proximity of progenitors to an IL-7 rich BM niche induces proliferation and therefore dilution of IRF8, which possibly allows for the expression of B cell lineage determining transcription factors such as *Ebf1* and *Pax5*. On the other hand, progenitors which progressively proliferate would move away from the IL-7-rich niche, thus reducing their proliferation rate, accumulate high IRF8 levels, and therefore commit to the pDC lineage. Indeed, we confirmed that expression of IRF8 plays a major role during pDC development: neither DP pre-pDCs nor conventional mature pDCs develop in *Irf8* deficient or *Irf8*^{R249C} mutant mice. Further, an alternative type of pDCs, which has reduced expression of pDC markers and is unable to produce Type I IFN, expands in these mice. This “pDC-like” cells also express several features reminiscent of cDCs, such as high levels of MHC-II, co-stimulatory molecules and CD11c, and are able to capture, process and present antigen to naïve CD4 T cells. The complete absence of mature pDCs and the expansion of these alternative pDC-like cells in IRF8 mutant mice, could suggest that deletion of IRF8 in hematopoietic progenitors may differently impair the generation of pDCs and pDC-like cells. While pDCs would strictly dependent on the expression of IRF8, its absence would not impair pDC-like development. Further, hypothesizing that pDCs would

mostly differentiate from lymphoid, while pDC-like cells from myeloid progenitors, IRF8 deficiency would only impair the lymphoid branch. To validate this hypothesis, we need to generate lines in which IRF8 is specifically deleted on individual progenitors. Those studies are currently ongoing. An Alternative scenario, would be compatible with a migratory defect in DP pre-pDCs of IRF8 deficient mice: excessive migration from the BM to the periphery, would result in reduced BM pDCs and increased splenic pDC-like cells. Other explanations are also possible, such as overall perturbed hematopoietic development in IRF8 deficient mice. Collectively, more studies are required to identify and characterize the key intrinsic and extrinsic factors of pDC development.

To better understand the transcriptional regulation that leads to the progressive differentiation and generation of pDC and pDC-like cells we plan to perform next generation single cell sequencing on distinct BM progenitors as well as mature pDCs. Cellular indexing of transcriptome and epitopes sequencing (CITE-Seq) is a new method that combines detection of surface antigens with whole RNA sequencing at a single cell level ²⁷⁵. Currently, most of the studies either use cell sorting to determine the lineage and differentiation potential of progenitors or use genome wide sequencing either on specific subsets or at a single cell level. The possibility to analyze the transcriptome of single cells gating on specific progenitors, for which we would know the developmental options, is an attractive approach. In parallel single cell ATAC sequencing (scATAC-seq) allows us to dissect the epigenomic regulation ²⁷⁶. The complexity of single cell approaches has exponentially increased over the past years and the challenge remains in developing the computational tools for the analysis. Efforts in designing lineage developmental maps based on single cell RNA sequencing exist, however how to translate them into epigenomic regulation is still an open question.

A novel computational fate-mapping analysis (FateID) that was recently developed was used to analyze hematopoiesis ²⁷⁷. In agreement with our data, this study shows that B cells and pDCs originate from a common progenitor, which expresses IL-7R. Furthermore, two recent studies highlighted the presence of a small fraction of cells in human peripheral blood that share pDC markers and which also have myeloid features ^{268, 269, 270}. This subset, defined as AS-DCs or pre-DCs, appears related to our pDC-like cells. What remains to be defined, besides the developmental origin of pDC and pDC-like cells, is their function. pDC-like cells resemble conventional pDCs but express myeloid specific markers, such as Zbtb46. The use of Zbtb46-GFP reporter mice allowed us to discriminate conventional pDCs from the newly identified pDC-like cells. A direct comparison of these two pDC subsets revealed that beyond phenotypical they also have functional differences. Both subsets produced equal amounts of

IFN- α upon CpG-A stimulation, but only conventional pDCs did respond to CpG-B. Importantly, only pDC like could process and present antigens to T cells, a feature characteristic of cDCs.

The identification of these two distinct pDC subsets has several implications. Firstly, we can now isolate and functionally characterize both subsets in greater detail. A multitude of functions have been attributed to pDCs, with often conflicting data in literature. It is conceivable that the presence of pDC-like cells could have accounted for the antigen presentation ability of conventional pDCs amongst the different functions. Furthermore, the involvement of pDCs in mediating and/or sustaining diseases has to be reevaluated. The presence of high levels of IFNs is a hallmark for many autoimmune conditions, such as SLE and arthritis, and has long been attributed to the sustained activation of pDCs in these patients. However, the pathogenesis of the disease is still unclear. On one hand, activated pDCs could sustain high IFN levels in the serum of these patients, while pDC like cells could account for the priming of autoreactive T cells. It will be essential to determine the role of both subsets during the priming as well as during the onset of disease. In this regard it becomes essential to specifically target each subset individually. By looking at the transcriptional profiles of conventional pDCs and pDC-like cells, we were able to identify *kallikrein 1* (Klk1) as a highly specific gene, exclusively expressed by both subsets but no other immune cells. Klk1 is a member of the peptidase S1 family, which belongs to the subgroup of serine proteases. It has been implicated in the regulation of inflammation, apoptosis, local blood pressure, as well as in the development of renal fibrosis and SLE^{278,279}. Lupus prone mice produce less klks than wild type controls and treatment with exogeneous klks leads to an amelioration of disease²⁷⁹. How the expression of KLK1 by pDCs and pDC-like cells is implicated in the pathogenesis of the disease is not clear. However, its exclusive expression on both subsets makes it an ideal target for specific depletion of either subset. In order to target pDCs we plan to generate a new mouse line by crossing the IL-7R^{Cre} or hCD2^{Cre} with a line expressing LoxP-STOP-LoxP cassette followed by a diphtheria toxin alpha (LSL-DTA) within the klk1 locus (Klk1^{LSL-DTA}). The cre recombinase expressed by lymphoid progenitors would induce the expression of the DTA, resulting in the depletion of conventional pDCs. In order to target pDC-like cells we plan to cross Zbtb46^{Cre} or Cx3cr1^{Cre} lines with Klk1^{LSL-DTA}. Expression of the cre recombinase on CDPs would result in the depletion of pDC-like cells but not conventional pDCs. We are currently designing the proposed lines. Preliminary studies will be required to assess the specificity of the expression. Nevertheless, understanding the specific function of conventional

pDCs and pDC like cells may be instrumental to dissect the pathogenesis of autoimmune diseases and be instrumental for the design of targeted therapies.

In summary, our investigation on the developmental trajectory of pDCs led to the identification of a committed pre-pDC within IL-7R expressing lymphoid precursors and to the reassignment of conventional pDCs to innate lymphocytes. Further, we characterized a novel subset of antigen-presenting cells, that we defined as pDC-like cells, which share transcriptional and functional features with both pDCs and cDCs. This subset appears myeloid derived and is capable to capture, process and efficiently present antigens to T cells. The role of this subset in shaping the immune response to pathogens will be the focus of our future studies. It will also be important to understand how developmental cues can change during infections and alter the mature pool. Further, the contribution of distinct lineages to the heterogeneity of pDCs raises the question whether other immune subsets in general or DCs in particular can also differentiate from lymphoid as well as myeloid biased progenitors, and if this developmental heterogeneity could reflect functional diversity.

Abbreviations:

bHLH	
basic Helix Loop Helix	13
BST2	
Bone marrow Stromal antigen 2	3, 7, 19, 21
cDCs	
conventional dendritic cells	1
CDP	
common dendritic cell progenitor	1, 4, 10, 13, 59
cGAS	
cGMP-AMP Synthetase	18
CLPs	
common lymphoid progenitors	1, 4, 6, 7, 8, 9, 10, 56
cMoP	
common Monocyte Progenitor	4
CMs	
Common Myeloid Progenitors	4, 6
CreER	
Tamoxifen inducible Cre recombinase Estrogen Receptor fusion protein	9
DC	
Dendritic Cell	2, 3, 5, 6, 7, 8, 9, 10, 11, 12, 13, 14, 25
DHX	
DexD H-box helicase	18
DiSNE	
Developmental interpolated t-distributed Stochastic Neighborhood Embedding	10, 70
DOTAP	
Dioleoyloxytrimethylammoniumpropane	17
DP	
double positive	1, 45, 46, 47, 48, 49, 56, 57, 58
EAE	
Experimental Autoimmune Encephalomyelitis	21
EBV	
Ebstein Barr Virus	17, 77

EMT	
Epithelial-to-Mesenchymal-Transition	13, 74
Flt3	
Fms-like tyrosine kinase 3	5, 11
Flt3L	
Fms-like tyrosine kinase 3 Ligand	3, 5, 48
GMP	
Granulocyte and Macrophage Precursor	4, 8
H3K27ac	
Histone H3 Lysin 27 acetylation	11
HCV	
Hepatocyte specific C Virus.....	17
HEV	
High Endothelial Venules.....	15
HSCs	
Hematopoietic Stem Cells.....	4
HSPCs	
Hematopoietic Stem and Progenitor Cells.....	10
HSV	
Herpes Simplex Virus.....	17, 21, 77, 80
HSV1	
Herpes Simplex Virus 1.....	21
Id	
Inhibitor of DNA binding.....	13, 73
IDO	
Indoleamine 2,3-dioxygenase	20
IFNs	
interferons.....	1, 2, 3, 16, 17, 18, 19, 20, 21, 22, 23, 24, 25
IL-7R	
Interleukin-7 receptor	1, 6, 7, 8, 12, 44, 45, 50, 56, 58, 59
IPCs	
Interferon Producing Cells	2, 3
IRF8	
interferon regulating factor 8	1, 11, 12, 23, 48, 49, 56, 57, 58
ISG	
Interferon Stimulated Genes	22

ITAM	
Intracellular Tyrosin based Activation Motif	19
ITIM	
Intracellular Tyrosine based Inhibitory Motifs	19
LCMV	
Lymphocytic Choriomeningitis Virus	17, 21, 22, 23, 74, 81
LCR	
Locus Control Region.....	8
LMPPs	
Lymphoid-primed Multi Potent Progenitors	6, 8, 10
MadCAM-1	
Mucosal addressin Cell Adhesion Molecule 1	16
MCMV	
Murine Cytomegalovirus	18, 21
MDP	
Monocyte and Dendritic cell Progenitor.....	4
MEP	
Megacaryocyte and Erythrocyte Progenitors.....	4, 8
MHV	
Mouse Hepatitis Virus	21
MPP	
Multi Potent Progenitor.....	4
MyD88	
Myeloid Differentiation primary response protein 88.....	16, 17, 23, 76, 82
NDV	
Newcastle Disease Virus.....	21
NETs	
Neutrophil Extracellular Traps	23
NF-kB	
Nuclear Factor-kb.....	16, 17, 18, 19
NOD	
Non Obese Diabetes.....	24
ODN	
Oligodeoxyribonucleotides.....	3, 4, 16
PBMCs	
Peripheral Blood Mononuclear Cells	25

pDCs	
plasmacytoid dendritic cells.....	
1, 2, 3, 4, 5, 6, 7, 8, 9, 10, 11, 12, 13, 14, 15, 16, 17, 18, 19, 20, 21, 22, 23, 24, 25, 27, 44, 45, 46, 47, 48, 49, 50, 51, 56, 57, 58, 59, 60	
PDL1	
Programmed cell Death Protein 1 Ligand 1.....	20
pre-pDCs	
precursors of pDCs.....	1
PRR	
Pattern Recognition Receptor.....	18
PSA	
Polysaccharide A.....	18
pTα	
pre-T cell receptor alpha	6
Siglech	
Sialic acid binding immunoglobulin-like lectin H.....	1, 3, 4, 19, 20, 44, 45, 46, 49, 51, 53, 56
SIV	
Simian Immunodeficiency Virus.....	22
SLE	
Systemic Lupus Erythematosus.....	23, 24, 59
STING	
Stimulator of IFN genes.....	18
T1D	
Type 1 Diabetes.....	23, 24
TCF4	
transcription factor 4.....	1, 13, 25, 56
T_h2	
T helper 2.....	3
TLR	
Toll Like Receptor.....	16, 17, 19, 20, 25, 76, 79, 81
T_{reg}	
regulatory T cells.....	20, 22, 24, 25
VEGF-A	
Vascular and Endothelial Growth Factor A.....	3
VSV	
Vesicular Stomatitis Virus.....	17, 21

Acknowledgment:

There are a number of people without whom this thesis might never have been written, and whom I am greatly indebted. I would like to express the deepest gratitude to my supervisor and mentor Prof. R. Tussiwand, who continuously motivated me and managed to convey the true spirit of science and research. Unlike anyone I have met, she has the ability to see clarity among complex topics and solve problems with ease. Her example has formed me as a scientist and I will always remember it. Without her guidance and persistent help this dissertation would not have been possible. Thank you for everything.

I would also like to thank to all my committee members, Prof. R. Zeller, Prof. C. King, Prof. M. Colonna and Prof. A. Rolink for their support, suggestions and encouragement.

Greater than any amount of knowledge I may have acquired during the time as PhD student, was the opportunity to work in the group of Prof. R. Tussiwand. The chance to have met all the lab members together with the joyful moments we were able to share made it an outstanding time in Roxanne's laboratory. I want to thank all the lab members in particular Jan, Anna, Fabian, Mladen, Gogi, Valentina, Thanos, Marzia and Jannes for being great teammates, whose collective input - scientific or not so scientific - always steered me towards progress. Special thanks go as well to the Rolink group in particular to Lucia, Panos, Lilly, Jonas, Mike, Stefan, Hannie, Corinne und Giusy. I also would like to thank all the collaborators such as Robert Ivanek, Alain Brülhart, Danny Labes, Ilda Blanco, Sofia Alves and Nicole Salvisberger for the indispensable support throughout the years.

Further, I am extremely thankful to my friends Lukas, Michi, Seline, Joel, Salome, Jeremy, Floride, Stefania and Sergio for their persistent support outside the lab in good times as well as bad.

A very special gratitude goes out to my family and girlfriend. Eu gostaria de aproveitar essa oportunidade e agradecer à minha família pelo apoio e a força prestada durante esse tempo todo. Quero registrar os meus sinceros agradecimentos ao meu pai Jorge, a minha mãe Maria, a minha irmã Sofia, ao meu cunhado Nelson, aos meus sobrinhos Isabel e Leandro, a minha sogra Daniela e ao amor da minha vida Alessandra. Vocês todos fostes o meu porto seguro em todas as minhas aventuras, até nas mais ousadas e sem o vosso apoio e amor, não teria tido a possibilidade de chegar onde estou hoje. Obrigado por tudo.

References:

1. Lennert, K. & Remmele, W. [Karyometric research on lymph node cells in man. I. Germinoblasts, lymphoblasts & lymphocytes]. *Acta Haematol* **19**, 99-113 (1958).
2. Muller-Hermelink, H.K., Kaiserling, E. & Lennert, K. [Pseudofollicular nests of plasmacells (of a special type?) in paracortical pulp of human lymph nodes (author's transl)]. *Virchows Arch B Cell Pathol* **14**, 47-56 (1973).
3. Papadimitriou, C.S., Stephanaki-Nikou, S.N. & Malamou-Mitsi, V.D. Comparative immunostaining of T-associated plasma cells and other lymph-node cells in paraffin sections. *Virchows Arch B Cell Pathol Incl Mol Pathol* **43**, 31-36 (1983).
4. Vollenweider, R. & Lennert, K. Plasmacytoid T-cell clusters in non-specific lymphadenitis. *Virchows Arch B Cell Pathol Incl Mol Pathol* **44**, 1-14 (1983).
5. Facchetti, F. *et al.* Plasmacytoid T cells. Immunohistochemical evidence for their monocyte/macrophage origin. *Am J Pathol* **133**, 15-21 (1988).
6. Kirchner, H. *et al.* Studies of the producer cell of interferon in human lymphocyte cultures. *Immunobiology* **156**, 65-75 (1979).
7. Ronnblom, L., Ramstedt, U. & Alm, G.V. Properties of human natural interferon-producing cells stimulated by tumor cell lines. *Eur J Immunol* **13**, 471-476 (1983).
8. Chehimi, J. *et al.* Dendritic cells and IFN-alpha-producing cells are two functionally distinct non-B, non-monocytic HLA-DR+ cell subsets in human peripheral blood. *Immunology* **68**, 486-490 (1989).
9. Feldman, M. & Fitzgerald-Bocarsly, P. Sequential enrichment and immunocytochemical visualization of human interferon-alpha-producing cells. *J Interferon Res* **10**, 435-446 (1990).
10. Sandberg, K., Eloranta, M.L., Johannisson, A. & Alm, G.V. Flow cytometric analysis of natural interferon-alpha producing cells. *Scand J Immunol* **34**, 565-576 (1991).
11. Fitzgerald-Bocarsly, P. Human natural interferon-alpha producing cells. *Pharmacol Ther* **60**, 39-62 (1993).
12. Perussia, B., Fanning, V. & Trinchieri, G. A leukocyte subset bearing HLA-DR antigens is responsible for in vitro alpha interferon production in response to viruses. *Nat Immun Cell Growth Regul* **4**, 120-137 (1985).
13. Starr, S.E. *et al.* Morphological and functional differences between HLA-DR+ peripheral blood dendritic cells and HLA-DR+ IFN-alpha producing cells. *Adv Exp Med Biol* **329**, 173-178 (1993).

14. Grouard, G. *et al.* The enigmatic plasmacytoid T cells develop into dendritic cells with interleukin (IL)-3 and CD40-ligand. *Journal of Experimental Medicine* **185**, 1101-1111 (1997).
15. Cella, M. *et al.* Plasmacytoid monocytes migrate to inflamed lymph nodes and produce large amounts of type I interferon. *Nat Med* **5**, 919-923 (1999).
16. Siegal, F.P. *et al.* The nature of the principal type 1 interferon-producing cells in human blood. *Science* **284**, 1835-1837 (1999).
17. Cella, M., Facchetti, F., Lanzavecchia, A. & Colonna, M. Plasmacytoid dendritic cells activated by influenza virus and CD40L drive a potent TH1 polarization. *Nat Immunol* **1**, 305-310 (2000).
18. Bjorek, P. Isolation and characterization of plasmacytoid dendritic cells from Flt3 ligand and granulocyte-macrophage colony-stimulating factor-treated mice. *Blood* **98**, 3520-3526 (2001).
19. Nakano, H., Yanagita, M. & Gunn, M.D. CD11c(+)B220(+)Gr-1(+) cells in mouse lymph nodes and spleen display characteristics of plasmacytoid dendritic cells. *J Exp Med* **194**, 1171-1178 (2001).
20. Asselin-Paturel, C. *et al.* Mouse type I IFN-producing cells are immature APCs with plasmacytoid morphology. *Nat Immunol* **2**, 1144-1150 (2001).
21. Dzionek, A. *et al.* BDCA-2, BDCA-3, and BDCA-4: three markers for distinct subsets of dendritic cells in human peripheral blood. *J Immunol* **165**, 6037-6046 (2000).
22. Dzionek, A. *et al.* BDCA-2, a novel plasmacytoid dendritic cell-specific type II C-type lectin, mediates antigen capture and is a potent inhibitor of interferon alpha/beta induction. *Journal of Experimental Medicine* **194**, 1823-1834 (2001).
23. Dzionek, A. *et al.* Plasmacytoid dendritic cells: from specific surface markers to specific cellular functions. *Hum Immunol* **63**, 1133-1148 (2002).
24. Asselin-Paturel, C., Brizard, G., Pin, J.J., Briere, F. & Trinchieri, G. Mouse strain differences in plasmacytoid dendritic cell frequency and function revealed by a novel monoclonal antibody. *J Immunol* **171**, 6466-6477 (2003).
25. Blasius, A.L., Cella, M., Maldonado, J., Takai, T. & Colonna, M. Siglec-H is an IPC-specific receptor that modulates type I IFN secretion through DAP12. *Blood* **107**, 2474-2476 (2006).
26. Blasius, A. *et al.* A cell-surface molecule selectively expressed on murine natural interferon-producing cells that blocks secretion of interferon-alpha. *Blood* **103**, 4201-4206 (2004).
27. Zhang, J. *et al.* Characterization of Siglec-H as a novel endocytic receptor expressed on murine plasmacytoid dendritic cell precursors. *Blood* **107**, 3600-3608 (2006).

28. Morrison, S.J. & Weissman, I.L. The long-term repopulating subset of hematopoietic stem cells is deterministic and isolatable by phenotype. *Immunity* **1**, 661-673 (1994).
29. Morrison, S.J., Wandycz, A.M., Hemmati, H.D., Wright, D.E. & Weissman, I.L. Identification of a lineage of multipotent hematopoietic progenitors. *Development* **124**, 1929-1939 (1997).
30. Pietras, E.M. *et al.* Functionally Distinct Subsets of Lineage-Biased Multipotent Progenitors Control Blood Production in Normal and Regenerative Conditions. *Cell Stem Cell* **17**, 35-46 (2015).
31. Kondo, M., Weissman, I.L. & Akashi, K. Identification of clonogenic common lymphoid progenitors in mouse bone marrow. *Cell* **91**, 661-672 (1997).
32. Akashi, K., Traver, D., Miyamoto, T. & Weissman, I.L. A clonogenic common myeloid progenitor that gives rise to all myeloid lineages 1. *Nature* **404**, 193-197 (2000).
33. Fogg, D.K. *et al.* A clonogenic bone marrow progenitor specific for macrophages and dendritic cells. *Science* **311**, 83-87 (2006).
34. Olsson, A. *et al.* Single-cell analysis of mixed-lineage states leading to a binary cell fate choice. *Nature* **537**, 698-702 (2016).
35. Hettinger, J. *et al.* Origin of monocytes and macrophages in a committed progenitor. *Nat.Immunol.* **14**, 821-830 (2013).
36. Liu, K. *et al.* In vivo analysis of dendritic cell development and homeostasis. *Science* **324**, 392-397 (2009).
37. Grajales-Reyes, G.E. *et al.* Batf3 maintains autoactivation of Irf8 for commitment of a CD8alpha(+) conventional DC clonogenic progenitor. *Nat Immunol* **16**, 708-717 (2015).
38. Mildner, A. & Jung, S. Development and function of dendritic cell subsets. *Immunity* **40**, 642-656 (2014).
39. Tussiwand, R. *et al.* Klf4 expression in conventional dendritic cells is required for T helper 2 cell responses. *Immunity* **42**, 916-928 (2015).
40. Murphy, T.L. *et al.* Transcriptional Control of Dendritic Cell Development. *Annu Rev Immunol* **34**, 93-119 (2016).
41. Sathe, P., Vremec, D., Wu, L., Corcoran, L. & Shortman, K. Convergent differentiation: myeloid and lymphoid pathways to murine plasmacytoid dendritic cells. *Blood* **121**, 11-19 (2013).
42. Shigematsu, H. *et al.* Plasmacytoid dendritic cells activate lymphoid-specific genetic programs irrespective of their cellular origin. *Immunity* **21**, 43-53 (2004).

43. Pelayo, R. *et al.* Derivation of 2 categories of plasmacytoid dendritic cells in murine bone marrow. *Blood* **105**, 4407-4415 (2005).
44. Waskow, C. *et al.* The receptor tyrosine kinase Flt3 is required for dendritic cell development in peripheral lymphoid tissues. *Nat Immunol* **9**, 676-683 (2008).
45. Eidenschenk, C. *et al.* Flt3 permits survival during infection by rendering dendritic cells competent to activate NK cells. *Proc Natl Acad Sci U S A* **107**, 9759-9764 (2010).
46. Mackarechtschian, K. *et al.* Targeted disruption of the flk2/flt3 gene leads to deficiencies in primitive hematopoietic progenitors. *Immunity* **3**, 147-161 (1995).
47. Karsunky, H., Merad, M., Cozzio, A., Weissman, I.L. & Manz, M.G. Flt3 ligand regulates dendritic cell development from Flt3⁺ lymphoid and myeloid-committed progenitors to Flt3⁺ dendritic cells in vivo. *Journal of Experimental Medicine* **198**, 305-313 (2003).
48. Laouar, Y., Welte, T., Fu, X.Y. & Flavell, R.A. STAT3 is required for Flt3L-dependent dendritic cell differentiation. *Immunity* **19**, 903-912 (2003).
49. Sathaliyawala, T. *et al.* Mammalian target of rapamycin controls dendritic cell development downstream of Flt3 ligand signaling. *Immunity* **33**, 597-606 (2010).
50. Chen, Y.L. *et al.* A type I IFN-Flt3 ligand axis augments plasmacytoid dendritic cell development from common lymphoid progenitors. *J Exp Med* **210**, 2515-2522 (2013).
51. Corcoran, L. *et al.* The lymphoid past of mouse plasmacytoid cells and thymic dendritic cells. *J Immunol* **170**, 4926-4932 (2003).
52. Res, P.C., Couwenberg, F., Vyth-Dreese, F.A. & Spits, H. Expression of pTalpha mRNA in a committed dendritic cell precursor in the human thymus. *Blood* **94**, 2647-2657 (1999).
53. Bendriss-Vermare, N. *et al.* Human thymus contains IFN-alpha-producing CD11c(-), myeloid CD11c(+), and mature interdigitating dendritic cells. *J Clin Invest* **107**, 835-844 (2001).
54. Pronk, C.J. *et al.* Elucidation of the phenotypic, functional, and molecular topography of a myeloerythroid progenitor cell hierarchy. *Cell Stem Cell* **1**, 428-442 (2007).
55. Olweus, J. *et al.* Dendritic cell ontogeny: a human dendritic cell lineage of myeloid origin. *Proc Natl Acad Sci U S A* **94**, 12551-12556 (1997).
56. Onai, N. *et al.* Identification of clonogenic common Flt3⁺M-CSFR⁺ plasmacytoid and conventional dendritic cell progenitors in mouse bone marrow. *Nat Immunol* **8**, 1207-1216 (2007).

57. Macdonald, K.P. *et al.* The colony-stimulating factor 1 receptor is expressed on dendritic cells during differentiation and regulates their expansion. *Ji* **175**, 1399-1405 (2005).
58. Hibbs, M.L. *et al.* Mice lacking three myeloid colony-stimulating factors (G-CSF, GM-CSF, and M-CSF) still produce macrophages and granulocytes and mount an inflammatory response in a sterile model of peritonitis. *J Immunol* **178**, 6435-6443 (2007).
59. Fancke, B., Suter, M., Hochrein, H. & O'Keeffe, M. M-CSF: a novel plasmacytoid and conventional dendritic cell poietin. *Blood* **111**, 150-159 (2008).
60. Onai, N. *et al.* A clonogenic progenitor with prominent plasmacytoid dendritic cell developmental potential. *Immunity* **38**, 943-957 (2013).
61. Schlitzer, A. *et al.* Identification of CCR9- murine plasmacytoid DC precursors with plasticity to differentiate into conventional DCs. *Blood* **117**, 6562-6570 (2011).
62. Schlitzer, A. *et al.* Tissue-specific differentiation of a circulating CCR9- pDC-like common dendritic cell precursor. *Blood* **119**, 6063-6071 (2012).
63. Sauer, B. & Henderson, N. Site-specific DNA recombination in mammalian cells by the Cre recombinase of bacteriophage P1. *Proc Natl Acad Sci U S A* **85**, 5166-5170 (1988).
64. Srinivas, S. *et al.* Cre reporter strains produced by targeted insertion of EYFP and ECFP into the ROSA26 locus. *BMC Dev Biol* **1**, 4 (2001).
65. Loschko, J. *et al.* Inducible targeting of cDCs and their subsets in vivo. *J Immunol Methods* **434**, 32-38 (2016).
66. Schlenner, S.M. *et al.* Fate mapping reveals separate origins of T cells and myeloid lineages in the thymus 1. *Immunity* **32**, 426-436 (2010).
67. de Boer, J. *et al.* Transgenic mice with hematopoietic and lymphoid specific expression of Cre. *European Journal of Immunology* **33**, 314-325 (2003).
68. Caton, M.L., Smith-Raska, M.R. & Reizis, B. Notch-RBP-J signaling controls the homeostasis of CD8- dendritic cells in the spleen. *J Exp.Med.* **204**, 1653-1664 (2007).
69. Schraml, B.U. *et al.* Genetic tracing via DNDR-1 expression history defines dendritic cells as a hematopoietic lineage. *Cell* **154**, 843-858 (2013).
70. Hawley, C.A. *et al.* Csf1r-mApple Transgene Expression and Ligand Binding In Vivo Reveal Dynamics of CSF1R Expression within the Mononuclear Phagocyte System. *J Immunol* **200**, 2209-2223 (2018).
71. Sasmono, R.T. *et al.* A macrophage colony-stimulating factor receptor-green fluorescent protein transgene is expressed throughout the mononuclear phagocyte system of the mouse. *Blood* **101**, 1155-1163 (2003).

72. Siegemund, S., Shepherd, J., Xiao, C. & Sauer, K. hCD2-iCre and Vav-iCre mediated gene recombination patterns in murine hematopoietic cells. *PLoS One* **10**, e0124661 (2015).
73. Abram, C.L., Roberge, G.L., Hu, Y. & Lowell, C.A. Comparative analysis of the efficiency and specificity of myeloid-Cre deleting strains using ROSA-EYFP reporter mice. *J.Immunol.Methods* **408**, 89-100 (2014).
74. Loschko, J. *et al.* Absence of MHC class II on cDCs results in microbial-dependent intestinal inflammation. *J Exp Med* **213**, 517-534 (2016).
75. Satpathy, A.T. *et al.* Zbtb46 expression distinguishes classical dendritic cells and their committed progenitors from other immune lineages. *Journal of Experimental Medicine* **209**, 1135-1152 (2012).
76. Sancho, D. *et al.* Tumor therapy in mice via antigen targeting to a novel, DC-restricted C-type lectin. *J.Clin.Invest* **118**, 2098-2110 (2008).
77. Caminschi, I. *et al.* The dendritic cell subtype-restricted C-type lectin Clec9A is a target for vaccine enhancement. *Blood* **112**, 3264-3273 (2008).
78. Sawai, C.M. *et al.* Hematopoietic Stem Cells Are the Major Source of Multilineage Hematopoiesis in Adult Animals. *Immunity* **45**, 597-609 (2016).
79. Pei, W. *et al.* Polylox barcoding reveals haematopoietic stem cell fates realized in vivo. *Nature* **548**, 456-460 (2017).
80. Naik, S.H. *et al.* Diverse and heritable lineage imprinting of early haematopoietic progenitors. *Nature* **496**, 229-232 (2013).
81. Lin, D.S. *et al.* DiSNE Movie Visualization and Assessment of Clonal Kinetics Reveal Multiple Trajectories of Dendritic Cell Development. *Cell Rep* **22**, 2557-2566 (2018).
82. Helft, J. *et al.* Dendritic Cell Lineage Potential in Human Early Hematopoietic Progenitors. *Cell Rep* **20**, 529-537 (2017).
83. Lee, J. *et al.* Lineage specification of human dendritic cells is marked by IRF8 expression in hematopoietic stem cells and multipotent progenitors. *Nat Immunol* **18**, 877-888 (2017).
84. Carotta, S. *et al.* The transcription factor PU.1 controls dendritic cell development and Flt3 cytokine receptor expression in a dose-dependent manner. *Immunity* **32**, 628-641 (2010).
85. Rosenbauer, F. *et al.* Acute myeloid leukemia induced by graded reduction of a lineage-specific transcription factor, PU.1. *Nat Genet* **36**, 624-630 (2004).

86. Dakic, A. *et al.* PU.1 regulates the commitment of adult hematopoietic progenitors and restricts granulopoiesis. *J Exp Med* **201**, 1487-1502 (2005).
87. Heinz, S., Romanoski, C.E., Benner, C. & Glass, C.K. The selection and function of cell type-specific enhancers. *Nat Rev Mol Cell Biol* **16**, 144-154 (2015).
88. Kurotaki, D. *et al.* Transcription Factor IRF8 Governs Enhancer Landscape Dynamics in Mononuclear Phagocyte Progenitors. *Cell Rep* **22**, 2628-2641 (2018).
89. Chopin, M. *et al.* Transcription Factor PU.1 Promotes Conventional Dendritic Cell Identity and Function via Induction of Transcriptional Regulator DC-SCRIPT. *Immunity* **50**, 77-90 e75 (2019).
90. Brass, A.L., Kehrli, E., Eisenbeis, C.F., Storb, U. & Singh, H. Pip, a lymphoid-restricted IRF, contains a regulatory domain that is important for autoinhibition and ternary complex formation with the Ets factor PU.1. *Genes & Development* **10**, 2335-2347 (1996).
91. Sharf, R. *et al.* Functional domain analysis of interferon consensus sequence binding protein (ICSBP) and its association with interferon regulatory factors. *J Biol Chem* **270**, 13063-13069 (1995).
92. Bovolenta, C. *et al.* Molecular interactions between interferon consensus sequence binding protein and members of the interferon regulatory factor family. *Proc Natl Acad Sci U S A* **91**, 5046-5050 (1994).
93. Rosenbauer, F. *et al.* Interferon consensus sequence binding protein and interferon regulatory factor-4/Pip form a complex that represses the expression of the interferon-stimulated gene-15 in macrophages. *Blood* **94**, 4274-4281 (1999).
94. Nagulapalli, S. & Atchison, M.L. Transcription factor Pip can enhance DNA binding by E47, leading to transcriptional synergy involving multiple protein domains. *Mol Cell Biol* **18**, 4639-4650 (1998).
95. Wang, H. *et al.* IRF8 regulates B-cell lineage specification, commitment, and differentiation. *Blood* **112**, 4028-4038 (2008).
96. Becker, A.M. *et al.* IRF-8 extinguishes neutrophil production and promotes dendritic cell lineage commitment in both myeloid and lymphoid mouse progenitors. *Blood* **119**, 2003-2012 (2012).
97. Kurotaki, D. *et al.* IRF8 inhibits C/EBPalpha activity to restrain mononuclear phagocyte progenitors from differentiating into neutrophils. *Nat Commun* **5**, 4978 (2014).
98. Aliberti, J. *et al.* Essential role for ICSBP in the in vivo development of murine CD8alpha + dendritic cells. *Blood* **101**, 305-310 (2003).
99. Hambleton, S. *et al.* IRF8 mutations and human dendritic-cell immunodeficiency. *N.Engl.J.Med.* **365**, 127-138 (2011).

100. Sichien, D. *et al.* IRF8 Transcription Factor Controls Survival and Function of Terminally Differentiated Conventional and Plasmacytoid Dendritic Cells, Respectively. *Immunity* **45**, 626-640 (2016).
101. Schiavoni, G. *et al.* ICSBP is essential for the development of mouse type I interferon-producing cells and for the generation and activation of CD8alpha(+) dendritic cells. *J Exp.Med.* **196**, 1415-1425 (2002).
102. Tailor, P., Tamura, T., Morse, H.C. & Ozato, K. The BXH2 mutation in IRF8 differentially impairs dendritic cell subset development in the mouse. *Blood* **111**, 1942-1945 (2008).
103. Tamura, T. *et al.* IFN regulatory factor-4 and -8 govern dendritic cell subset development and their functional diversity. *J Immunol* **174**, 2573-2581 (2005).
104. Molnar, A. & Georgopoulos, K. The Ikaros gene encodes a family of functionally diverse zinc finger DNA-binding proteins. *Mol Cell Biol* **14**, 8292-8303 (1994).
105. Wang, J.H. *et al.* Selective defects in the development of the fetal and adult lymphoid system in mice with an Ikaros null mutation. *Immunity* **5**, 537-549 (1996).
106. Nichogiannopoulou, A., Trevisan, M., Neben, S., Friedrich, C. & Georgopoulos, K. Defects in hemopoietic stem cell activity in Ikaros mutant mice. *J Exp Med* **190**, 1201-1214 (1999).
107. Kirstetter, P., Thomas, M., Dierich, A., Kastner, P. & Chan, S. Ikaros is critical for B cell differentiation and function. *Eur J Immunol* **32**, 720-730 (2002).
108. Dumortier, A., Kirstetter, P., Kastner, P. & Chan, S. Ikaros regulates neutrophil differentiation. *Blood* **101**, 2219-2226 (2003).
109. Morgan, B. *et al.* Aiolos, a lymphoid restricted transcription factor that interacts with Ikaros to regulate lymphocyte differentiation. *EMBO J* **16**, 2004-2013 (1997).
110. Wang, J.H. *et al.* Aiolos regulates B cell activation and maturation to effector state. *Immunity* **9**, 543-553 (1998).
111. Hahm, K. *et al.* Helios, a T cell-restricted Ikaros family member that quantitatively associates with Ikaros at centromeric heterochromatin. *Genes Dev* **12**, 782-796 (1998).
112. Kelley, C.M. *et al.* Helios, a novel dimerization partner of Ikaros expressed in the earliest hematopoietic progenitors. *Curr Biol* **8**, 508-515 (1998).
113. Wu, L., Nichogiannopoulou, A., Shortman, K. & Georgopoulos, K. Cell-autonomous defects in dendritic cell populations of Ikaros mutant mice point to a developmental relationship with the lymphoid lineage. *Immunity* **7**, 483-492 (1997).

114. Allman, D. *et al.* Ikaros is required for plasmacytoid dendritic cell differentiation. *Blood* **108**, 4025-4034 (2006).
115. Mastio, J. *et al.* Ikaros cooperates with Notch activation and antagonizes TGFbeta signaling to promote pDC development. *PLoS Genet* **14**, e1007485 (2018).
116. Cytlak, U. *et al.* Ikaros family zinc finger 1 regulates dendritic cell development and function in humans. *Nat Commun* **9**, 1239 (2018).
117. Liu, P. *et al.* Bcl11a is essential for normal lymphoid development. *Nat Immunol* **4**, 525-532 (2003).
118. Sankaran, V.G. *et al.* Developmental and species-divergent globin switching are driven by BCL11A. *Nature* **460**, 1093-1097 (2009).
119. Xu, J. *et al.* Transcriptional silencing of {gamma}-globin by BCL11A involves long-range interactions and cooperation with SOX6. *Genes Dev* **24**, 783-798 (2010).
120. Wu, X. *et al.* Bcl11a controls Flt3 expression in early hematopoietic progenitors and is required for pDC development in vivo. *PLoS One* **8**, e64800 (2013).
121. Ippolito, G.C. *et al.* Dendritic cell fate is determined by BCL11A. *Proc Natl Acad Sci U S A* **111**, E998-1006 (2014).
122. Wang, D. *et al.* The basic helix-loop-helix transcription factor HEBAIt is expressed in pro-T cells and enhances the generation of T cell precursors. *J Immunol* **177**, 109-119 (2006).
123. Cisse, B. *et al.* Transcription factor E2-2 is an essential and specific regulator of plasmacytoid dendritic cell development 1. *Cell* **135**, 37-48 (2008).
124. Nagasawa, M., Schmidlin, H., Hazekamp, M.G., Schotte, R. & Blom, B. Development of human plasmacytoid dendritic cells depends on the combined action of the basic helix-loop-helix factor E2-2 and the Ets factor Spi-B. *European Journal of Immunology* **38**, 2389-2400 (2008).
125. Ghosh, H.S., Cisse, B., Bunin, A., Lewis, K.L. & Reizis, B. Continuous expression of the transcription factor e2-2 maintains the cell fate of mature plasmacytoid dendritic cells. *Immunity* **33**, 905-916 (2010).
126. Engel, I. & Murre, C. The function of E- and Id proteins in lymphocyte development. *Nat Rev Immunol* **1**, 193-199 (2001).
127. Hacker, C. *et al.* Transcriptional profiling identifies Id2 function in dendritic cell development. *Nat Immunol* **4**, 380-386 (2003).
128. Grajkowska, L.T. *et al.* Isoform-Specific Expression and Feedback Regulation of E Protein TCF4 Control Dendritic Cell Lineage Specification. *Immunity* **46**, 65-77 (2017).

129. Denecker, G. *et al.* Identification of a ZEB2-MITF-ZEB1 transcriptional network that controls melanogenesis and melanoma progression. *Cell Death Differ* **21**, 1250-1261 (2014).
130. Seuntjens, E. *et al.* Sip1 regulates sequential fate decisions by feedback signaling from postmitotic neurons to progenitors. *Nat Neurosci* **12**, 1373-1380 (2009).
131. Weng, Q. *et al.* Dual-mode modulation of Smad signaling by Smad-interacting protein Sip1 is required for myelination in the central nervous system. *Neuron* **73**, 713-728 (2012).
132. van den Berghe, V. *et al.* Directed migration of cortical interneurons depends on the cell-autonomous action of Sip1. *Neuron* **77**, 70-82 (2013).
133. Van de Putte, T. *et al.* Mice lacking ZFH1B, the gene that codes for Smad-interacting protein-1, reveal a role for multiple neural crest cell defects in the etiology of Hirschsprung disease-mental retardation syndrome. *Am J Hum Genet* **72**, 465-470 (2003).
134. Vandewalle, C., Van Roy, F. & Berx, G. The role of the ZEB family of transcription factors in development and disease. *Cell Mol Life Sci* **66**, 773-787 (2009).
135. Goossens, S. *et al.* The EMT regulator Zeb2/Sip1 is essential for murine embryonic hematopoietic stem/progenitor cell differentiation and mobilization. *Blood* **117**, 5620-5630 (2011).
136. van Helden, M.J. *et al.* Terminal NK cell maturation is controlled by concerted actions of T-bet and Zeb2 and is essential for melanoma rejection. *J Exp Med* **212**, 2015-2025 (2015).
137. Dominguez, C.X. *et al.* The transcription factors ZEB2 and T-bet cooperate to program cytotoxic T cell terminal differentiation in response to LCMV viral infection. *J Exp Med* **212**, 2041-2056 (2015).
138. Li, J. *et al.* The EMT transcription factor Zeb2 controls adult murine hematopoietic differentiation by regulating cytokine signaling. *Blood* **129**, 460-472 (2017).
139. Wu, X. *et al.* Transcription factor Zeb2 regulates commitment to plasmacytoid dendritic cell and monocyte fate. *Proc Natl Acad Sci U S A* **113**, 14775-14780 (2016).
140. Scott, C.L. *et al.* The transcription factor Zeb2 regulates development of conventional and plasmacytoid DCs by repressing Id2. *J Exp Med* **213**, 897-911 (2016).
141. Ray-Gallet, D., Mao, C., Tavitian, A. & Moreau-Gachelin, F. DNA binding specificities of Spi-1/PU.1 and Spi-B transcription factors and identification of a Spi-1/Spi-B binding site in the c-fes/c-fps promoter. *Oncogene* **11**, 303-313 (1995).
142. Schotte, R., Nagasawa, M., Weijer, K., Spits, H. & Blom, B. The ETS transcription factor Spi-B is required for human plasmacytoid dendritic cell development. *Journal of Experimental Medicine* **200**, 1503-1509 (2004).

143. Schotte, R. *et al.* The transcription factor Spi-B is expressed in plasmacytoid DC precursors and inhibits T-, B-, and NK-cell development. *Blood* **101**, 1015-1023 (2003).
144. Sasaki, I. *et al.* Spi-B is critical for plasmacytoid dendritic cell function and development. *Blood* **120**, 4733-4743 (2012).
145. Karrich, J.J. *et al.* The transcription factor Spi-B regulates human plasmacytoid dendritic cell survival through direct induction of the antiapoptotic gene BCL2-A1. *Blood* **119**, 5191-5200 (2012).
146. Collins, A., Littman, D.R. & Taniuchi, I. RUNX proteins in transcription factor networks that regulate T-cell lineage choice. *Nat Rev Immunol* **9**, 106-115 (2009).
147. Long, F. Building strong bones: molecular regulation of the osteoblast lineage. *Nat Rev Mol Cell Biol* **13**, 27-38 (2011).
148. Sawai, C.M. *et al.* Transcription factor Runx2 controls the development and migration of plasmacytoid dendritic cells. *J Exp Med* **210**, 2151-2159 (2013).
149. Chopin, M. *et al.* RUNX2 Mediates Plasmacytoid Dendritic Cell Egress from the Bone Marrow and Controls Viral Immunity. *Cell Rep* **15**, 866-878 (2016).
150. Drobits, B. *et al.* Imiquimod clears tumors in mice independent of adaptive immunity by converting pDCs into tumor-killing effector cells. *J Clin Invest* **122**, 575-585 (2012).
151. Umemoto, E. *et al.* Constitutive plasmacytoid dendritic cell migration to the splenic white pulp is cooperatively regulated by CCR7- and CXCR4-mediated signaling. *J Immunol* **189**, 191-199 (2012).
152. Zou, W. *et al.* Stromal-derived factor-1 in human tumors recruits and alters the function of plasmacytoid precursor dendritic cells. *Nat Med* **7**, 1339-1346 (2001).
153. Krug, A. *et al.* IFN-producing cells respond to CXCR3 ligands in the presence of CXCL12 and secrete inflammatory chemokines upon activation. *J Immunol* **169**, 6079-6083 (2002).
154. Diacovo, T.G., Blasius, A.L., Mak, T.W., Cella, M. & Colonna, M. Adhesive mechanisms governing interferon-producing cell recruitment into lymph nodes. *J Exp Med* **202**, 687-696 (2005).
155. Sisirak, V. *et al.* CCR6/CCR10-mediated plasmacytoid dendritic cell recruitment to inflamed epithelia after instruction in lymphoid tissues. *Blood* **118**, 5130-5140 (2011).
156. Hadeiba, H. *et al.* Plasmacytoid dendritic cells transport peripheral antigens to the thymus to promote central tolerance. *Immunity* **36**, 438-450 (2012).

157. Wendland, M. *et al.* CCR9 is a homing receptor for plasmacytoid dendritic cells to the small intestine. *Proc Natl Acad Sci U S A* **104**, 6347-6352 (2007).
158. Wurbel, M.A., McIntire, M.G., Dwyer, P. & Fiebiger, E. CCL25/CCR9 interactions regulate large intestinal inflammation in a murine model of acute colitis. *PLoS One* **6**, e16442 (2011).
159. Clahsen, T., Pabst, O., Tenbrock, K., Schippers, A. & Wagner, N. Localization of dendritic cells in the gut epithelium requires MAdCAM-1. *Clin Immunol* **156**, 74-84 (2015).
160. Gutzmer, R. *et al.* Human plasmacytoid dendritic cells express receptors for anaphylatoxins C3a and C5a and are chemoattracted to C3a and C5a. *J Invest Dermatol* **126**, 2422-2429 (2006).
161. Gilliet, M., Cao, W. & Liu, Y.J. Plasmacytoid dendritic cells: sensing nucleic acids in viral infection and autoimmune diseases. *Nat Rev Immunol* **8**, 594-606 (2008).
162. Blasius, A.L. & Beutler, B. Intracellular toll-like receptors. *Immunity* **32**, 305-315 (2010).
163. Kawai, T. & Akira, S. Toll-like receptors and their crosstalk with other innate receptors in infection and immunity. *Immunity* **34**, 637-650 (2011).
164. Honda, K. *et al.* Spatiotemporal regulation of MyD88-IRF-7 signalling for robust type-I interferon induction. *Nature* **434**, 1035-1040 (2005).
165. Lee, B.L. & Barton, G.M. Trafficking of endosomal Toll-like receptors. *Trends Cell Biol* **24**, 360-369 (2014).
166. Lund, J., Sato, A., Akira, S., Medzhitov, R. & Iwasaki, A. Toll-like receptor 9-mediated recognition of Herpes simplex virus-2 by plasmacytoid dendritic cells. *J Exp Med* **198**, 513-520 (2003).
167. Kumagai, Y. *et al.* Cutting Edge: TLR-Dependent viral recognition along with type I IFN positive feedback signaling masks the requirement of viral replication for IFN- α production in plasmacytoid dendritic cells. *J Immunol* **182**, 3960-3964 (2009).
168. Deal, E.M., Jaimes, M.C., Crawford, S.E., Estes, M.K. & Greenberg, H.B. Rotavirus structural proteins and dsRNA are required for the human primary plasmacytoid dendritic cell IFN α response. *PLoS Pathog* **6**, e1000931 (2010).
169. Bave, U. *et al.* Fc gamma RIIa is expressed on natural IFN- α -producing cells (plasmacytoid dendritic cells) and is required for the IFN- α production induced by apoptotic cells combined with lupus IgG. *J Immunol* **171**, 3296-3302 (2003).
170. Barrat, F.J. *et al.* Nucleic acids of mammalian origin can act as endogenous ligands for Toll-like receptors and may promote systemic lupus erythematosus. *J Exp Med* **202**, 1131-1139 (2005).

171. Kim, S. *et al.* Self-priming determines high type I IFN production by plasmacytoid dendritic cells. *Eur J Immunol* **44**, 807-818 (2014).
172. Takahashi, K. *et al.* Plasmacytoid dendritic cells sense hepatitis C virus-infected cells, produce interferon, and inhibit infection. *Proc Natl Acad Sci U S A* **107**, 7431-7436 (2010).
173. Frenz, T. *et al.* Independent of plasmacytoid dendritic cell (pDC) infection, pDC triggered by virus-infected cells mount enhanced type I IFN responses of different composition as opposed to pDC stimulated with free virus. *J Immunol* **193**, 2496-2503 (2014).
174. Dreux, M. *et al.* Short-range exosomal transfer of viral RNA from infected cells to plasmacytoid dendritic cells triggers innate immunity. *Cell Host Microbe* **12**, 558-570 (2012).
175. Lepelley, A. *et al.* Innate sensing of HIV-infected cells. *PLoS Pathog* **7**, e1001284 (2011).
176. Rua, R., Lepelley, A., Gessain, A. & Schwartz, O. Innate sensing of foamy viruses by human hematopoietic cells. *J Virol* **86**, 909-918 (2012).
177. Wieland, S.F. *et al.* Human plasmacytoid dendritic cells sense lymphocytic choriomeningitis virus-infected cells in vitro. *J Virol* **88**, 752-757 (2014).
178. Decembre, E. *et al.* Sensing of immature particles produced by dengue virus infected cells induces an antiviral response by plasmacytoid dendritic cells. *PLoS Pathog* **10**, e1004434 (2014).
179. Feng, Z. *et al.* Human pDCs preferentially sense enveloped hepatitis A virions. *J Clin Invest* **125**, 169-176 (2015).
180. Baglio, S.R. *et al.* Sensing of latent EBV infection through exosomal transfer of 5'pppRNA. *Proc Natl Acad Sci U S A* **113**, E587-596 (2016).
181. Megjugorac, N.J. *et al.* Image-based study of interferogenic interactions between plasmacytoid dendritic cells and HSV-infected monocyte-derived dendritic cells. *Immunol Invest* **36**, 739-761 (2007).
182. Assil, S.C., E. Decembre, L. Sherry, O. Allatif, B. Webster, M. Dreux. Antiviral Response by Plasmacytoid Dendritic Cells via Interferogenic Synapse with Infected Cells. *BioRxiv* (2018).
183. Tomasello, E. *et al.* Molecular dissection of plasmacytoid dendritic cell activation in vivo during a viral infection. *EMBO J* **37** (2018).
184. Dasgupta, S., Erturk-Hasdemir, D., Ochoa-Reparaz, J., Reinecker, H.C. & Kasper, D.L. Plasmacytoid dendritic cells mediate anti-inflammatory responses to a gut

- commensal molecule via both innate and adaptive mechanisms. *Cell Host Microbe* **15**, 413-423 (2014).
185. Koblansky, A.A. *et al.* Recognition of profilin by Toll-like receptor 12 is critical for host resistance to *Toxoplasma gondii*. *Immunity* **38**, 119-130 (2013).
 186. Kim, T. *et al.* Aspartate-glutamate-alanine-histidine box motif (DEAH)/RNA helicase A helicases sense microbial DNA in human plasmacytoid dendritic cells. *Proc Natl Acad Sci U S A* **107**, 15181-15186 (2010).
 187. Li, X.D. *et al.* Pivotal roles of cGAS-cGAMP signaling in antiviral defense and immune adjuvant effects. *Science* **341**, 1390-1394 (2013).
 188. Paijo, J. *et al.* cGAS Senses Human Cytomegalovirus and Induces Type I Interferon Responses in Human Monocyte-Derived Cells. *PLoS Pathog* **12**, e1005546 (2016).
 189. Bode, C. *et al.* Human plasmacytoid dendritic cells elicit a Type I Interferon response by sensing DNA via the cGAS-STING signaling pathway. *Eur J Immunol* **46**, 1615-1621 (2016).
 190. Bao, M. & Liu, Y.J. Regulation of TLR7/9 signaling in plasmacytoid dendritic cells. *Protein Cell* **4**, 40-52 (2013).
 191. Swiecki, M. & Colonna, M. The multifaceted biology of plasmacytoid dendritic cells. *Nat Rev Immunol* **15**, 471-485 (2015).
 192. Swiecki, M. *et al.* Cell depletion in mice that express diphtheria toxin receptor under the control of SiglecH encompasses more than plasmacytoid dendritic cells. *J Immunol* **192**, 4409-4416 (2014).
 193. Blasius, A.L. *et al.* Bone marrow stromal cell antigen 2 is a specific marker of type I IFN-producing cells in the naive mouse, but a promiscuous cell surface antigen following IFN stimulation. *The Journal of Immunology* **177**, 3260-3265 (2006).
 194. Tai, L.H. *et al.* Positive regulation of plasmacytoid dendritic cell function via Ly49Q recognition of class I MHC. *J Exp Med* **205**, 3187-3199 (2008).
 195. Watarai, H. *et al.* PDC-TREM, a plasmacytoid dendritic cell-specific receptor, is responsible for augmented production of type I interferon. *Proc Natl Acad Sci U S A* **105**, 2993-2998 (2008).
 196. Mitsuhashi, Y. *et al.* Regulation of plasmacytoid dendritic cell responses by PIR-B. *Blood* **120**, 3256-3259 (2012).
 197. Chiang, E.Y., Johnston, R.J. & Grogan, J.L. EBI2 is a negative regulator of type I interferons in plasmacytoid and myeloid dendritic cells. *PLoS One* **8**, e83457 (2013).
 198. Karrich, J.J. *et al.* MicroRNA-146a regulates survival and maturation of human plasmacytoid dendritic cells. *Blood* **122**, 3001-3009 (2013).

199. Zhou, H. *et al.* miR-155 and its star-form partner miR-155* cooperatively regulate type I interferon production by human plasmacytoid dendritic cells. *Blood* **116**, 5885-5894 (2010).
200. Agudo, J. *et al.* The miR-126-VEGFR2 axis controls the innate response to pathogen-associated nucleic acids. *Nat Immunol* **15**, 54-62 (2014).
201. Meier, A. *et al.* Sex differences in the Toll-like receptor-mediated response of plasmacytoid dendritic cells to HIV-1. *Nat Med* **15**, 955-959 (2009).
202. Segura, E. & Villadangos, J.A. Antigen presentation by dendritic cells in vivo. *Curr Opin Immunol* **21**, 105-110 (2009).
203. Reizis, B., Bunin, A., Ghosh, H.S., Lewis, K.L. & Sisirak, V. Plasmacytoid dendritic cells: recent progress and open questions. *Annu Rev Immunol* **29**, 163-183 (2011).
204. Mouries, J. *et al.* Plasmacytoid dendritic cells efficiently cross-prime naive T cells in vivo after TLR activation. *Blood* **112**, 3713-3722 (2008).
205. Hoeffel, G. *et al.* Antigen crosspresentation by human plasmacytoid dendritic cells. *Immunity* **27**, 481-492 (2007).
206. Munn, D.H. *et al.* Expression of indoleamine 2,3-dioxygenase by plasmacytoid dendritic cells in tumor-draining lymph nodes. *J Clin Invest* **114**, 280-290 (2004).
207. Fallarino, F. *et al.* Murine plasmacytoid dendritic cells initiate the immunosuppressive pathway of tryptophan catabolism in response to CD200 receptor engagement. *J Immunol* **173**, 3748-3754 (2004).
208. Boasso, A. *et al.* HIV inhibits CD4+ T-cell proliferation by inducing indoleamine 2,3-dioxygenase in plasmacytoid dendritic cells. *Blood* **109**, 3351-3359 (2007).
209. Pallotta, M.T. *et al.* Indoleamine 2,3-dioxygenase is a signaling protein in long-term tolerance by dendritic cells. *Nat Immunol* **12**, 870-878 (2011).
210. Ito, T. *et al.* Plasmacytoid dendritic cells prime IL-10-producing T regulatory cells by inducible costimulator ligand. *J Exp Med* **204**, 105-115 (2007).
211. Diana, J. *et al.* NKT cell-plasmacytoid dendritic cell cooperation via OX40 controls viral infection in a tissue-specific manner. *Immunity* **30**, 289-299 (2009).
212. Diana, J. *et al.* Viral infection prevents diabetes by inducing regulatory T cells through NKT cell-plasmacytoid dendritic cell interplay. *J Exp Med* **208**, 729-745 (2011).
213. Jahrsdorfer, B. *et al.* Granzyme B produced by human plasmacytoid dendritic cells suppresses T-cell expansion. *Blood* **115**, 1156-1165 (2010).
214. Hadeiba, H. *et al.* CCR9 expression defines tolerogenic plasmacytoid dendritic cells able to suppress acute graft-versus-host disease. *Nat Immunol* **9**, 1253-1260 (2008).

215. Lombardi, V., Speak, A.O., Kerzerho, J., Szely, N. & Akbari, O. CD8alpha(+)beta(-) and CD8alpha(+)beta(+) plasmacytoid dendritic cells induce Foxp3(+) regulatory T cells and prevent the induction of airway hyper-reactivity. *Mucosal Immunol* **5**, 432-443 (2012).
216. Chappell, C.P. *et al.* Targeting antigens through blood dendritic cell antigen 2 on plasmacytoid dendritic cells promotes immunologic tolerance. *J Immunol* **192**, 5789-5801 (2014).
217. Loschko, J. *et al.* Antigen targeting to plasmacytoid dendritic cells via Siglec-H inhibits Th cell-dependent autoimmunity. *J Immunol* **187**, 6346-6356 (2011).
218. Loschko, J. *et al.* Antigen delivery to plasmacytoid dendritic cells via BST2 induces protective T cell-mediated immunity. *J Immunol* **186**, 6718-6725 (2011).
219. Kumagai, Y. *et al.* Alveolar macrophages are the primary interferon-alpha producer in pulmonary infection with RNA viruses. *Immunity* **27**, 240-252 (2007).
220. Cervantes-Barragan, L. *et al.* Control of coronavirus infection through plasmacytoid dendritic-cell-derived type I interferon. *Blood* **109**, 1131-1137 (2007).
221. Cervantes-Barragan, L. *et al.* Type I IFN-mediated protection of macrophages and dendritic cells secures control of murine coronavirus infection. *J Immunol* **182**, 1099-1106 (2009).
222. Swiecki, M., Wang, Y., Gilfillan, S. & Colonna, M. Plasmacytoid dendritic cells contribute to systemic but not local antiviral responses to HSV infections. *PLoS Pathog* **9**, e1003728 (2013).
223. Swiecki, M., Gilfillan, S., Vermi, W., Wang, Y. & Colonna, M. Plasmacytoid dendritic cell ablation impacts early interferon responses and antiviral NK and CD8(+) T cell accrual. *Immunity* **33**, 955-966 (2010).
224. Cervantes-Barragan, L. *et al.* Plasmacytoid dendritic cells control T-cell response to chronic viral infection. *Proc Natl Acad Sci U S A* **109**, 3012-3017 (2012).
225. Ciancanelli, M.J. *et al.* Infectious disease. Life-threatening influenza and impaired interferon amplification in human IRF7 deficiency. *Science* **348**, 448-453 (2015).
226. Webster, B. *et al.* Plasmacytoid dendritic cells control dengue and Chikungunya virus infections via IRF7-regulated interferon responses. *Elife* **7** (2018).
227. Lehmann, C. *et al.* Longitudinal analysis of distribution and function of plasmacytoid dendritic cells in peripheral blood and gut mucosa of HIV infected patients. *J Infect Dis* **209**, 940-949 (2014).
228. Reeves, R.K. *et al.* SIV infection induces accumulation of plasmacytoid dendritic cells in the gut mucosa. *J Infect Dis* **206**, 1462-1468 (2012).

229. Li, H., Goepfert, P. & Reeves, R.K. Short communication: Plasmacytoid dendritic cells from HIV-1 Elite Controllers maintain a gut-homing phenotype associated with immune activation. *AIDS Res Hum Retroviruses* **30**, 1213-1215 (2014).
230. O'Brien, M. *et al.* Spatiotemporal trafficking of HIV in human plasmacytoid dendritic cells defines a persistently IFN-alpha-producing and partially matured phenotype. *J Clin Invest* **121**, 1088-1101 (2011).
231. Macal, M. *et al.* Self-Renewal and Toll-like Receptor Signaling Sustain Exhausted Plasmacytoid Dendritic Cells during Chronic Viral Infection. *Immunity* **48**, 730-744 e735 (2018).
232. Manches, O., Fernandez, M.V., Plumas, J., Chaperot, L. & Bhardwaj, N. Activation of the noncanonical NF-kappaB pathway by HIV controls a dendritic cell immunoregulatory phenotype. *Proc Natl Acad Sci U S A* **109**, 14122-14127 (2012).
233. Sandler, N.G. *et al.* Type I interferon responses in rhesus macaques prevent SIV infection and slow disease progression. *Nature* **511**, 601-605 (2014).
234. Blasius, A.L., Krebs, P., Sullivan, B.M., Oldstone, M.B. & Popkin, D.L. Slc15a4, a gene required for pDC sensing of TLR ligands, is required to control persistent viral infection. *PLoS Pathog* **8**, e1002915 (2012).
235. Rogers, G.L. *et al.* Plasmacytoid and conventional dendritic cells cooperate in crosspriming AAV capsid-specific CD8(+) T cells. *Blood* **129**, 3184-3195 (2017).
236. Brewitz, A. *et al.* CD8(+) T Cells Orchestrate pDC-XCR1(+) Dendritic Cell Spatial and Functional Cooperativity to Optimize Priming. *Immunity* **46**, 205-219 (2017).
237. Wang, Y. *et al.* Timing and magnitude of type I interferon responses by distinct sensors impact CD8 T cell exhaustion and chronic viral infection. *Cell Host Microbe* **11**, 631-642 (2012).
238. Wilson, E.B. *et al.* Blockade of chronic type I interferon signaling to control persistent LCMV infection. *Science* **340**, 202-207 (2013).
239. Teijaro, J.R. *et al.* Persistent LCMV infection is controlled by blockade of type I interferon signaling. *Science* **340**, 207-211 (2013).
240. Means, T.K. *et al.* Human lupus autoantibody-DNA complexes activate DCs through cooperation of CD32 and TLR9. *J Clin Invest* **115**, 407-417 (2005).
241. Garcia-Romo, G.S. *et al.* Netting neutrophils are major inducers of type I IFN production in pediatric systemic lupus erythematosus. *Sci Transl Med* **3**, 73ra20 (2011).
242. Lande, R. *et al.* Neutrophils activate plasmacytoid dendritic cells by releasing self-DNA-peptide complexes in systemic lupus erythematosus. *Sci Transl Med* **3**, 73ra19 (2011).

243. Morshed, M. *et al.* NADPH oxidase-independent formation of extracellular DNA traps by basophils. *J Immunol* **192**, 5314-5323 (2014).
244. Baccala, R. *et al.* Anti-IFN-alpha/beta receptor antibody treatment ameliorates disease in lupus-predisposed mice. *J Immunol* **189**, 5976-5984 (2012).
245. Guiducci, C. *et al.* Autoimmune skin inflammation is dependent on plasmacytoid dendritic cell activation by nucleic acids via TLR7 and TLR9. *J Exp Med* **207**, 2931-2942 (2010).
246. Baccala, R. *et al.* Essential requirement for IRF8 and SLC15A4 implicates plasmacytoid dendritic cells in the pathogenesis of lupus. *Proc Natl Acad Sci U S A* **110**, 2940-2945 (2013).
247. Teichmann, L.L., Schenten, D., Medzhitov, R., Kashgarian, M. & Shlomchik, M.J. Signals via the adaptor MyD88 in B cells and DCs make distinct and synergistic contributions to immune activation and tissue damage in lupus. *Immunity* **38**, 528-540 (2013).
248. Rowland, S.L. *et al.* Early, transient depletion of plasmacytoid dendritic cells ameliorates autoimmunity in a lupus model. *J Exp Med* **211**, 1977-1991 (2014).
249. Lande, R. *et al.* Plasmacytoid dendritic cells sense self-DNA coupled with antimicrobial peptide. *Nature* **449**, 564-569 (2007).
250. Ganguly, D. *et al.* Self-RNA-antimicrobial peptide complexes activate human dendritic cells through TLR7 and TLR8. *J Exp Med* **206**, 1983-1994 (2009).
251. Lande, R. *et al.* Cationic antimicrobial peptides in psoriatic skin cooperate to break innate tolerance to self-DNA. *Eur J Immunol* **45**, 203-213 (2015).
252. Nestle, F.O. *et al.* Plasmacytoid predendritic cells initiate psoriasis through interferon-alpha production. *J Exp Med* **202**, 135-143 (2005).
253. Karthaus, N. *et al.* Vitamin D controls murine and human plasmacytoid dendritic cell function. *J Invest Dermatol* **134**, 1255-1264 (2014).
254. Glitzner, E. *et al.* Specific roles for dendritic cell subsets during initiation and progression of psoriasis. *EMBO Mol Med* **6**, 1312-1327 (2014).
255. Wohn, C. *et al.* Langerin(neg) conventional dendritic cells produce IL-23 to drive psoriatic plaque formation in mice. *Proc Natl Acad Sci U S A* **110**, 10723-10728 (2013).
256. Allen, J.S. *et al.* Plasmacytoid dendritic cells are proportionally expanded at diagnosis of type 1 diabetes and enhance islet autoantigen presentation to T-cells through immune complex capture. *Diabetes* **58**, 138-145 (2009).
257. Diana, J. *et al.* Crosstalk between neutrophils, B-1a cells and plasmacytoid dendritic cells initiates autoimmune diabetes. *Nat Med* **19**, 65-73 (2013).

258. Hansen, L. *et al.* E2-2 Dependent Plasmacytoid Dendritic Cells Control Autoimmune Diabetes. *PLoS One* **10**, e0144090 (2015).
259. Conrad, C. *et al.* Plasmacytoid dendritic cells promote immunosuppression in ovarian cancer via ICOS costimulation of Foxp3(+) T-regulatory cells. *Cancer Res* **72**, 5240-5249 (2012).
260. Labidi-Galy, S.I. *et al.* Quantitative and functional alterations of plasmacytoid dendritic cells contribute to immune tolerance in ovarian cancer. *Cancer Res* **71**, 5423-5434 (2011).
261. Sisirak, V. *et al.* Impaired IFN-alpha production by plasmacytoid dendritic cells favors regulatory T-cell expansion that may contribute to breast cancer progression. *Cancer Res* **72**, 5188-5197 (2012).
262. Terra, M. *et al.* Tumor-Derived TGFbeta Alters the Ability of Plasmacytoid Dendritic Cells to Respond to Innate Immune Signaling. *Cancer Res* **78**, 3014-3026 (2018).
263. Tel, J. *et al.* Targeting uptake receptors on human plasmacytoid dendritic cells triggers antigen cross-presentation and robust type I IFN secretion. *J Immunol* **191**, 5005-5012 (2013).
264. Le Mercier, I. *et al.* Tumor promotion by intratumoral plasmacytoid dendritic cells is reversed by TLR7 ligand treatment. *Cancer Res* **73**, 4629-4640 (2013).
265. Liu, C. *et al.* Plasmacytoid dendritic cells induce NK cell-dependent, tumor antigen-specific T cell cross-priming and tumor regression in mice. *J Clin Invest* **118**, 1165-1175 (2008).
266. Bar-On, L. *et al.* CX3CR1+ CD8alpha+ dendritic cells are a steady-state population related to plasmacytoid dendritic cells. *Proc.Natl.Acad.Sci.U.S.A* **107**, 14745-14750 (2010).
267. Zhang, H. *et al.* A distinct subset of plasmacytoid dendritic cells induces activation and differentiation of B and T lymphocytes. *Proc Natl Acad Sci U S A* **114**, 1988-1993 (2017).
268. Villani, A.C. *et al.* Single-cell RNA-seq reveals new types of human blood dendritic cells, monocytes, and progenitors. *Science* **356** (2017).
269. See, P. *et al.* Mapping the human DC lineage through the integration of high-dimensional techniques. *Science* **356** (2017).
270. Alcantara-Hernandez, M. *et al.* High-Dimensional Phenotypic Mapping of Human Dendritic Cells Reveals Interindividual Variation and Tissue Specialization. *Immunity* **47**, 1037-1050 e1036 (2017).

271. Mega, T. *et al.* Zinc finger protein 521 antagonizes early B-cell factor 1 and modulates the B-lymphoid differentiation of primary hematopoietic progenitors. *Cell Cycle* **10**, 2129-2139 (2011).
272. Garrison, B.S. *et al.* ZFP521 regulates murine hematopoietic stem cell function and facilitates MLL-AF9 leukemogenesis in mouse and human cells. *Blood* **130**, 619-624 (2017).
273. Fleenor, C.J. *et al.* Zinc Finger Protein 521 Regulates Early Hematopoiesis through Cell-Extrinsic Mechanisms in the Bone Marrow Microenvironment. *Mol Cell Biol* **38** (2018).
274. Kueh, H.Y., Champhekar, A., Nutt, S.L., Elowitz, M.B. & Rothenberg, E.V. Positive feedback between PU.1 and the cell cycle controls myeloid differentiation. *Science* **341**, 670-673 (2013).
275. Stoeckius, M. *et al.* Simultaneous epitope and transcriptome measurement in single cells. *Nat Methods* **14**, 865-868 (2017).
276. Cusanovich, D.A. *et al.* Multiplex single cell profiling of chromatin accessibility by combinatorial cellular indexing. *Science* **348**, 910-914 (2015).
277. Herman, J.S., Sagar & Grun, D. FateID infers cell fate bias in multipotent progenitors from single-cell RNA-seq data. *Nat Methods* **15**, 379-386 (2018).
278. Liu, K. *et al.* Kallikrein genes are associated with lupus and glomerular basement membrane-specific antibody-induced nephritis in mice and humans. *J Clin Invest* **119**, 911-923 (2009).
279. Li, Q.Z. *et al.* The lupus-susceptibility gene kallikrein downmodulates antibody-mediated glomerulonephritis. *Genes Immun* **10**, 503-508 (2009).

Appendix:

Curriculum Vitae

Patrick F. Rodrigues

Address	Birsstrasse 242 4052 Basel Switzerland	
Email	Patrick.Rodrigues@unibas.ch	
Phone number	+41 76 457 73 93	
Date of birth	09 th of March 1990	
Nationality	Portugal	
Languages	German	native (bilingual)
	Portuguese	native (bilingual)
	English	fluent
	Italian	fluent
	French	good knowledge

Education

- 02/2015 – 03/2019 Doctor of Philosophy (PhD) in Cell Biology**
 Department of Biomedicine, Faculty of Science, University of Basel
 PhD Thesis: "Dissecting the development of plasmacytoid DCs"
 Laboratory: Prof. R. Tussiwand
 Final mark: 6.0 (summa cum laude)
- 03/2013 – 10/2014 Master of Science in Molecular Biology**
 Department of Biomedicine, Faculty of Science, University of Basel
 Master Thesis: "The role of BAFF-R in B-cell development & autoimmunity"
 Laboratory: Prof. A. Rolink
 Final mark: 5.5 (magna cum laude)
- 09/2009 – 02/2013 Bachelor of Science in Biology with Major in Molecular Biology**
 Faculty of Science, University of Basel
 Major Subjects: Structure Biology/Biophysics
 Biochemistry
 Microbiology/Immunology
 Neurobiology/Cell Biology
-

Additional Education

- 03/2018 – 06/2018 Analysis of genomic data with R/Bioconductor**
 University of Basel – An advanced R course where an overview was given in the analysis of different NGS data files from microarray, chip Seq and RNA Seq experiments.

09/2017 – 12/2017	Introduction to R University of Basel – Basic Introduction to R.
06/2016 – 06/2016	LTK Module 1 University of Zürich – Introductory Course in Laboratory Animal Science (FELASA category B)
05/2015 – 05/2015	BD FACS ARIA III operator training A one-week operator training on the BD FACS ARIA III cell sorter at the BD Bioscience headquarter in Erembodegem (Belgium).
09/2008 – 09/2009	Bachelor of Science in Informatics Faculty of Science, University of Basel

Research Experience

03/2019 – present	Postdoc in Prof. R. Tussiwand's Laboratory The characterization and functional role of pDC like cells.
02/2015 – 03/2019	PhD student in Prof. R. Tussiwand's Laboratory The identification and characterization of a specific pDC precursor.
10/2014 – 02/2015	Continuation in Prof. A. Rolink's Laboratory as an internship The role of the pro survival cytokine BAFF and its receptor BAFF-R in B cell development and autoimmunity.
03/2013 – 10/2014	Master student in Prof. A. Rolink's Laboratory The role of the pro survival cytokine BAFF and its receptor BAFF-R in B cell development and autoimmunity.

Supervision of Students

09/2018 – 03/2019	Athanasios Kouklas Department of Biomedicine, Faculty of Science, University of Basel Master Thesis: "Characterizing the development of DCs". Laboratory: Prof. R. Tussiwand
-------------------	--

Oral and Poster Presentations

10/2018	URI Group Meeting – Freiburg, Germany Annual meeting of the Upper Rhine Immunology groups Poster: "Heterogeneity of pDCs is revealed by a Distinct Lineage of Origin" Presentation: "Distinct progenitor lineages contribute to the heterogeneity of pDCs"
---------	--

- 06/2018 **DC 2018 – Aachen, Germany**
The 15th International Symposium on Dendritic Cells.
Poster: "Heterogeneity of pDCs is revealed by a Distinct Lineage of Origin"
- 06/2018 **TOLL 2018 – Porto, Portugal**
A meeting with the focus on recent advances in innate immunity.
Poster: "Heterogeneity of pDCs is revealed by a Distinct Lineage of Origin"
- 09/2017 **Innate Immunity Symposium 2017 – Freiburg, Germany**
International meeting with the focus on Innate Immunity.
Poster prize: "Heterogeneity of pDCs is revealed by a Distinct Lineage of Origin"
- 03/2017 & 02/2018 **Junior myeloid group meeting – Engelberg, Switzerland**
Conference organized by Prof. R. Tussiwand where groups working on myeloid cells have the chance to discuss about ongoing research in innate immunity.
Presentation: "Dissecting the development of pDC development" (2018)
Presentation: "Defining pDC commitment" (2017)
- 11/2016 & 11/2017 **UBICO Retreat – Engelberg, Switzerland**
Yearly conference of the Uni Basel Immune Community.
Poster: "Dissecting the development of pDC development" (2017)
Presentation: "Defining pDC commitment" (2016)
-

Membership in Scientific Societies

- 02/2016 - present **SGAI**
Swiss Society for Allergology and Immunology
-

Publications

- Rodrigues, P. F.**, Alberti-Servera, L., Eremin, A., Grajales-Reyes, G. E., Ivanek, R., & Tussiwand, R.
"Distinct progenitor lineages contribute to the heterogeneity of plasmacytoid dendritic cells"
Nature immunology, 1 (2018)
-